HHS Public Access

Author manuscript

Chem Rev. Author manuscript; available in PMC 2016 October 14.

Published in final edited form as:

Chem Rev. 2015 October 14; 115(19): 10967–11011. doi:10.1021/acs.chemrev.5b00135.

Polymeric Nanostructures for Imaging and Therapy

Mahmoud Elsabahy[1,2,*], **Gyu Seong Heo**[1], **Soon-Mi Lim**[1], **Guorong Sun**[1], and **Karen L. Wooley**[1,*]

[1]Department of Chemistry, Department of Chemical Engineering, Department of Materials Science & Engineering, Laboratory for Synthetic-Biologic Interactions, Texas A&M University, P.O. Box 30012, 3255 TAMU, College Station, Texas 77842-3012, United States

[2]Department of Pharmaceutics, Faculty of Pharmacy, Assiut International Center of Nanomedicine, Al-Rajhy Liver Hospital, Assiut University, 71515 Assiut, Egypt, and Misr University for Science and Technology, 6th of October City, Egypt

1. Introduction

Medical diagnosis and therapy are essential for providing patients with proper care, although inefficient diagnosis and therapy are usually associated with either improper detection of the diseases, unsatisfactory therapeutic outcomes and/or serious adverse reactions. Advances in the design of various diagnostic and therapeutic agents, and the recent trend of utilizing molecules for both therapeutic and diagnostic applications (*i.e.* theranostics), still have not achieved the maximum benefits of controlling the navigation and biodistribution of these molecules within the biological system. The key challenges towards the use of these agents, from small molecules to macromolecular drugs (*e.g.* natural, proteins and nucleic acids-based drugs, or synthetic, polymer-based conjugates, carriers or other systems), are, for example, the loss of activity *via* rapid clearance or degradation, inefficient delivery to the target sites, and inappropriate probing of the disease states, dependent on the particular disease and its location in the body. The concept of nanotechnology has been initiated early in 1959 by Richard Feynman in his famous historical talk at Caltech "There's Plenty of Room at the Bottom", with introduction of the possibility of manipulating materials at the atomic and molecular levels.[1] In 1974, Norio Taniguchi, at Tokyo University, first utilized the term "nanotechnology" referring to the design of materials on the nanoscale.[2] In the early 1990's and until now, the use of nanomaterials of different nature (organic and inorganic), and for various applications (multiple disciplines) has been greatly expanded, in particular, over the last couple of decades.[3-4] In the medical field, nanotechnology has emerged to include non-invasive systems for probing of disease and also capable of carrying cargo for localized high concentration delivery, known as "nanomedicine", with reduction of off-target effects. The use of nanomaterials, in particular polymeric nanostructures, has demonstrated efficiency in improving delivery of diagnostic and therapeutic agents to the target sites, and the feasibility of incorporating several therapeutic/diagnostic/targeting moieties within specific compartments of the nanoparticles, with control of their navigation

*Correspondence to: Tel.: +1 979 845 4077, Fax: +1 979 862 1137, mahmoud.elsabahy@chem.tamu.edu and wooley@chem.tamu.edu.

in the body and to the target sites. Further understanding of the nature and microenvironments of biological systems (*e.g.* different pH, temperature, permeability, drainage, or overexpressing proteins, enzymes or receptors), and the barriers towards the delivery of various moieties to their destinations, which could be either intra- or extracellular, has aided the design of nanomaterials that could evade the various physiological barriers. Selective delivery to the site of the disease can increase the therapeutic efficacy, imaging contrast and accuracy, reduce adverse reactions, and reduce the dose and cost of medications.

Initially, platform technologies were the target for nanostructure designs, but with the complications of biological systems, it has been recognized over the past decade that disease- and patient-specific medical treatment is needed for efficacy—this review highlights a few examples developed within the past couple of years, with a focus on *in vivo* studies together with novel designs and significant advances in syntheses. The advantages of polymeric nanostructures over other types of nanomaterials are based upon the flexibility over which their structures can be modified to yield materials of various compositions, morphologies, sizes, surface properties, with possibility of hierarchical assembly of several nanomaterials of various components into one construct that can be accommodated with a variety of therapeutic, diagnostic and/or targeting moieties, within selective compartments of the nanodevices. High efficiency in diagnosis and treatment of diseases and improving patient quality of life and compliance can be achieved through understanding the molecular events associated with various diseases, and combining the advances in the design of therapeutic and diagnostic agents and nanomaterials, together with the innovative instruments utilized for monitoring these agents. This review will focus on several recent advances in the design of polymeric nanoparticles that have been utilized for delivery of diagnostic and/or therapeutic agents, and the various barriers towards the clinical development of these materials. After a brief overview of the capabilities and challenges with medical imaging and therapy, in general, disease-specific examples of polymer nanoparticles designed specifically to overcome the challenges and address unmet medical needs will be discussed in detail.

2. Capabilities and challenges for medical imaging

Non-invasive medical imaging, including the use of X-ray computed tomography (CT), magnetic resonance imaging (MRI), optical imaging, positron emission tomography (PET), and single photon emission computed tomography (SPECT), is an essential tool for the diagnosis of several critical diseases, such as cancer, cardiovascular diseases, and infectious diseases, and for monitoring the progression and prognosis of these diseases, through visualizing organs and internal structures with limited damage to surrounding tissues. The anatomic and functional information obtained from medical imaging can provide evaluation/estimation of disease staging, while also enabling guidance of therapeutic processes. While each medical imaging modality has its own advantages and disadvantages, regarding the sensitivity, spatial resolution, probing depth and time limitations (Table 1), it is often necessary to acquire and combine information from more than one imaging method to improve the diagnostic accuracy.[5] The intrinsic nature of the versatile construction and functionalization of polymeric nanoparticles (*i.e.*, multiple functionalities of imaging probes,

biodistribution “tuners”, targeting ligands, and therapeutic agents can be accommodated throughout the entire macromolecular frameworks in chemo- and regioselective manners) have enabled facile and practical strategies for developing multimodal medical imaging that can compensate disadvantages of one imaging modality from another.[6]

As the most commonly used medical imaging modality, the relatively faster and less costly CT, compared with MRI and PET, generates three-dimensional (3D) images through the reconstructions of cross sectional 2D x-ray pictures. The pathological tissues are identified from the surrounding healthy tissues, based upon their different densities and the resulting x-ray absorption variations.[7-8] To enhance the contrast between normal and anomalous tissues during CT scanning, CT contrast agents, mostly based iodine or barium, are administered to patients before imaging, thereby, improving the image resolution and specificity. The current small molecule-based CT contrast agents, especially the most widely used iodinated compounds, require relatively higher dosage (molar concentration range) than other imaging modalities, such as MRI (millimolar concentration range), nuclear imaging (micromolar concentration range), and optical imaging (nanomolar concentration range).[9] Although the radiotoxicity of CT imaging is still controversial, development of contrast agents with higher x-ray absorption coefficients is beneficial. For instance, other high K-line transition metals and semiconducting materials have been exploited as contrast agents with higher x-ray absorption coefficients. In addition, further improvement of CT agents should be addressed to allow for specific localization, non-toxic metabolites, sufficiently long (2-4 h) blood retention time, water solubility, and short clearance time from the body.[9] Therefore, polymeric nanoparticles are under development, with comparable loading/conjugation capacities of iodinated (or other contrast elements) moieties and prolonged blood circulation times.[10-12]

MRI generates high resolution images (up to single-cell resolution) of soft tissues such as muscles, joints, and brain. MRI uses strong magnetic field to align the nuclear spins and generates images from emitted radio frequency (RF) from the nuclei when they return to their original states. ^{1}H signals from water molecules are most frequently visualized, however, ^{13}C, ^{31}P, and ^{19}F can also be observed, and abnormalities of tissues appear as darker (T_1-weighted) or brighter (T_2-weighted) than healthy tissues, due to differences in relaxation times. Contrast agents that are used to improve visibility of organs and clinically-used MRI contrast agents are paramagnetic gadolinium (Gd) reagents for T_1 imaging and superparamagnetic iron oxide (SPIO) for T_2 imaging.[13-16] One of the limitations of MRI imaging is the relatively long acquisition times required to obtain high quality images, where patients are uncomfortable and restrained. There are limited applications of MRI for patients with implanted metal devices because the metal could interfere with imaging, and malfunction of the implanted metal device is possible during MRI acquisition within the high magnetic field instrumentation. Both CT and MRI generate high resolution images, but they provide only morphological information, with some exceptions such as functionalized MRI (fMRI).

On the other hand, PET and SPECT can provide functional information *via* tracking biochemical changes in specific tissues, a feature that is not available in CT and MRI.[17] PET and SPECT rely on detection of gamma rays, and allow for 3D tomographic image

reconstruction. PET tracers emit positrons (anti-electron)-emitting radioisotopes, which emit pairs of opposing gamma rays upon annihilation. SPECT tracers directly emit gamma rays. The gamma rays are then collected by detectors surrounding the patient in PET or rotating around the patient in SPECT.[18] Recent CT scanners are equipped also with the SPECT imaging module, which enables co-registration of high resolution CT images with functional SPECT images. Commonly used tracers are ^{18}F, ^{13}N, ^{11}C, ^{15}O, ^{82}Rb, ^{68}Ga and ^{64}Cu,[19-21] for PET, and ^{67}Ga, ^{99m}Tc and ^{111}In for SPECT. PET is highly sensitive and quantitative, as compared to SPECT. PET requires only 10^{-11}-10^{-12} M of radioactive tracers, while SPECT requires 10^{-10}-10^{-11} M.[8,10] Due to the high sensitivity of PET, it is challenging to minimize nonspecific uptake of tracers, which interferes with quantitative analysis.[22] Also, challenges result from the lifetimes of radioactive tracers that decay much faster than image acquisition times. Therefore, it will be beneficial to develop tracers having lifetimes that coincide with the time periods required for sample preparation, purification, distribution to remote imaging facilities and completion of stable imaging.

Optical imaging, with fluorescent dyes and quantum dots, is a highly sensitive imaging method that can detect up to 10^{-9} to 10^{-12} M concentration, while also avoiding x-ray irradiation or the use of radionuclides and, therefore, being safer than CT and PET. However, the most significant limitation for non-invasive optical imaging is the limited depth of detection. Traditionally, quantum dots experienced issues related to their toxicities, however, advances have been made with non-toxic inorganic Cornell Dots (C Dot) and other materials, which are currently undergoing clinical trial.[23] Optical imaging also can provide functional imaging, by designing dyes with selective localization in target tissues, and/or selective turn-on or turn-off capabilities in the presence of external or biological stimuli (*e.g.*, reactive oxygen species present at elevated levels at sites of inflammation).[24-25] The Phillips group developed small molecules that undergo signal amplification reactions in the presence of singlet oxygen and generate a colorimetric output signal.[26] Optical imaging is the only imaging method that can acquire multi-channel images, simultaneously. Recent progress in near IR dyes (680 ~ 880 nm) has expanded the possibilities for non-invasive tissue imaging at depths approaching several cm without damaging tissues and organs.[27-30] The development of near-infrared (NIR) dyes with higher quantum efficiency, greater brightness, more selective stimuli-responsiveness,[31] and lack of toxicity remains an active area of research for clinical application of optical imaging.

The greatest potential impact of polymeric nanoparticles toward imaging, in general, is the ability to increase contrast locally, by directing the biodistribution of high concentrations of packaged small molecule contrast agents to a target organ/site *in vivo*, and also the possibility that multiple types of contrast agents can be coincidentally carried within a polymer nanoparticle package to achieve multi-modality imaging. Various imaging modalities are compared in Table 1 with their ranges of spatial resolution, imaging depth, and sensitivity. For anatomical (structural) imaging, MRI, CT, and ultrasound can be applied, while physiological imaging of diseased tissues can be acquired by all of the medical imaging methods, and molecular information such as protein composition in cells can be acquired from MRI, PET, SPECT, and optical imaging. In addition to the imaging modalities mentioned here, there are others. For instance, photoacoustic imaging is

emerging, especially as advances are made with sensitive imaging agents, beyond non-degradable inorganic materials (*e.g.*, carbon nanotube, gold nanorod, *etc*.), including organic polymer-based nanoparticle materials.[32] Each medical imaging modality has its own advantages and disadvantages. Therefore, multimodal imaging with multiple imaging methods could provide complementary information and more accurate diagnosis.

3. Capabilities and challenges for medical therapy

Medical therapy, in particular the systems that target special events related to a disease, is promising in treatment of several diseases on the molecular level, for instance, *via* correcting genetic mutations or protein misfolding, or interfering with one or more of the pathway cascades involved in disease progression. Diseased tissues are usually different from healthy ones in several aspects, such as, having different microenvironment (pH or temperature), permeability, drainage, or overexpressing specific proteins, enzymes or receptors. These differences can be utilized to allow selective delivery once the therapeutic molecules could overcome the various biological barriers and reach the diseased tissues and molecular targets. The same principles apply for therapy as for imaging, where selective binding or release of the diagnostic agents to the diseased tissues can improve the imaging contrast and provide more efficient diagnosis and information on the disease status and progression. Theranostic agents are being currently developed *via* either utilizing a particular probe or drug that has therapeutic and diagnostic capabilities, or labeling therapeutic agents with imaging probes, for both therapy and imaging. The use of a theranostic approach, in addition to providing simultaneous therapy and imaging, reducing the frequency of administration, enhancing patient compliance and decreasing the burden on patients and caregivers, can also provide useful information on the drug biodistribution and clearance.

Selective delivery to the site of the disease can increase the therapeutic and imaging efficacy, reduce adverse reactions, and reduce the cost. However, there are several challenges towards this efficient delivery (Figures 1 and 2). Several of these drugs have poor aqueous solubilities and, thus, cannot be solubilized, dispersed, or diluted in saline prior to injection, or solubilized in other aqueous solutions for administration *via* other routes of administration. Rapid degradation, enzymatic or hydrolytic, of some drugs, both *in vitro* during storage and *in vivo* after administration (extra- or intracellularly), hinders drugs from reaching their target sites in an intact form. Interaction between drugs and various biological environments (depending on the administration route and target site) may destabilize the drug, prevent their penetration to the target site or re-direct their distribution in the body (Figure 1). The detailed biological barriers (external, en-route, internal) have been reviewed previously by our group (Figure 2) and others.[35-38]

The main barriers towards the delivery of therapeutic and diagnostic agents to their target sites are the external barriers that prevent them from entering the body (skin and mucosa that cover body surface), blood, blood components, and extracellular matrices that hinder them from reaching the targeted cells or sites in the various organs, and cellular barriers (limited uptake, degradation in the endosomes/lysosomes or the cytoplasm, and low nuclear uptake, if the nucleus is the target site). These barriers could also destabilize the various agents before reaching their target sites. The tightly packed layers of the stratum corneum of the

skin usually hinder penetration of various drugs, whereas the viscoelastic hydrogel of the mucus that covers various body surface areas hinders the delivery to the underlying tissues *via* several mechanisms.[39-40] The mucus has various compositions (cells, bacteria, lipids, salts, proteins, macromolecules, and cellular debris), thicknesses and pHs, depending on the physiological region and disease status. Adhesiveness, steric hindrance and mucociliary clearance are the main mechanisms for hindering efficient delivery through mucus. Drugs that reach the bloodstream are subjected to opsonization, degradation, immune response, non-specific biodistribution, renal, hepatic and/or splenic clearance.[41] Drugs on the cellular surface are usually not at their final destination yet, and they may not have the capability of entering cells, especially for hydrophilic macromolecules, and after uptake, they may degrade within the endosomal/lysosomal compartments. When the target site is a subcellular organelle, such as mitochondria or the nucleus, one more barrier is included into the journey, as these organelles do not allow non-specific uptake of various moieties (Figure 3).

4. Cardiovascular diseases, cancer and infectious maladies as targets for medical diagnosis and therapy

4.1 Cardiovascular diseases

Cardiovascular diseases are the number one death-causing disease and according to the World Health Organization, in 2012, 3 in every 10 people worldwide died from cardiovascular diseases (CVD).[44] In the United States, in 2010, more than 300 billion dollars were spent on medical expenses due to CVD.[45] Diseases related to the cardiovascular system include atherosclerosis, hypertension, and coronary artery diseases (CAD), which could result in heart attack or stroke. The majority of cardiovascular diseases are related to plaque formation in blood vessels. Atherosclerosis is an immune disease in arteries, initiated from low density lipoprotein (LDL) permeation into vessel walls, due to endothelial dysfunction. Atherosclerotic plaques stiffen blood vessels and the progression of plaques may lead to coronary artery disease, which could eventually block the artery, hinder blood flow to the heart and, thereby, cause cellular death in the heart and heart failure. Plaques covered by an unstable cap could be ruptured and block blood flow to the heart. Blood vessels are composed of three layers, tunica intima, tunica media, and tunica adventitia. The inner-most layer is the tunica intima and the interface between the intima and vessel lumen is protected by a monolayer of endothelial cells. When the endothelium is damaged by high blood pressure, high cholesterol intake, smoking, obesity, diabetes and LDL, components in blood lumen leak into the intima, and, thus causing inflammation and recruitment of monocytes from the blood stream. Monocytes differentiate into macrophages, which then ingest oxidized LDL and change into foam cells (Figure 4). Cell debris and lipids from dead cells can promote accumulation of extracellular lipids to the site and spread out plaques in the vessel wall.[46] This plaque area is later covered by a fibrous cap composed of vascular smooth muscle cells, macrophages, and extracellular matrix components, such as collagen. Some plaques are stable enough to last for a long time without undergoing a rupture event, but plaques with large lipid cores, low smooth muscle cell content, high macrophage content, and a thin fibrous cap are prone to rupture that leads to arterial blockage.

Early and specific detection of atherosclerotic plaques are crucial for treatment and to avoid fatal consequences from rupture. Monocytes and macrophages could serve as biomarkers of disease progression for atherosclerosis, as well as, cancer and myocardial infarction. Monocyte recruitment to sites of inflammation is mediated by C-C cytokine receptors (CCR), such as CCR2.[47] Therefore, imaging agents conjugated with CCR2 ligands could be used for targeted imaging for early detection of atherosclerosis. Likewise, translocator protein (TSPO) receptors and somatostatin receptors on macrophage membranes are characteristic markers for early stages of atherosclerosis. Macrophages in the inflammation site require high energy, which is provided from glucose. The most common PET tracer, ^{18}F-2-deoxy-2-fluoro-D-glucose (^{18}F-FDG), recognizes increased uptake of glucose by macrophages in the intima, which is a sign of inflammation. Progression of atherosclerotic plaques can be recognized by hypoxia, angiogenesis from the *vasa vasorum*, and microcalcification in the stiffened arteries. Smooth muscle cells also play a significant role in blood vessel stiffening. Tanaka and co-workers reported the regulation of vascular smooth muscle cells (SMCs) by nuclear factor (NF)-κB.[48-49] It has been reported that the late stage of atherosclerosis is associated with CCR5 activation, which could also be utilized as a potential biomarker for plaque instability.[50] Natriuretic peptides (NPs) have potent antiproliferative and antimigratory effects on vascular smooth-muscle cells (VSMCs) and, in atherosclerosis, the expression of NP clearance receptors (NPR-Cs) is upregulated both in endothelium and VSMCs and participate in vascular remodeling.[51] Application of C-type atrial natriuretic factor (CANF) fragment in atherosclerosis diagnosis and treatment has been proposed, and recently nanoparticles labeled with CANF have been approved for human clinical trials.[52] Figure 4 summarizes mechanisms of atherosclerosis progression and therapeutic strategies using nanomedicine.[53]

4.2 Cancer

Tumor/neoplasm is uncontrolled growth of cells, where this group of cells might have the ability to spread in the body *via* invasion and metastasis through the blood and lymph systems. The main characteristics of cancer are sustaining proliferative signaling, evading growth suppressors, avoiding immune destruction, enabling replicative immortality, promoting inflammation, invading and metastasizing, inducing angiogenesis, accruing genome instability and mutation, resisting cell death, and deregulating cellular energetics,[54] which are shared by more than 100 cancer-related diseases. These diseases can be categorized by the type of cell or tissue in which cancer originates, including carcinoma, sarcoma, leukemia, lymphoma and myeloma, central nervous system cancers, *etc*. Cancer usually acquires these characteristics due to genetic and epigenetic alterations, which consequently result in molecular variations, such as, overexpression of receptors and proteins, changes in upstream and downstream effectors, and tumor progression.[55-61] Alteration in signaling pathways is commonly observed in cancer and usually affects cellular proliferation, angiogenesis and apoptosis. Some of the molecules that are overexpressed in cancer are vascular endothelial growth factor (VEGF), platelet-derived growth factor receptor β (PDGFR β), and basic fibroblast growth factor (bFGF), which are key factors in the growth of new blood vessels and in increasing the vascular permeability.[62-64] Sometimes, overexpression of specific molecules or receptors serves as a "benchmark" for some tumors. For instance, ASGP-R (endocytic cell surface receptors) and

glycyrrhetinic acid (GA) receptors are highly expressed in hepatocytes and, thus, can be utilized for targeted drug delivery for treatment of liver cancer.[65-69] Understanding these fundamental biological processes of cancer facilitates the advancement of treatment strategies.

Cancer can be treated in several ways, including surgery, chemotherapy, radiation therapy, hormonal therapy, immunotherapy, hyperthermia, stem cell transplantation, photodynamic therapy, laser surgery, *etc.*, where more than one strategy can be combined together, depending on the type and stage of cancer. To date, complete removal of cancerous tissues remains challenging, since cancer cells can invade normal adjacent tissues and metastasize to distant body parts. As biological information about cancer has been accumulated, development and modification of treatments have been pursued in order to eradicate cancer cells selectively from the patient and minimize side effects.

The two main goals for the treatment of cancer with various therapeutic agents are the selective delivery of drugs to the target sites and interfering with molecular events involved in the cancer progression without affecting normal healthy cells. Characteristics of cancerous tissues, such as the leaky vasculature and impaired lymphatic drainage, can be utilized to enhance selective delivery and accumulation of various therapeutics and/or diagnostics into tumor tissues. However, small molecules usually extravasate quickly from blood vessels within short blood circulation times that do not allow for sufficient accumulation in the tumor tissues, and usually clear rapidly from tumors after accumulation *via* elevated interstitial fluid pressure. Extravasation into tumor tissues, due to the leaky vasculature and accumulation at the cancerous tissues of impaired lymphatic drainage, is most well-known as the “enhanced permeability and retention (EPR)” effect.[70]

A variety of biomarkers and receptors associated with cancer progression could be employed to improve the extravascular transport of drugs to reach the target tumor sites by specific ligand-receptor interactions.[71-73] The effect of utilizing various ligands conjugated to drugs or carriers that contain the drugs, including antibodies and antibody fragments, aptamers, peptides, and small molecules, or targeting molecular events specific to cancer underlying mechanisms, has been confirmed to improve therapeutic efficiency. However, there are still several challenges towards effective delivery, including the rapid clearance of small therapeutic molecules, environmental or enzymatic degradation of therapeutic agents, limited aqueous solubility and low selectivity of conventional anticancer drugs, biological and biophysical barriers that hinder targeting, such as, the tight junctions between epithelial cells in the blood-brain barrier, *etc*.

4.3 Infectious diseases, with a focus on pulmonary infections

Infectious diseases are usually caused by bacteria, viruses, parasites or fungi. They usually spread from one to another, and, sometimes, could become serious, difficult to treat, and life-threatening. More recently, the outbreaks of Ebola, influenza, salmonella, HIV, *etc.* have brought worldwide attention to zoonotic diseases that can be transmitted to humans by infected animals. Since the expansion of the global transport network, infectious diseases have become more broadly transmissible,[74] increasing the urgency to develop efficient treatment methods. Although there are several therapeutics and diagnostics that have been

tested with varying degrees of success for management of infectious diseases, the poor bioavailability (due to rapid metabolism and excretion from the body or inactivation of drugs) and serious side effects of some of these agents, development of resistant microorganisms, and biological barriers that hinder the efficient delivery of therapeutic and diagnostic agents to the infection sites, compromise the expected therapeutic outcomes.[75-77] We have a keen interest in the treatment of pulmonary infectious diseases, due to their prevalence, limited diagnosis and treatment strategies, and promise for direct routes of administration, which may avoid complications from systemic delivery and damage to the human microbiome, among other beneficial microflora. Examples of infectious diseases that affect the lung are pneumonia, tuberculosis, and chronic obstructive pulmonary diseases. Barriers towards the delivery of antimicrobials for the treatment of infectious diseases depend upon the type and site of infections, and could include but are not limited to, multi-drug resistant bacteria, need for high doses, which often results in toxicity, mucociliary clearance, steric hindrance of drug uptake, presence of enzymes and macrophages in the mucus gel and tissues, and high viscosity of sputum, especially in the case of cystic fibrosis.[9,36,46-54] For instance, mucus is a viscoelastic hydrogel secreted by the mucosal glands to protect regions that are not covered by the skin, with varying composition, thickness and permeability depending on the region and disease status.[40] The use of physical or chemical methods to hydrolyze mucin and mucolytic agents can enhance penetration of the drug by reducing the viscosity of mucus.[78-80]

5. The design of polymer nanostructures to address challenges in imaging and therapy

5.1 Significance and versatility

Polymeric nanostructures have the potential to improve the medical outcomes of various therapeutics and diagnostics by enhancing the accumulation of the embedded active species into the target sites of diseased tissues *via* passive and/or active targeting (Figure 5-7). They can also be utilized for combinational therapy/diagnosis. In passive targeting, nanoparticles accumulate into pathological sites with leaky vasculature (*e.g.* tumor and inflammation sites) due to the EPR effect (*vide supra*), whereas active targeting is achieved through decorating the surface of nanoparticles with targeting ligands that bind to receptors overexpressed on the diseased tissues. Active targeting features can also be incorporated into the nanostructures *via* including stimuli-responsive components into the nanomaterials. Ideally, both targeting mechanisms aim to concentrate the nanomaterials, while containing the embedded drugs and/or diagnostic probes, at the diseased tissues and avoiding accumulation or drug-release at healthy tissues. No matter which targeting strategy is employed, a common characteristic of nanoparticulate materials is that loading drugs into nanoparticles redirects the biodistribution, preventing small molecule drugs from passing through normal blood vasculature, renal tubules, and other pores < 10 nm to eliminate rapid biological clearance and alleviate severe side effects systemically. Instead, nanomaterials can permeate through and accumulate into pathological areas with leaky vasculature (pores > 100 nm). Local routes of administration offer opportunities to further narrow the selective region of access of nanomaterials, for instance to diseased skin, lungs, urinary tracts, *etc.*

Typically, nanoparticle-based carrier materials possess a core-shell morphology, for which the nature of the core-forming polymer dictates the type of therapeutics/diagnostics that can be incorporated into the nanomaterials, whereas the composition and structure of the shell-forming polymer components (*e.g.*, the polymer chain length, spacing and the incorporation of crosslinking moieties) control the stability of nanoparticles and their blood circulation time. Although there remain several challenges towards the development of effective therapeutics, the ability to control their characteristics *via* chemical modifications of the building blocks is an exciting strategy to improve the utility of nanomaterials for biomedical applications. The building blocks can be modified to encapsulate hydrophobic drugs, nucleic acids, enzymes, hormones, small peptides and other macromolecules. They can also be modified to respond to external or internal stimuli.

5.2 Nanoparticle design principles, components and types of structures

There are several types of nanomaterials that are summarized in Table 2 and Figure 8. The main focus of this review is on polymeric nanoparticles that have been utilized for therapy and/or imaging. Multifunctional polymeric nanoparticles with precise control over the architectures of the individual polymer components and overall nanoparticle composition can be engineered *via* bottom-up controlling the polymer chemistry and supramolecular assembly (Figure 9). The chemistry of polymer precursors can be modified for efficient encapsulation of various therapeutic molecules. For example, chemical modification with hydrophobic side chains or cationic functional groups can be utilized for incorporation of hydrophobic drugs and nucleic acids, respectively. These drugs can also be covalently attached onto polymers to afford drug-polymer conjugates, which consequently eliminate the diffusion-dominated premature release and provide further tunability of either hydrolytically- or enzymatically-induced controlled release. Diagnostic probes can be included into these materials through orthogonal chemical modifications. Hierarchical assembly of various nanostructures could be utilized to incorporate all these functionalities into one set of nanomaterials, as will be explained later.

Hydrophilic polymer components/segments should be carefully selected to mask the hydrophobic domains of the nanoparticles and the embedded cargoes, and to allow for prolonged blood circulation time, low interaction with extracellular matrices and with the immune system components. Poly(ethylene glycol) (PEG), also known as poly(ethylene oxide) (PEO) or polyoxyethylene (POE), is the most commonly-used polymer to coat various types of nanomaterials and to impart stealth properties. Other polymers have been investigated also to form the corona of nanoparticles, such as poly(*N*-(2-hydroxypropyl) methacrylamide) (PHPMA), poly(acrylic acid) (PAA), poly(*N*-vinylpyrrolidone), poly(*N*-isopropylacrylamide) and poly(carboxybetaine) (PCB).[82-87] Although still controversial, it was reported that PCB can impart antibiofouling effect better than PEG, possibly due to better hydration of corona *via* electrostatic binding of water molecules more tightly than hydrogen bonding in case of PEG, and thus minimizing protein adsorption on the surface of nanoparticles.[85-87] Antibiofouling means lower competences for adsorbing proteins or other opsonins in the surrounding environment.

Wooley and coworkers have performed rigorous *in vitro* and *in vivo* comparisons between two sets of shell crosslinked knedel-like nanoparticles (SCKs) coated with either non-ionic PEG or zwitterionic PCB, in terms of physicochemical characteristics, stability, pharmacokinetic profiles, immunotoxicity and antibiofouling properties (Figure 10).[88-89] SCKs are polymeric nanoparticles formed *via* self-assembly of amphiphilic block copolymers into micelles, followed by selective crosslinking of some of the functionalities in the shell layer to provide greater stability against dilution, prolonged circulation time, reduced toxicity, as compared to the non-crosslinked micellar analogs.[35,90-100] These nanoparticles were formed through first synthesizing poly(acrylic acid)-*block*-polylactide (PAA-*b*-PLA) copolymers and then utilizing the PAA block segment to graft PEG and PCB of various molecular weights (2 and 5 kDa PEG and PCB).[88] To prepare multifunctional nanoparticles that can be utilized for both PET imaging and potential therapy, DOTA chelator and tyramine were covalently incorporated by following an established "pre-grafting" strategy.[101-102] Significant differences in the physicochemical properties and *in vivo* characteristics were found between the SCKs grafted with PEG and PCB. Both PEG_{5k}- and PCB_{5k}-SCKs had similar size distribution and zeta-potential values, whereas the nanoparticles before functionalization with PEG or PCB had larger sizes, broader size distributions and higher negative zeta-potential values (in particular, as compared to the PEG_{5k}- and PCB_{5k}-SCKs), which highlights the benefits from the steric stability imparted by the PEG and PCB polymers of higher molecular weights. It was found that the parent PAA-*b*-PLA was immunotoxic, with grafting by either PEG or PCB leading to a reduction of immunotoxicity, however, SCKs derived from both of the PEG- and PCB-grafted polymers remained immunotoxic. PCB-based nanoparticles induced a higher release of proinflammatory cytokines, both *in vitro* and *in vivo*, than did PEG-SCKs. The uncoated nanoparticles resulted in high release of most of the measured cytokines, probably due to the absence of the shielding effect of PEG and PCB for the coated nanoparticles. The uncoated nanoparticles resulted in higher adsorption of the measured cytokines, which is due to the anionic nature of these SCKs and the lack of stealth properties. The higher adsorption of proteins on PCB polymers and nanoparticles, as compared to those which were PEGylated, together with the higher *in vitro* and *in vivo* immunotoxicity, correlated well with the longer blood circulation time and lower clearance in the immune organs of the PEG_{5k}-SCKs, as compared to PCB_{5k}-SCKs.[88] Biocompatible nanoparticles should not induce a massive release of cytokines. As potential toxicities and immunogenicities of PEGylated therapeutics were previously reported,[103-105] alternative degradable PEG analogs are currently under investigation to improve the safety profiles of PEG-based therapeutics.[106] However, it is worth mentioning that safety, biocompatibility and performance of nanomaterials depend on the overall nanoparticle composition, and not only that of the shell.

The recently-developed controlled polymerization methodologies not only provide a powerful toolbox for incorporation of diverse functionalities into polymers, but also enable precise rationalization of drug/targeting ligand/probes-to-polymer or unimer-to-unimer ratio, beyond the "conventional" polymer structures outlined in Figure 9, and, thus providing a possibility of predefined control over the size and shape of the formed nanoparticles. The size and morphology of polymer nanoparticles serve as critical characteristics for their *in vivo* fates, such as, blood circulation time and organ biodistribution. While spherical

nanostructures with hydrodynamic diameters (D_hs) ranging from tens to hundreds of nanometers have been extensively studied, recent research activities on ultrasmall nanoparticles with D_h at the sub-10 nm scale revealed noticeable advantages of enabling effective renal excretion[132] and minimizing off-target accumulation,[133] which are attractive features for developing nanoparticulates for imaging applications. However, the decrease of nanoparticle size can enhance its permeability to both healthy and diseased tissues, and can also result in rapid clearance from the blood and thus reduced accumulation in the targeted tissues, which deceases the benefits from nanoparticles in some therapeutic applications, such as in the case of cancer therapy. Regardless of the size of nanoparticles, imparting stability that prevents premature dissociation and release of the loaded therapeutic/diagnostic cargoes is crucial.

5.3 Crosslinking

Premature disassembly of nanoparticles into the polymer constituents and/or breakdown into degradation products result in premature release of their loaded cargoes, and is considered as one of the main challenges towards the effective delivery of nanoparticle-packaged therapeutics to their target sites. Not only releasing the drug prematurely, but also the free polymeric chains may induce cyto/immunotoxicity. Stereocomplexation, non-covalent interactions and crosslinking of one or more components of the polymers components are some of the most commonly-utilized strategies to enhance the stability of nanomaterials.[134-136] Crosslinking can be performed within either the core or the corona of pre-formed micelles (Figure 11). Synthesis of unimolecular/hyperbranched structures that are not prone to dissociation upon dilution is another way to yield stable nanostructures.

The effect of chemical composition and crosslinking of different block copolymers and the relative copolymer block length on the size, core/shell dimensions, loading and release kinetics and pH- and thermo-responsiveness of SCKs were previously reviewed by our group and others.[90,137-139] The focus of this section is on the superior characteristics of the crosslinked nanomaterials over their non-crosslinked precursors, such as allowing for unique processing opportunities, including overcoming complications of aggregation during lyophilization processes, biological advantages, including slower kinetics of release of therapeutic guests,[83,140] higher kinetic- and blood stability,[92,141] longer pulmonary retention to provide for extended release,[140] and lower cyto/immuno/toxicities, introductions of structural/functional factors that enable stimuli-responsive functions, as well as, affording unusual nanoparticle properties and structures, including stabilization of nanocrystals and the formation of nanocages.

Effect on the stability of nanoparticles during lyophilization processes— Freeze-drying is one of the most valuable techniques to improve the long-term stability of nanoparticles to overcome the limited stability in aqueous solutions.[142] However, lyophilization had a limited success due to nanoparticle aggregation events that often occur during the process and prevent resuspension. Lyoprotectants (*e.g.* sugars and polyalcohols) have been utilized to prevent aggregation during the freezing step of the lyophilization, although the use of these materials might be limited with some patients, as in the case of diabetic patients. Crosslinking has been shown to be a useful tool for overcoming

aggregation during freeze-drying. For instance, stable, freeze-dried polyplexes consisting of a crosslinked thiolated poly(L-lysine) core and PEG shell and plasmid DNA (pDNA) were prepared.[94] The disulfide-crosslinked polyplexes showed excellent stability during freeze-drying and reconstitution processes, whereas the non-crosslinked analogs formed visible agglomerates. The freeze-dried nanoparticles achieved a similar *in vitro* transfection, as compared to the original formulations, and have also demonstrated gene expression *in vivo* in mice.

Effect on pharmacokinetics and biodistribution—Shell length, spacing and crosslinking of the shell are critical parameters that dictate the blood circulation time and stability of nanoparticles with ~1 nm spacing found to be efficient in preventing protein adsorption.[22,35,143-144] Special efforts have focused on increasing the kinetic stability of these nanoassemblies to enable them to withstand the harsh biological barriers that they experience during circulation in the blood and down to the cellular and subcellular levels, until they deliver their guest molecules. Among the different strategies to enhance the kinetic stability of polymer micelles, shell- and core-crosslinking have been shown to limit the premature disassembly and slow the release of the encapsulated drug. Seminal work by Kabanov and coworkers, involving direct comparison of crosslinked and non-crosslinked nanoparticle materials, showed that the crosslinked analogs exhibited enhanced blood-stability and accumulation in the brain tissues of treated mice than the non-crosslinked complexes.[92] In an attempt to study the effect of crosslinking on the ability of nanomaterials to provide sustained release of high concentrations of therapeutics locally in the lung *via* direct administration, Wooley and coworkers have developed biodegradable polyphosphoester-based polymeric micelles and SCKs loaded with ultra-high levels of paclitaxel (PTX). Upon intratracheal administration into mice, SCKs were retained in the lung of the treated mice for almost twice the time of their micellar counterparts (*ca.* 8 d *vs*. 4 d, respectively).[140]

Effect on toxicity and immunogenicity—Kabanov and coworkers have found that crosslinked PEG-*b*-poly(L-lysine hydrochloride)-based nanoparticles had lower cytotoxicity than their non-crosslinked complexes, which was explained by reducing the release of free copolymer chains and, thereby, limiting the molecular-level interactions with the cell membrane.[92] As a follow-up, Wooley and coworkers investigated the immunotoxicities of nanoparticles of various compositions by incubating RAW 264.7 mouse macrophages with various formulations of micellar assemblies *vs*. their shell-crosslinked nanoparticle analogs for 24 h, and measuring the levels of 23 different cytokines. Induction of cytokines by polyphosphoester-based nanoparticles was substantially reduced by the introduction of crosslinks within the shells of the zwitterionic and cationic micelles.[145] In another study, poly(acrylamidoethylamine)-*block*-poly(DL-lactide) (PAEA-*b*-PDLLA) copolymers were synthesized, self-assembled in water to yield nanoscopic polymeric micelles, and the effects of decorating the micellar surface with PEG and crosslinking the PAEA layer to varying extents on the immunotoxicity of the nanoparticles were studied. It was observed that a nominal 20%-crosslinking of the micelle shell functionalities was more efficient than PEGylation of micelles and PEGylation of the 5%-crosslinked SCKs in reducing the release of cytokines.[146] Immunotoxicity associated with non-crosslinked PEG-micelles highlights

the advantages of using crosslinked nanoparticles. In comparison, Lipofectamine™ induced significantly higher expression of almost all the tested cytokines as compared to both PDLLA- and polyphosphoester-based nanoparticles, which confirm the usefulness of designing degradable nanomaterials in reducing immunotoxicity. The reasons for the lower toxicity could be the suppression of block copolymer release, reducing the flexibility of the outer shell, and minimizing the accessibility of the surrounding biomolecules to the shell/core components (Figure 11). Limiting the flexibility of the shell with crosslinking hinders the nanoparticles from rapid dissociation and interaction with the surrounding biomolecules.

Functional crosslinking—Crosslinking can be utilized to incorporate imaging probes to nanostructures by utilizing functional crosslinkers. For instance, Achilefu *et al.* reported NIR fluorescent nanoparticles prepared from core-crosslinking of micelles with cypate-diamine crosslinkers.[147] Through optimizing the stoichiometry of cypate-diamine *vs.* aldehyde reactive moieties, NIR nanoparticulates could achieve nine-fold increase of brightness over small molecule cypate fluorophore, while maintaining comparable quantum yield. Polymer nanostructures crosslinked with fluorophore-containing crosslinkers also provided profound and beneficial "feedbacks" to the photophysical properties of fluorescent probes, as evidenced by Wooley, Dorshow, Neumann, and coworkers.[148-150] The covalent incorporations of pyrazine, a pH-insensitive fluorophore, into nanostructures with different chemical compositions, sizes, and morphologies through crosslinking chemistry produced notably pH-driven high *vs.* low fluorescence outputs or ratiometric dual-emissions.

Structural pH-responsivity can also be introduced to nanoparticles through functional shell-crosslinking of micelles with acetal-based hydrolytically-labile crosslinkers.[151] The chromophore acetals were "inert" at physiological pH, which enabled sufficient integrities to SCKs and the chromophores. Upon exposure to cancer cell lysosomal pH, rapid hydrolysis of acetals occurred and released the chromophore aldehydes. Cui and coworkers developed oligopeptide-based enzymatically-degradable crosslinker and demonstrated the prompt disassembly of crosslinked nanostructures after selective cleavage of the GPQGIAGQ or IPVSLRSG sequences on crosslinkers by matrix metalloproteases-2 (MMP-2).[152]

Nanocages—Crosslinking has also been an efficient strategy for stabilizing nanocages and drug crystals.[96-97,153-154] For instance, Leroux and coworkers have crosslinked the stabilizer molecules on the surface of PTX nanocrystals to yield stable nanocages that retained the drug nanocrystals within the inner compartment.[97] The advantage of utilizing this technique is that it provides a great stability for the entrapped drug without covalent interactions, which ensures that the drug is maintained in an active form. Shell-crosslinking has also been utilized to transform shell-crosslinked nanoparticles or polymer brushes to nanocages *via* chemical degradation of the core domains,[154-157] with control over nanoparticle shape,[158] as well as size.[159-160] The water-filled core of nanocages can host large quantities or sizes of various drugs, such as proteins and nucleic acids. The shell can be crosslinked using diamine, dicarboxylate or disulfide crosslinkers, among other chemistries, depending on the pendant functionalities on the shell polymer chains, followed by chemical degradation of the core, for example, *via* ozonolysis of polyisoprene[154-157] or hydrolysis of polyester[161-162] to form the nanocages, of course, with proper optimization of the polymer chemistry and

reaction conditions.[155-156] Recently, an elegant synthesis of polyelectrolyte nanocages has been developed by Cheng and coworkers.[163] Different from the conventional excavation of the core domains of crosslinked nanoparticles, their "crystal-forming" mini-emulsion approach involved the facile construction of well-defined emulsion droplets comprised of crystalized *n*-docosane and adsorbed surfactant monolayer. Followed by polymerization and crosslinking of the acrylol groups located within the aqueous/organic interface, nanocages with monolayer-thick shells were obtained. They further advanced this droplet-first synthetic strategy to cationic amphiphilic PLA copolymers bearing pendent alkene functionalities and prepared novel cationic nanocages loaded with doxorubicin.[160] After rendering the nanocages with siRNA, it was demonstrated that the nanocages could be used for drug-gene co-delivery.

Factors to be considered in crosslinking—Intermediate stability to circumvent physiological barriers and at the same time be able to release the drug at the target sites is required and can be achieved with different methods, for instance, by crosslinking. Considering the approximate size of plasma proteins and constituents (~1-10 nm), it is desirable to maintain the spacing between PEG chains as small as possible to minimize the interactions between the plasma components and the core material. Crosslinking the corona by biodegradable crosslinkers is also important to retain the spacing and avoid the dissociation and segregation of the PEG chains. However, elimination of these entities and hindrance of the release of their cargoes should be considered, as the efficiency of crosslinking could be varied by several factors.[164] A balance between the appropriate degree of crosslinking that reduces toxicity and increases stability, but at the same time does not induce aggregation during the crosslinking or hinder *in vivo* clearance is critical.

6. Polymeric nanostructures for theranostic applications

6.1 Medical imaging

6.1.1 Unimodal medical imaging—There have been great efforts to improve medical imaging agents to enhance the significantly differing characteristics of high resolution and sensitivity during imaging and long-term shelf-life and high formulation stability of the agents during storage and utilization. However, there are few imaging agents that have been approved by the FDA over the past five years.[165-166] FDA-approved contrast agents and molecular imaging probes and contrast agents are listed in the Molecular Imaging and Contrast Agent Database (MICAD).[167] Among the few recent FDA-approved agents are ^{11}C-based PET imaging agent (Choline C-11) for prostate cancer detection, ^{18}F-based PET imaging agent (AMYVID™) for β-amyloid neuritic plaque detection, Gd^{3+}-based MRI agent (Gadavist®) for brain and spine imaging, ^{123}I-based SPECT agent (DaTscan™) for Parkinsonian syndromes evaluation, and iodinated CT agent (Scanlux). In this article, we will focus on newly-developed imaging agents with a main interest in polymeric nanostructures.

Polymeric imaging agents have contrast agents or tracers conjugated or chelated to the polymer structures and/or physically encapsulated in the polymeric matrix.[168] CT is one of the most popular imaging modalities in clinical settings. Nano-sized CT contrast agents have been developed by many research groups to increase the sensitivity of CT imaging.[169-170]

Among them are iodine-containing micelles,[171] dendrimeric imaging agents,[172] and nanoparticle- or polymer-based contrast agents comprised of gold (Au),[11,173] gadolinium (Gd),[174] ytterbium (Yb),[175] tantalum (Ta),[176] or bismuth (Bi).[177-179] Iodinated oil, such as Lipiodol®, is approved by the FDA for clinical imaging, and iodinated oil-containing polymeric nanoparticles have been developed with methoxy-terminated poly(ethylene glycol)-*block*-poly(ε-caprolactone) (mPEG-*b*-PCL).[171,180] Iodinated mPEG-*b*-PCL nanocapsules showed enhancement in contrast, improved blood persistence and superior stability (up to 3 months in aqueous suspension). Poly(sebacic-*co*-ricinoleic acid) with iodinated oil was used for implant visualization with CT and showed a possibility to trace changes in biodegradable implants.[181]

Polymeric nanoparticles have been shown to improve MRI by delivering Gd or SPIO nanoparticles with limited success in targeting selective tissues, and also, in some cases, achieving therapeutic delivery (see section 6.3 for details of theranostic examples). For instance, the Zhang group developed a degradable Gd-based nanoparticle system, comprised of a mixture of multiblock polymers poly(lactic acid)-poly(ethylene glycol)-poly(L-lysine)-diethylenetriamine pentaacetic acid (PLA-PEG-PLL-DTPA) and the pH-sensitive poly(L-histidine)-poly(ethylene glycol)-biotin (PLHPEG-biotin) for MRI of hepatocellular carcinoma.[182] Gd ions were chelated to the DTPA groups for MRI and biotinylated vascular endothelial growth factor receptor (VEGFR) antibodies were linked to the PLHPEG-biotin through the avidin linkers for targeting. The polymeric nanoparticle exhibited 3.6 times longer T_1 relaxivity (17.3 mM^{-1} s^{-1}) than the commercial agent and also showed great potential as a theranostic agent (*vide infra*). Folate targeted SPIO-encapsulated PEG-*b*-PCL nanomicelles (Fa-PEG-PCL-SPIONs) exhibited unique spatial resolution for MRI of cancer cells in Bel 7402 tumor-bearing mice.[183] Recently, Boyer and co-workers reported a versatile and efficient *in situ* method to prepare complex assemblies of iron oxide nanoparticles encased within triblock copolymer chains comprised of poly-(oligoethylene glycol methacrylate)-*block*-(methacrylic acid)-*block*-polystyrene (POEGMA-*b*-PMAA-*b*-PST).[184] As the polymerization proceeded, the heterogeneous inorganic-organic polymeric nanoparticles assembled into different morphologies including spherical, rod-like and worm-like micelles, and vesicles, where vesicles showed the highest relaxivity, and, thus can be utilized as effective MRI agents.

Commonly-used isotopes for PET imaging have various half-lives from 110 min (^{18}F) to 4.18 d (^{124}I). The choice of radiotracer should be correlated to the circulation time of the nanomaterial.[185] Polymeric nanomaterials can be optimized for such demand by customizing their compositions and structures, including their internal volumes and external surface areas, with differentiation and independent chemical control. The surface also can be modified with biologically-active ligands for specific targeting.[22] In one of the most systematic early studies, Hawker, Welch and co-workers synthesized star[186] and comb[187] polymer nanostructures containing methoxy-terminated-PEG (mPEG) and 1,4,7,10-tetraazacyclododecanetetraacetic acid (DOTA) labeled with ^{64}Cu acetate, and demonstrated that their chemistries allowed for tunability of their blood circulation lifetimes. For instance by using 5.0 kDa, 2.0 kDa, and 1.1 kDa mPEG chains, 31 ± 2% of the 5.0 kDa combs remained in blood circulation at 48 h post-injection, which was *ca*. 10-fold higher than for

the 1.1 kDa mPEG comb, with the 2.0 kDa comb exhibiting intermediate biodistribution behavior. In contrast, the small molecule DOTA-^{64}Cu complex cleared renally within minutes. The comb having 5 kDa mPEG chains was further conjugated with C-type atrial natriuretic factor (CANF) peptides and used for PET detection of upregulated natriuretic peptide clearance receptor (NPR-C) associated with atherosclerotic-like lesions in an animal model.[52] The nanoparticles have demonstrated longer blood circulation time, higher standard uptake value (SUV), and higher specificity in PET imaging compared to CANF alone. Because of the simplicity of the labeling strategy by chelation in a final step after nanoparticle production, there have been several polymer-based nanoparticle scaffolds to which ^{64}Cu has been chelated, including SCKs constructed from DOTA-lysine pre-grafted PAA-*b*-PS precursors,[101] 1,4,7,10-tetraazacyclododecane-1,4,7-triacetic acid (DO3A) functionalized dextran-coated manganese doped silicon (Si_{Mn}) QDs,[188] polymeric micelles assembled from 1,4,8,11-tetraazabicyclo[6.6.2]hexadecane (CB-TE2A) conjugated triblock copolymer,[189] and polymer nanoparticle based on elastin-like polypeptides.[19] Of great importance to the translation of nanotechnology to clinical medicine, the CANF-comb polymer nanoparticles represent one of the few examples of nanomaterials that have entered human clinical trials.

^{18}F-FDG is the most commonly used PET tracer in cardiovascular imaging, but it can accumulate in any cells that metabolize glucose and cause high background signal. To overcome the limitation, novel PET tracers have been developed to track precursors to plaque rupture and its clinical sequelae.[190] These tracers include ^{68}Ga-[1,4,7,10-tetraazacyclododecane-*N*,*N*′,*N*″,*N*‴;- tetraacetic acid]-$_{D}$-Phe^{1},Tyr^{3}-octreotate (DOTATATE), ^{18}F-fluoromethylcholine (FMCH), and ^{11}C-PK11195 for macrophages, ^{18}F-fluoromisonidazole (FMISO) for hypoxia, ^{68}Ga-1,4,7-triazacyclononane-1,4,7-triacetic acid-Arg–Gly–Asp (NOTA-GDD) for neoangiogenesis, and ^{18}F-NaF for microcalcification detections (Figure 12). Future directions for nanoscopic imaging agents may take advantage of these small molecule developments, however, challenges are likely to result due to the covalent ^{18}F chemistry and its short half-life. A couple of initial approaches have combined the rapid, near quantitative coupling of “click” chemistry[191-192] or oxime chemistry[193] with ^{18}F or ^{64}Cu labeling of nanostructures to achieve radiolabeling yields with high efficiency. Meanwhile, the recently-developed fluorination toolboxes in organic chemistry[194-195] can also be adapted as additional synthetic pathways to effectively construct the C-^{18}F bonds within 30 min.

6.1.2 Multimodal medical imaging—Each imaging method has inherent limitations, therefore, complementary information from multimodal imaging can provide more accurate information and, as a result, avoid false diagnosis.[5] Polymeric nanoparticles have the ability to carry several different types of imaging agents as cargoes or *via* conjugation to the polymer structure.[168] Ligand or peptide modification to the polymeric structure also allows targeted delivery of imaging agents to the site of interest.[6] There have been numerous studies to develop polymeric nanoparticles as contrast agents for multimodal medical imaging.[22] In this section, combinations of imaging modalities are addressed, each with a focus on recent progress in developing polymeric nanoparticles as multimodal imaging

tracers. Table 3 summarizes recently developed multimodal imaging agents based on polymeric nanoparticles.

Fluorescence optical imaging has high sensitivity and has great advantage of producing multi-channel data from a single imaging step, a feature that is not available from other imaging modalities. Florescence imaging is known for low penetration depth and low resolution, which can be resolved by dual imaging with MRI or CT. Furthermore, lack of functional information from optical imaging can be compensated by PET imaging. Polymeric nanoparticles have been reported as platforms for many MR/optical imaging probes due to versatility of surface modification and ability to accommodate cargoes of different sizes and structures. Fitzgerald and coworkers reported a MRI/optical probe made from poly(glycidyl methacrylate) (PGMA) with Rhodamine B conjugation as a fluorophore and SPIO nanoparticles as a MRI contrast agent.[201] The nanostructures were coated with polyethyleneimine (PEI) and used to visualize optic nerve or whole eye with fluorescence analysis and MRI. Another MRI/optical probe reported by other researchers was made from poly(lactic acid)-D-α-tocopheryl poly(ethylene glycol)$_{1000}$ succinate (PLA-TPGS), which encapsulated quantum dots (QDs) for fluorescence imaging and SPIO nanoparticles for MRI.[203] PLA-TPGS nanostructure with QDs and SPIO nanoparticles improved biocompatibility and increased blood circulation time for controlled delivery of imaging agents to a tumor site by passive targeting effects. MRI/fluorescence images showed that nanoparticles were mainly found in tumor areas. Both the PGMA-PEI and PLA-TPGS probes were also proposed for therapeutic applications, which would be useful for imaging and therapeutic applications, and also for trafficking of nanoparticles *in vivo*.

Researchers from Weissleder and Nahrendorf groups accomplished numerous research studies for development of nanomaterials for management of cardiovascular diseases. In earlier work, they have used ^{18}F-FDG for PET imaging of macrophages on atherosclerotic sites. However, specificity of ^{18}F-FDG was questionable because cells with increased glucose uptake were also recognized. In a recent publication, they reported a specificity-enhanced PET/optical imaging agent, ^{89}Zr-dextran nanoparticle (^{89}Zr-DNP), which is biocompatible and biodegradable, therefore, being a suitable material for clinical translation. Dextran was crosslinked by epichlorohydrin and partially aminated with ethylenediamine, and then modified with *p*-isothiocyanatobenzyl desferoxamine (SCN-Bz-Df) and the *N*-hydroxysuccinimidyl ester of the NIR fluorochrome VivoTag 680 (VT680), followed by complexing ^{89}Zr to DNP to form ^{89}Zr-DNP. Flow cytometry results from the VT680 signal showed that DNP uptake was dominated by monocyte and macrophages (76.7 %), while lower signal was detected from other leukocytes.[199] Along with anatomical guide from MRI, the *in vivo* PET signal from ^{18}F-FDG was 30% higher in atherosclerotic plaques of ApoE$^{-/-}$ mice than wild-type controls. When the animal was treated with siRNA silencing C-C chemokine receptor type 2 (CCR2), which plays a significant role in recruiting monocytes to inflammation sites,[210] the PET signal was significantly decreased and the inflammation was reduced in plaque areas. The results showed that the ^{89}Zr-DNP with fluorophore conjugation is a non-invasive and specific agent for PET/optical imaging of inflammation, and therefore, could be applied to clinical diagnosis of inflammatory diseases.

Thurecht and coworkers developed a multimodal imaging agent with hyperbranched polymer (HBP) nanoparticles made from poly(ethylene glycol) methyl ether methacrylate (PEGMA), trifluoroethyl acrylate (FEA), and ethylene glycol dimethacrylate (EDGMA), with structure- and size-control by reversible addition/fragmentation chain-transfer (RAFT) polymerization. For MRI/optical application, the polymeric nanoparticle was labeled with ^{19}F for MRI and Rhodamine B or NIR797, which enabled multispectral fluorescence imaging (Figure 13).[202] The HBP was also conjugated with folate for targeted delivery to tumor sites and, thus, can be utilized for targeted therapeutic applications. High resolution MRI imaging and optical imaging allowed estimation of the tumor mass across various size scales *in vivo*, from millimeters to tens of micrometers. ^{19}F probes can eliminate background issues in biological imaging because there is minimal endogenous fluorine in the body and, this work is considered as the first demonstration of a polymeric agent in tumor detection by ^{19}F-based MRI. For PET/optical application, ^{64}Cu was added to the HBP nanoparticle as a PET probe and Alexa Fluor-647 or NIR-750 near IR dyes as fluorescence probes.[200] *In vivo* PET/CT/optical images showed that the ^{64}Cu-labeled polymer mainly localized to the tumor site after 24 h, presumably, *via* the EPR effect.

Most imaging agents carry heavy-metal ions, but, recently, a new class of polymeric and entirely organic imaging agent was reported by Johnson and co-workers.[211] They prepared redox-responsive organic radical contrast agents (ORCAFluors) from spirocyclohexyl nitroxide and Cy5.5-conjugated macromolecules, and successfully demonstrated *in vivo* MRI and fluorescence imaging. When the ORCAFluor was excited at 640 nm, nitroxide radical was generated and quenched the fluorescence while enhancing the MRI signal. On the other hand, the same ORCAFluor excitation in the presence of ascorbate or ascorbate/glutathione led to reduction of nitroxide, and, thus resulted in enhancement of fluorescence intensity by 2-3.5-fold and deactivation of the MRI functionality. This unique behavior of the ORCAFluor enabled targeted imaging in mice with high correlation of MRI contrast and fluorescence intensity to the ascorbate content in tissues (Figure 14).

Ultrasound imaging is a non-invasive imaging modality widely used in clinical settings for prenatal check, echocardiography and cancer diagnosis. Conventional ultrasound imaging uses acoustic waves of high frequency (2-20 MHz), which penetrate much deeper into tissues and organs than photons, and have lower scattering in imaging *in vivo*. Ultrasound imaging does not require a contrast agent, but microbubbles or nanobubbles filled with gas have been used to improve specificity and image contrast.[212-213] Moreover, development of nanostructures for photoacoustic imaging agents enabled dual imaging with ultrasound, such as optical/ultrasound and MR/ultrasound imaging.[205,214] Miki and Ohe groups reported on the synthesis of amphiphilic hyaluronic acid (HA) derivatives that is conjugated with high dose of indocyanine green (ICG) dye derivatives and hydrophilic PEG for high-contrast optical tumor imaging *in vivo*.[204] The HA derivatives accumulated in tumor site after intravenous injection were irradiated with near-IR laser, which generated intense fluorescence signal and enhanced photoacoustic image. Furthermore, photoacoustic imaging agents are highly feasible to be used for image-guided therapy, such as photothermal therapy, and controlled drug release pplications.[215-216]

Due to the flexible structure of polymeric nanostructures, many research groups have utilized polymeric nanostructures for multimodal medical imaging beyond dual imaging. In 2008, Weissleder and coworkers reported a multimodal imaging agent for medical applications. They used dextranated and diethylene triamine pentaacetic acid (DTPA)-modified magnetofluorescent nanoparticles with ^{64}Cu for PET, iron oxide core for MR, and Vivotag-680 (VT680) for optical imaging.[206] The multimodal capability of the ^{64}Cu-trireporter nanoparticle (^{64}Cu-TNP) facilitated *in vivo* visualization of atherosclerotic lesions in the aortic root of an animal model at cellular and anatomical levels. Some examples of polymeric structures that were used for trimodal imaging are listed in Table 3 (*vide supra*).

6.2 Therapy (cardiovascular, cancer and infectious diseases)

6.2.1 Cardiovascular diseases—Polymeric nanoparticles with specific biomarkers have been highly investigated in medical imaging for diagnosis and treatment of cardiovascular diseases, such as, atherosclerosis, hypertension, and coronary artery diseases.[199,206,217-221] Polymeric nanoparticles could offer better treatment for the blood vessel narrowing and for cell therapy, and provide suitable materials for stent and stent coating materials. Peptide-based therapy is one of the frequently applied methods in treating diabetes, cancer, metabolic, cardiovascular, and infectious diseases, but it has suffered from rapid clearance or degradation of the peptides *in vivo*. Polymer-conjugated peptides, on the other hand, prolong the circulation time of peptide drugs and increase their bioactivities.[222] As one example, researchers from the Langer, Tabas, and Farokhzad laboratories developed a core-shell nanoparticle to deliver the anti-inflammatory peptide Ac2-26, an annexcin A1/lipocortin 1-mimetic peptide, encapsulated in the biodegradable diblock copolymer PEG-*b*-PLGA that was conjugated with peptides for targeting collagen IV (Col IV), which comprises 50% of vascular basement membrane (Figure 15). In their previous studies, Col IV-targeting peptide conjugated-polymeric nanoparticles encapsulated with paclitaxel reduced the thickness of neointima to 50%, compared to a carotid injury model control group.[223-225] Ac2-26 peptide delivery using collage IV-targeted nanoparticles showed 30% higher effect in blocking tissue damage with much lower dosage (1μg *per* mouse) than free peptide.[226] The results showed that the peptide treatment using polymeric nanostructures and specific targeting have potential for treatment of inflammation-involved diseases like atherosclerosis.

Current treatment of coronary artery diseases are conservative management with medical therapies and invasive management with mechanical revascularization by percutaneous coronary interventions (PCI) or coronary artery bypass graft (CABG) surgeries. One major concern in vascular surgeries is injury to the vascular wall that leads to inflammation and delayed recovery of the vessel, which could induce late stent thrombosis and significant clinical complications.[217] Therapies based on nanotechnology have contributed in developing biocomparable materials for stents, polymeric nanofibers as a stent surface coating substances, and drug eluting stents (DES).[227-230] The first generation of DES effectively reduced in-stent restenosis, but profoundly delayed healing. Oh and Lee reported the preparation of nanofibers as a drug (β-estradiol) eluting coating on a stent. They used Eudragit S-100 (ES) as a nanoparticle (NP) base, and the mixtures of hexafluoro-2-propanol (HFIP), PLGA and PLA as a nanofiber base at tunable ratios.[229] The β-estradiol is known to

suppress activity of reactive oxygen species (ROS), which induces procoagulation and apoptosis of endothelial cells, but clinical trials showed that the β-estradiol did not exhibit sufficient activity, even though the drug effect had been observed in cell studies. Enhanced drug effect was obtained by delivering the drug in nanofiber coating on a stent due to maintaining biological effect of β-estradiol. The β-estradiol was dissolved in the nanoparticle solution and the nanofibers were coated onto the stent *via* electrospinning. The maximum loading of β-estradiol was obtained at a 4:1 ratio of PLGA and PLA, and the drug eluting nanofiber coating provided high coating stability and prevented stent-induced restenosis.

There have been debates over either using biodegradable polymer drug eluting stents (BP-DES) that is lower in long-term polymer toxicity, or durable polymer drug eluting stents (DP-DES), which last longer and has higher stability on stent surface. Most of BP-DES were based on PLA (BioMatrix Flex™, Elixir DESyne™, Nobori™) or PLGA (CoStar™, Nevo™), while DP-DES polymers include poly(*n*-butyl methacrylate) PBMA/poly(ethylene-*co*-vinyl acetate) (PEVA) (Cypher™) and poly (vinylidene fluoride-*co*-hexafluoropropylene) (PVDF-HFP) (PREMIER™, XIENCE PRIME™). According to a recent report based on 20,005 patients, BD-DES significantly lowered later lumen loss and late stent thrombosis.[231] Current on-going clinical trials for DES include physical improvement of stent structures, comparing various drug elusions, clinical evaluation of developed polymers for DES, but few of them are focused on novel polymer structures.[232]

Polymeric nanoparticles were also exploited for cell therapy and one of the applications used Tetronic-tyramine (Tet-TA)-RGD hydrogel embedded with C2C12 myoblast cells, which were transfected with vascular endothelial growth factor (VEGF) plasmids using poly(β-amino ester) nanoparticles. The genetically engineered cell sheet was transplanted into a hind limb ischemic mouse and promoted the formation of capillaries and arterioles in ischemic muscles, which is promising for effective treatment of peripheral arterial diseases with improved angiogenesis after transimplantation.[233] Currently, there are several on-going clinical trials of drug eluting stent based on polymeric nanostructures targeted for Coronary Artery Disease.[232] Although there have been numerous polymeric structures developed for therapeutic applications, there is still demand for developing noble polymeric platform and further optimization for clinical applications.

6.2.2 Cancer—Although numerous nanoparticle-based formulations for treatment of cancer have been developed and showed greater efficacy *in vitro* and *in vivo*, translation of those promising pre-clinical results to successful clinical trials has been challenging.[234] Only few nanoparticulate systems have been approved for clinical usage [*e.g.* Abraxane®, DaunoXome®, DepoCyt®, Doxil®/Caelyx®/Myocet®, Genexol-PM®, Lipo-Dox®, Marqibo®, Mepact®, Oncaspar®, and Zinostatin stimalamer®] and few additional candidates are undergoing clinical trials [*e.g.* BIND-014 (Phase 2), NC-6004 (Phase 1/2), NK012 (Phase 2), NK105 (Phase 3), CT-2106 (Phase 2), CRLX101 (Phase 2), PK1 (Phase 2), *etc.*].[71,235-236] Clinical responses to treatments have mostly resulted in temporary remission and have eventuated in recurrence and disease progression.[54] There is a thorough review on details of nanomedicines in cancer clinical trials and treatments.[236]

Intravenous injection is the most common administration method for cancer nanomedicines to increase delivery of drug carriers to tumor sites *via* the EPR effect. However, entry into the vasculature also has the complications of allowing for systemic access, and, thus further improvement on delivery efficiency should consider routes of administration that offer more direct and confined biodistribution. Local drug delivery methods can be considered for specific types of cancer, which are located in readily-accessible sites, such as the skin, lung, bladder, *etc*.[37] For example, inhalation treatment may be one option for the treatment of lung cancer, since it can improve biodistribution of nanostructures and their retention in the lungs compared to intravenous administrations.[237-238] The design and development of well-defined polymer-based nanodelivery systems, with control over their composition, structure and morphology, is expected to provide for ultra-high drug loading within intact nanoparticles, followed by sustained release, facilitated by optimized biodistribution and polymer degradation, and timed to the rate of disease progression.[140]

High loading capacity is a desirable trait for any drug carriers to maximize the amount of delivered drug at the target site, while minimizing the burden of clearance of the drug carrier. From a chemical perspective, reducing the volume of carrier required is analogous to atom economy, a term used in synthetic methodology, whereby waste and cost are minimized. There are varying degrees of affinity of drug guest molecules to the nanoscopic host system, with two extreme cases of loading methods: physical encapsulation and covalent conjugation. Physical encapsulation is straightforward and the most common method to load drugs in nanocarriers. However, there are intrinsic limitations, including relatively low loading efficiency, premature diffusion-based release of drugs, difficulty of multi-drug loading, *etc*. Covalent conjugation of drug molecules to the polymer nanoparticle components could avoid some of these limitations. However, conjugation of drug molecules and/or multiple numbers and types of drugs can complicate the nanoparticle assembly process, can limit the ability to cleave the covalent linkage, and once the drug-polymer particle covalent bond is cleaved, the drug molecule initially exists as a physically-encapsulated species (unless it had been conjugated onto the particle surface), which then undergoes diffusion-based release. In addition, stimuli-responsive cleavage of conjugated drugs could minimize release of drug at non-target sites to reduce side effects. With either the physical encapsulation or covalent conjugation strategy, there are additional influences from degradation of the polymer backbones, which can further accelerate the rate of drug release. Proper chemistries need to be selected to prevent a decrease of therapeutic efficacy of conjugated drugs and the unexpected toxicity of additional linker moieties and/or contaminants, such as metal catalysts. A significant complication is how to translate detailed degradation studies conducted *in vitro* (where differentiation of conjugated *vs*. encapsulated *vs*. active drugs and the state of nanoparticle disassembly and polymer degradation can be made) to accurate *in vivo* determination of the release of free drug, its pharmacokinetics and the biological clearance of the nanoparticle and polymer components.

The micelles of PEG-*b*-(PPE-*g*-PTX) drug conjugates had the highest reported PTX loading capacity. The conjugates were developed by organocatalytic ring-opening polymerization (ROP) of propargyl-functional cyclic phosphotriester monomer and consecutive click reaction with PTX prodrug.[239] The high drug loading was attributed to the high water

solubility of the polyphosphoester backbone to which PTX was conjugated. Although the initial system involved conjugation of PTX to the polymer backbone *via* a relatively-stable ester linkage,[239] accelerated hydrolytic degradability of the polyphosphoester backbones under acidic conditions was accomplished by incorporation of a β-thiopropionate functionality,[240] and is a promising feature of this system for selective release of payloads in tumor acidic microenvironments.

Cisplatin and cisplatin prodrugs are broad-spectrum chemotherapeutics that have been loaded into polymeric nanoparticles, in attempts at avoiding systemic delivery of these relatively-hydrophilic small molecule drug complexes. Lippard, Langer, Farokhzad, and coworkers have actively pursued improved delivery methods using polymeric nanoparticles.[241-244] Recently, they have reported mitaplatin-loaded PEG-*b*-PLGA nanoparticles, stabilized with poly(vinyl alcohol) (PVA), using a double emulsion method.[245] Mitaplatin is a water-soluble Pt(IV) prodrug, which releases two dichloroacetate (DCA) ligands upon intracellular reduction.[246] Since DCA is a mitochondria targeting compound that has potential as a cancer therapeutic,[247] encapsulation of mitaplatin is equivalent to the dual loading of cisplatin and DCA for combinational therapy. The resulting nanoparticles showed prolonged circulation times, reduced accumulation of Pt in the kidneys, and long-term efficacy by controlled drug release *in vivo*. In addition, the hydrophobic cisplatin prodrug, Platin-M, which has mitochondrial targeting ligand, triphenylphosphonium (TPP) cation, was synthesized by strain-promoted alkyne-azide cycloaddition (SPAAC) between azide-functional Pt(IV) prodrug and dibenzocyclooctyne (DBCO)-TPP conjugate. Platin-M-loaded polymeric nanoparticles of TPP-PEG-*b*-PLGA were prepared to damage mitochondrial DNA and, thereby, overcome chemoresistance against cisplatin therapy (Figure 16).[248]

Cationic polymers have been also utilized for electrostatic complexation of negatively-charged therapeutic nucleic acids that can be utilized for cancer therapy *via*, for example, knocking down specific oncogenes or expressing therapeutic proteins. Anderson, Langer and coworkers developed multilamellar vesicles prepared from lipid (C_{13})-conjugated low-molecular weight PEI_{600} (lipid : PEI = 14 : 1), and C14-PEG2000 for efficient delivery of multiple siRNAs to endothelial cells.[249] Although it is unclear how the nanoparticle promotes delivery of siRNAs to endothelial cells without considerable gene silencing in hepatocytes, immune cells, and pulmonary cells, resulting nanoparticles concurrently delivered multiple siRNAs and enabled multi-endothelial gene silencing. In addition, they showed the most long-lasting reduction of target gene expression in various mouse models.

However, the potential toxicity of cationic polymers has led to the exploration of safer delivery vehicles. For instance, DeSimone *et al*. applied their particle replication in non-wetting templates (PRINT®) technology to physically entrap siRNA within neutral PLGA nanoparticles with high loading efficiency, without the need to form potentially toxic polyplexes.[250] The resulting nanoparticles showed luciferase gene knockdown transfection efficiency *in vitro* as a model system for siRNA therapy of prostate cancer. As the PRINT technology allows for the preparation of nanoparticles with precise size, shape, and composition,[251] PRINT nanoparticles could enable fundamental studies on nanocarrier design factors, such as size and shape on various biological events.[252-253] For example, it

was found that particle shapes of cylinder or rod gave efficient cellular internalization, and the rate was faster as the aspect ratio was increased.[254] In addition, when two cylindrical nanoparticles (diameter = 80 nm, height = 320 nm, aspect ratio = 4 *vs*. diameter = 200 nm, height = 200 nm, aspect ratio = 1) were compared, the nanoparticle with smaller size and higher aspect ratio exhibited lower clearance by the mononuclear phagocyte system (MPS).[255]

A drug cocktail, a combination of drugs with different anticancer mechanisms, has the potential to overcome the genetic complexity and heterogeneity of cancer and to overcome drug resistance in cancer therapy, compared to individual-drug therapy.[256-264] However, co-encapsulation of multiple drugs into single polymeric nanoparticles is often challenging when drugs have different physicochemical properties, which lead to differential degrees of favorable interactions with the polymer matrix. In addition, the concomitant administration of more than one drug using a single nanoparticle structure can be either synergistic or antagonistic and the dose ratio is one of the critical factors to determine the synergistic combinations.[265-267]

A clever controlled loading and release strategy was recently developed for multiple anti-cancer drugs incorporated within a single type of brush-arm star polymer (BASP) nanoparticle.[268] Simultaneous delivery of camptothecin, doxorubicin, and cisplatin was expected to achieve maximum therapeutic effect at their optimal doses without increasing toxicity. Johnson and coworkers synthesized the BASPs by sequentially “grafting-through” a mixture of drug-conjugated macromonomers and then a drug-based crosslinker through ring-opening metathesis polymerizations (ROMP) (Figure 17). For the two drug-conjugated macromonomers, camptothecin or doxorubicin was incorporated through ester or *o*-nitrobenzyl linkages, respectively, and the crosslinker was based upon cisplatin-type Pt-carboxylate coordination, each of which was designed to release the drug molecules by orthogonal stimuli, including, pH, light, and reduction, respectively. This synthetic approach allowed a single nanoparticle to carry precise molar ratios of multiple drugs *via* simply modifying the feed ratios of macromonomers and crosslinker. The triple-drug-loaded nanoparticle system showed better *in vitro* cytotoxicity against OVCAR3 human ovarian cancer cells than did the mono- and double-drug-loaded systems. This elegant design of polymeric nanoparticle platform, together with the modulated synthetic approach, provided precise tunability of multiple drug loading and release and facilitated the development of nanoparticle-based combinational cancer therapies that can be finely-optimized for specific cancer types.

Multi-compartment polymeric nanostructures can be prepared by self-assembly or hierarchical assembly of multiple components to increase structural complexity with unprecedented properties.[269-270] Multiple sequestered environments within the unique morphologies allow for loading of multiple incompatible therapeutic agents selectively within discrete compartments, which has the potential to solve challenges in cancer therapy. For example, the simultaneous delivery of nucleic acids and photosensitizers realized successful application of photochemical internalization (PCI) *in vivo*.[271] PCI is a promising concept to promote delivery of nucleic acids into the cytoplasm for gene transduction *via* photochemical disruption of the endo-/lysosomal membrane. The probable inactivation of

nucleic acids by reactive oxygen species (ROS), generated by photosensitizers, requires compartmentalization of the payloads in the nanocarrier. Nishiyama, Kataoka and coworkers reported the seminal *in vivo* PCI-mediated gene transfection by systemically-administered light-responsive multi-compartment micelles.[271] They designed and prepared multi-compartmentalized nanostructures, which were comprised of an outer hydrophilic PEG shell, a photosensitizer-loaded intermediate compartment, and a plasmid DNA (pDNA)-encapsulated polyplex core within a single nanostructure. Initial polyplex formation between pDNA and PEG-poly[*N*-[*N*-(2-aminoethyl)-2-aminoethyl]aspartamide]-poly(L-lysine) [PEG-*b*-PAsp(DET)-*b*-PLys] was assumed to favor electrostatic interactions predominantly with the poly($_{L}$-lysine) terminal chain segments, and was followed by incorporation of a carboxylate-terminated dendrimeric phthalocyanine-based photosensitizer (Figure 18). Electrostatic interactions between the anionic carboxylates on the dendrimeric photosensitizer and the cationic PAsp(DET) middle block segment granted the formation of stable ternary photosensitizer-pDNA-polyplex nanostructures (DPc loaded ternary polyplex micelles) under physiological conditions. Translocation of photosensitizers from the nanocarrier to the endo-/lysosomal membrane were promoted by protonation of the carboxylates under the relatively acidic endo-/lysosomal environment, which then facilitated light-responsive disruption of the endo-/lysosomal membranes and escape of the polyplexes to deliver pDNA into the nucleus for gene expression. It is unclear what was the mechanism for the release of the pDNA, however, the nanocarriers exhibited >100-fold enhanced gene transfection efficiency in HeLa cells *in vitro* after photoirradiation than for the non-photosensitizer-loaded polyplex analogs. In addition, light-induced *in vivo* transfection of Venus (yellow fluorescent protein)-encoding reporter gene into subcutaneous HeLa and HCT 116 tumor models showed higher fluorescence by Venus expression compared to the non-photoirradiated tumors, ~4.4-fold and ~6.0-fold, respectively.

Another interesting multi-compartment nanostructure was reported for photodynamic therapy (PDT).[272] Photosensitizer-encapsulated micelles were prepared by self-assembly of polybutadiene-*b*-poly(1-methyl-2-vinyl pyridinium methyl sulfate)-*b*-poly(methacrylic acid) (poly(BVqMAA)) triblock terpolymers and a porphyrazine derivative. The negatively-charged PMAA corona of the resulting micelles was functionalized with positively-charged PLL-*b*-PEG diblock copolymers *via* inter-polyelectrolyte complexation and the resulting multi-compartment nanostructures were further stabilized by amidation-based crosslinking (Figure 19). The degree of complexation could be controlled by changing the feed ratio of poly(BVqMAA) *vs*. PLL-*b*-PEG, and a bottlebrush-on-sphere morphology was observed at higher degrees of complexation. The surface charge of the micelles was dependent on the composition of the corona, which was closely related to their cellular uptake and PDT activity *in vitro* against A594 human lung adenocarcinoma cells, as well as blood circulation, tumor accumulation, and PDT activity *in vivo* against a subcutaneous A594 tumor model. These results suggest that the resulting micelles could be a versatile platform for various functional multi-compartment nanostructures by incorporation of other polymers containing positively-charged blocks. In this current study, only the hydrophobic core domain was utilized for packaging of photosensitizers to accomplish PDT, however, other hydrophobic drugs, or hydrophilic or amphiphilic charged or non-charged drugs have the potential to also be loaded within the core, shell or core-shell domains, respectively.

Furthermore, this initial system provides a foundation for development of the chemical compositions of the polymer frameworks, with particular need to translate the materials from non-degradable to biodegradable polymer building blocks.

One of major challenges in nanoparticle-based drug delivery is the incompatibility between prolonged blood circulation for enhanced EPR effects, which requires neutral or slightly negative surface charges, and efficient tumor cell uptake, in which positive surface charges are preferred. Two strategies, switch of surface charge and removal of stabilization layer, have been applied to address this issue. Example of the surface charge switching strategy was reported by Wang and coworkers.[273] They developed interesting polymeric nanostructures, which have the capability to adjust their surface charge to the surrounding pH conditions. Polymeric micelles were prepared by self-assembly of block copolymers comprised of a hydrophilic zwitterionic polyphosphoester block and a hydrophobic PCL segment [PCL-*b*-P(AEP-*g*-TMA/DMA)]. The zwitterionic surface enabled elongated circulation of the nanocarriers in blood. Once they reached tumor sites, however, cleavage of amide bonds between 2,3-dimethylmaleic anhydride (DMA or DMMA) and primary amine under acidic tumor extracellular environment, decreased the anionic character in the zwitterionic segments and resulted in positively-charged nanoparticles that could be internalized more easily into tumor cells (Figure 20). Doxorubicin-loaded into these nanoparticles inhibited growth of human breast cancer cell MDA-MB-231 xenografts in nude mice.

A stabilization layer removal strategy was also accomplished using similar chemistry by the same research group.[274] Positively-charged PEI/siRNA polyplexes were stabilized with PEG-based block copolymers, which had a negatively-charged polyphosphoester segment [mPEG-*b*-P(AEP-Cya-DMMA)], *via* electrostatic interactions. Exposed primary amine groups by deprotection of acid-responsive DMMA groups induced electrostatic repulsion between the PEG layer and polyplex, which led to the removal of PEG stabilization layer. Exposure of the positively-charged surface of the polyplexes promoted tumor cell uptake and RNAi efficiency to silence Polo-like kinase 1 (Plk1) expression in MDA-MB-231 xenograft tumor-bearing mice.

Torchilin and coworkers also devised another smart drug delivery system, which had a stabilization layer removing feature as well as active targeting with cell-penetrating peptide (CPP).[275] PEG_{2000} and PTX were connected by a matrix metalloproteinase 2 (MMP2)-cleavable peptide linkage. PEG_{2000}-PTX conjugate, TAT targeting peptide-PEG_{1000}-phosphoethanolamine (PE), and PEG_{1000}-PE were assembled into micelles (Figure 21). The resulting nanoparticles displayed improved tumor targeting by elongated blood circulation, conferred by longer PEG_{2000}. Once reaching the tumor microenvironment, longer PEG_{2000} chains were separated from the micelles *via* cleavage of the peptide linkages by extracellular MMP2, which led to release of PTX, and also cell internalization of micelles promoted by exposed TAT on the chain-end of shorter PEG_{1000}. This stimuli-responsive targeted drug delivery system has the additional attributes of preventing undesired drug leakage while possessing high drug loading capacity.

6.2.3 Infectious diseases—Nanoparticles have been utilized to improve delivery efficiency of antimicrobials to the site of infection, together with the use of auxiliary devices for localized delivery.[41,276-277] Nanoparticles could improve the stability and pharmacokinetics of the encapsulated antimicrobials, allow prolonged retention and sustained release of the drugs at the sites of infections, and overcome the drug resistance of the bacteria.[35,73,81,90,278-282] They can also overcome the challenges towards the treatment of multidrug-resistant bacteria in infected lungs (*e.g.* cystic fibrosis and tuberculosis).[283]

Cationic polymers are promising antimicrobials for multidrug resistant bacteria since they physically disrupt microbial membranes, which decrease the potential to develop antimicrobial resistance.[284-285] A seminal biodegradable antimicrobial polymeric nanostructure was cationic micelles self-assembled from amphiphilic triblock polycarbonates containing pendant quaternary ammonium moieties on the middle block (Figure 22).[286] The resulting micelles exhibited selective targeting and lysis of bacterial membranes to kill Gram-positive bacteria including methicillin-resistant *Staphylococcus aureus* (MRSA), as well as, fungi. The minimum inhibitory concentrations (MICs) of the cationic polymers were higher than their critical micelle concentrations, which indicated that micelle formation was crucial for the microbicidal function of these polymers by increasing local charge density and polymer mass on the surface of bacterial cells. In addition, more dynamic micelles from random copolycarbonates showed broader antimicrobial activity towards Gram-positive, as well as, Gram-negative bacteria.[287] Cationic polymers could also protect antibiotics by ionic complexation. Cationic cobaltocenium polymers were prepared to treat MRSA infection.[288] Ionic complexation between cationic metallopolymers and carboxylate in β–lactam antibiotics inhibited β–lactamase activity to protect β–lactam antibiotics from hydrolysis, which improved antimicrobial efficacy. In addition, these cationic polymers have capability to selectively lyse MRSA cells with low cytotoxicity towards red blood cells and splenocytes of the mice, both *in vitro* and *in vivo*. These polymeric scaffolds could provide potential treatment methods for multidrug-resistant bacteria, due to their synergistic effects. However, clinical applications of cationic polymers for delivery of antimicrobials might be limited, as they would have lower capability of mucus penetration in the case of inhalational administration, and non-selectivity and systemic toxicity after systemic administration, as compared to PEG-shielded neutral nanoparticles.

Nebulized nanoparticles have been utilized for the pulmonary delivery of broad-spectrum silver cation or silver carbene complexes (SCCs), which were loaded into the shell and/or the core of polymeric nanoparticles. The initial study was conducted using non-degradable SCKs prepared by self-assembly of PAA-*b*-PS and subsequent crosslinking. All silver antimicrobial-loaded nanoparticles provided a sustained delivery of silver species over at least 2-4 d, with superior survival advantages of the SCKs loaded with the SCCs in the core of the nanoparticles, when tested *in vivo* in a mouse model of *Pseudomonas aeruginosa* pneumonia.[289] Fully degradable polymeric nanoparticles were then developed and their antimicrobial activities were evaluated *in vitro* against *Staphylococcus aureus* and *Escherichia coli*.[290] Silver cation and SCCs were loaded into the self-assembled micelles of anionic PPE-*b*-PLLA, which was designed to load silver antimicrobials *via* not only

electrostatic interaction with carboxylates and/or coordination with 1,2-dithioethers within the hydrophilic corona, but also hydrophobic interaction with PLLA core. SCC-loaded polymeric micelles showed lower MICs than for the SCCs alone. Degradable PPE-based polymeric nanoparticles were also developed to carry silver cations using different loading mechanisms to modify release kinetics. Silver cations were loaded by coordination with pendant alkyne groups of PEBP-*b*-PBYP-*g*-PEG to form silver acetylides.[291] The resulting silver-loaded nanoparticles showed much slower release kinetics ($t_{1/2}$ = 28 h in nanopure water and 16 h in 10 mM phosphate buffer containing 10 mM NaCl) compared to the anionic PPE-*b*-PLLA systems (2.5–5.5 h in nanopure water) and exhibited antimicrobial activities against cystic fibrosis pathogens *in vitro*. These results suggest that the duration of drug release could be adjusted to the target disease *via* alteration of the chemistry employed for the drug-loading mechanism.

DNAs have also been delivered to the lung *via* inhalation of gene nanocarriers. Nanoparticles, based on PEG coating of either polyethylenimine (PEI) or poly-L-lysine (PLL), were developed for delivering plasmid DNA encoding for the cystic fibrosis transmembrane conductance regulator protein to the lung. Nanoparticles could efficiently penetrate human cystic fibrosis mucus *ex vivo*, and upon intranasal administration, they enhanced particle retention and gene expression in the mouse lungs and induced negligible toxicity and inflammation.[292] In another study, pH-sensitive PEG-*b*-poly-L-histidine-*b*-poly-L-lysine nanoparticles were used for delivery of plasmid DNA.[293] The formed nanoparticles were rod-like in shape. These nanoparticles could improve the *in vitro* and *in vivo* gene transfer to lung airways in BALB/c mice, by *ca.* 20-fold and 3-fold over PEG-*b*-poly-L-lysine/DNA nanoparticles, respectively, while maintaining a favorable toxicity profile. The enhanced efficacy might be due to the incorporated poly-L-histidine that increased the buffering capacity of the nanoparticles.

Intravenous injection is also a viable administration method for antimicrobial-loaded nanocarriers, since long-circulating nanoparticles could accumulate at the site of infection *via* enhanced vascular permeability caused by inflammation. In addition, acidic environments at the infection sites could be utilized as a stimulus for the development of smart nanoparticles. For example, a pH-responsive surface charge-switching drug delivery system was developed using PLGA-*b*-poly(L-histidine)-*b*-PEG-based nanoparticles.[294] After systemic administration and extravasation, protonation of imidazoles in the poly(L-histidine) segment could produce positively-charged nanoparticles at acidic infection sites, which could facilitate binding of nanoparticles to negatively-charged bacterial cell walls *via* electrostatic interactions. Even though *in vivo* studies were not presented, *in vitro* results showed promise, including the binding of nanoparticles to both Gram-positive and Gram-negative bacteria and maintaining the antimicrobial efficacy of the nanoparticles under acidic conditions.

An enzyme-sensitive polymeric nanoparticle was developed for on-demand delivery of antimicrobials to the site of bacterial infection. The star copolymer-based drug delivery system was prepared *via* the “arm-first” approach, ROP of difunctional cyclic phosphotriester crosslinker with monofunctional mPEG-*b*-PCL-OH macroinitiator.[295] The hydrophobic PCL intermediate layer minimized undesirable release of antibiotics from the

polyphosphoester core to reduce side effects. When the nanocarriers were incubated with lipase or lipase-secreting bacteria, degradation of the PCL protective layer facilitated release of the payload. Even more accelerated release could be achieved by the addition of phosphatase, or other bacterial secreting enzymes that degrade the polyphosphoester core. Furthermore, this nanostructure was internalized into infected cells to deliver antimicrobials, while many antibiotics showed poor cellular internalization. This stimuli-responsive drug delivery system can be a potential treatment option for a variety of infections caused by lipase-secreting bacteria. A similar system, polyphosphoester-based multifunctional nanogel, was also reported as a bacterial phosphatase- or phospholipase-responsive antimicrobial nanocarrier, which can release payloads by enzyme-catalyzed core degradation.[296]

6.3 Theranostic nanoparticles utilized for both imaging and therapy

Polymeric nanoparticles have been utilized for both therapy and imaging *via* various concepts and strategies.[297-303] In this section, after a brief overview of some terminologies and concepts that have been commonly utilized for theranostic applications, some of the recent and successful examples of multifunctional nanoparticles utilized for combinational delivery of various imaging agents, drugs, and nucleic acids, for treatment, diagnosis and monitoring of several diseases, will be highlighted.

Photodynamic theragnosis is a recent strategy that has demonstrated promising potential application in photodynamic therapy and diagnosis, for a wide variety of applications, in oncology, cardiovascular, dermatology and ophthalmic fields. The therapeutic part is based on utilizing a chemical photosensitizer (relatively non-toxic) for accumulation at the targeted tumor tissues. After accumulation, when irradiated with light at certain wavelengths, the chemical moiety generates cytotoxic compounds (*i.e.* reactive singlet oxygen or reactive oxygen species) that kill the tumor tissues *via* apoptosis or necrosis. The use of some photosensitizer, such as porphyrin derivatives, can also provide fluorescence that can be utilized for drug trafficking and for imaging applications. The use of nanomaterials to enhance the accumulation of these photosensitizers into tumor tissues could reduce the potential phototoxicity in other organs. Nanoparticles based on quenching/dequenching systems may also allow specific toxicity only in the targeted tumor tissues. This reversible system is “quenched” in normal tissues or during circulation in the blood, to avoid photo-induced toxicity or fluorescence. However, in response to various stimuli in the tumor tissues (*e.g.* acidic pH or presence of certain enzymes), dissociation of nanoparticles leads to a “dequenched” state and, upon light exposure, will allow specific therapeutic and imaging capabilities in the tumor tissues with high selectivity.[304-309] Photothermal and photodynamic therapy have been also combined into a single nanostructure platform of upconversion nanoparticles. Upconversion nanoparticles are a recent category of “smart nanomaterials” that contain rare-earth elements (*e.g.* lanthanide-doped nanocrystals) to overcome the problem of limited tissue penetration of UV and visible light wavelengths, which are required for activation of several photosensitizers. These materials, upon excitation by NIR light, emit high energy photons that can excite the photosensitizers. The NIR light has minimal absorption and fluorescence background in biological tissues and, thus, it is currently one of the most suitable modalities for optical imaging.

PEG-*b*-PCL-based biodegradable plasmonic gold nanovesicles were developed for photoacoustic (PA) imaging and photothermal therapy (Figure 23).[310] Gold nanoparticles were densely packed during the assembly *via* disulfide bonds available at the terminus of the copolymer, resulting in a strong plasmonic coupling between nanoparticles. NIR absorption allowed simultaneous thermal/PA imaging and enhanced PTT efficacy. In addition, the dissociated nanoparticles can be cleared after the completion of the treatment course. A new organic photothermal therapy agent based on a conductive polymer mixture with strong NIR absorbance, poly-(3,4-ethylenedioxythiophene):poly(4-styrenesulfonate), was also developed for *in vivo* PTT. The dye was coated by layers of charged polymers, and then grafted with branched PEG. High *in vivo* tumor uptake in a mouse tumor model under NIR light irradiation at a low laser power density was demonstrated.[311]

Magnetic polymer-modified gold nanorods were prepared by coating the gold nanorods with poly(*N*-isopropylacrylamide-*co*-methacrylic acid) polymer, followed by conjugation with magnetic nanoparticles, for application as dual MR and PA imaging contrast agents, and PTT (Figure 24). Localization and targeting of nanoparticles were achieved with the use of an external magnet. The nanoparticles significantly enhanced the NIR-laser-induced photothermal effect due to their increased thermal stability.[312]

Magnetic nanoparticles were coated with chitosan, and the chitosan was loaded with doxorubicin and verapamil, and then entrapped into PLGA nanoparticles *via* a double emulsion solvent evaporation technique.[313] After entrapment, it is expected that amounts of the two drugs will be dispersed in the PLGA, in addition to the chitosan. PVA was also used as an emulsifier to stabilize the nanoparticles. Finally, cRGD peptide targeting moieties were introduced through amide linkages. Irradiation with NIR laser triggered rapid drug release *in vitro*. In addition, preferential accumulation of the targeted nanoparticles in the tumor tissues has been demonstrated in mice under guidance of an external magnetic field, together with the capability of whole mouse optical imaging.

Tumor areas contain heterogeneous cell populations, which lower the efficiency of ligand-receptor targeting of tumor cells and result in drug-resistance. Research groups led by Hyeon and Na developed a pH-dependent MR imaging and PDT agent *via* self-assembly of extremely small iron oxide nanoparticles (ESIONs, ~3 nm) with PEG-*b*-poly(*β*-benzyl-L-aspartate) chlorin e6 (Ce6)-based polymers.[314] Ce6 is a commonly used natural photosensitizer originated from green plants, such as, chlorella. Additionally, three different functional groups, imidazole as a pH responsive moiety, catechol as a ligand for ESIONs, and 3-phenyl-1-propylamine as a hydrophobic group, were introduced to the polymer platform. Micellar structures of polymers disassembled in the tumor cells, which have lower pH (~ 5.5) than normal cells, after protonation of the imidazole groups onto the polymer, and, as a result, iron oxide particles and Ce6 were exposed and activated for MR imaging and PDT in the tumor cells. The pH-sensitive bimodal agent was able to detect small tumors (~3 mm in diameter) and exerted 2-fold higher targeted delivery to heterogeneous tumor cells implanted into a mouse, as compared to the pH-insensitive nanoparticles (prepared without the pH-sensitive functionalities) or photosensitizer alone, which offered an effective targeted cancer therapy without the complications (*i.e.* cost, scale up, immunogenicity, *etc*.) of decorating nanoparticles with surface moieties.

Research groups led by Li, Pan and Lam recently developed an "all-in-one" smart and versatile nanoporphyrin platform that is biocompatible and demonstrated high efficacy for multimodal imaging, photothermal/photodynamic therapies, and light-activated drug release in both an ovarian cancer xenograft model and a murine transgenic breast cancer model. The nanoparticle was composed of four pyropheophorbide-a (Por) molecules and four cholic acids (CA) attached to the PEG chain (PEG_{5k}-Por_4-CA_4) and nanoparticles of size ~21 ± 6 nm were formed *via* self-assembly (Figure 25).[208] The Por molecule enabled chelation of metal ions used in medical imaging, such as, Cu^{2+}, Pd^{2+}, Gd^{3+}, and Ga^{3+}, with capability of MRI and PET dual imaging *in vivo* by incorporating $Gd^{3+}$and $^{64}Cu^{2+}$. In the same study, the polymer structure was modified with cysteine (PEG_{5k}-Cys_4-Por_4-CA_4) to form disulfide-crosslinked nanoparticles (CNPs) to enhance the stability in the blood and to avoid premature release of loaded drug. The particle size of the CNPs were measured under destabilizing conditions with 50% (*v*/*v*) of human plasma and the particle size did not change up to 50 h, and, thus high stability is expected upon *in vivo* administration. The synthesis of porphyrin/CA nanoparticles was highly reproducible and scalable to kilogram levels at low cost without losing functionality. Hence, these nanoparticles might have great potential for clinical translation. Furthermore, activation of the nanoparticle requires a portable, single-wavelength NIR laser, while previously developed nanoparticles for photothermal/photodynamic therapies require multi-wavelength lasers.

Park and coworkers reported on the development of an optical/MRI multimodal transfection agent based on SPION and a rhodamine fluorophore, that could be utilized for tracing human mesenchymal stem cells in transplanted mice with optical and MR imaging (Figure 26).[315] SPION- and catechol-functionalized polypeptides were covalently conjugated with rhodamine-labeled PEI, which electrostatically binds to negatively-charged pDNA. The nanoparticles were successfully transfected into the stem cells, and the transfected cells were transplanted into mice and visualized with optical and MR imaging over 14 days.

Nanoparticles were developed for targeted (fragment of anti-amyloid antibody) treatment (immunosuppressant cyclophosphamide that can reduce cerebrovascular inflammation) and early detection (MRI) of cerebral amyloid angiopathy (CAA), that results from deposition of amyloid beta proteins within the walls of the cerebral vasculature, with possibility of inducing vascular inflammation and hemorrhagic strokes.[316] Cyclophosphamide (*i.e.* drug) was loaded into the polymeric nanocore made from Magnevist® (MRI contrast agent) conjugated chitosan, and the core was further modified with putrescine modified F(ab′)2 fragment of anti-amyloid antibody for selective delivery of the nanoparticles to the cerebrovascular amyloid. *In vitro* and *in vivo* data demonstrated the ability of the nanoparticles to provide contrast for MR imaging of CAA and to have better therapeutic efficacy than the cyclophosphamide alone.

A multifunctional pH-sensitive polymeric nanoparticle system was developed by self-assembly of PLA-PEG-PLL-diethylenetriamine pentaacetic acid and poly(L-histidine)-PEG-biotin, and the nanoparticles were loaded with sorafenib (anticancer drug for treatment of hepatocellular carcinoma), and, furthermore, gadolinium ions were chelated with the diethylenetriamine pentaacetic acid for MRI application (Figure 27). Biotinylated vascular endothelial growth factor receptor (VEGRR) antibodies were linked to the surface biotin

groups of the nanoparticles through avidin linkers to form the targeted pH-sensitive theranostic nanoparticles. *In vivo*, the nanoparticles have demonstrated higher antitumor effect in H22 tumor (VEGFR-overexpressing cell line) bearing mice compared to the solubilized sorafenib solution and better MRI than Magnevist®.[182]

Lee *et al*. have developed targeted polypeptide-based nanoparticles for targeted imaging and treatment of cancer.[317] The nanoparticles were constructed from antibody-conjugated poly(γ-glutamic acid)-*graft*-cetylester (γ-PGA-*g*-cetylester), and were loaded with paclitaxel, and pH-switchable fluorophores that were activated at the acidic pH of endosomes (Figure 28). Both hydrophobic paclitaxel and fluorophores were incorporated into the nanoparticles after modifying the poly(γ-glutamic acid) with hydrophobic moieties (~48.9% of the carboxylates were modified with cetylesters). Decoration of the nanoparticles with the anti-HER2 antibody (Herceptin) significantly enhanced the cytotoxic effect of the paclitaxel-loaded nanoparticles *in vitro* against SKBR3 cells, in addition to the demonstrated high target-to-background signal ratio in the images obtained for HeLa cells treated with the switchable fluorophore-loaded nanoparticles.

MRI-visible and T-cell-targeted polymeric nanoparticles were constructed from PEG-*g*-PEI that was functionalized with the CD3 single-chain antibody, and loaded with pDNA and SPION for delivery into primary T cells expressing CD3 receptors. In the heart transplanted rat model, nanoparticles were able to transfect T cells and detect the post-transplantation acute rejection with high efficiency (Figure 29). Upon intravenous injection of the nanoparticles, on the third day after transplantation, T-cell gathering was detected at the endocardium of the transplanted heart as hypo-intense areas on the MRI T_2*-weighted images. Interestingly, the use of nanoparticles loaded with diacylglycerol kinase-α gene (a regulator of immune function) suppressed the immune response in the allogeneic heart transplantation rat model, which could be monitored by MRI during the treatment course.[318]

Development of multifunctional nanostructures that can be tuned to co-deliver multiple drugs and diagnostic agents to diseased tissues is of great importance, and has been accomplished *via* several strategies, for instance, by combining several nanostructures into one template.[140,240,319-321] Hierarchically-assembled theranostic (HAT) nanostructures based on anionic shell crosslinked rod-like nanoparticles and cationic spherical SCKs have recently been developed by our group to deliver siRNA intracellularly, and to undergo radiolabeling.[319] In addition, paclitaxel, a hydrophobic anticancer drug, and siRNA have been successfully loaded into the cylindrical and spherical components of the hierarchical assemblies, respectively (Figure 30).[320] Cytotoxicity, immunotoxicity and intracellular delivery mechanisms of the HAT nanostructures and their individual components have been investigated by using several methods under different conditions, and in some cases, in the presence of chemical inhibitors to understand the intracellular trafficking pathway of the nanoparticles. Decoration of nanoparticles with F3-tumor homing peptide enhanced the selective cellular uptake of the spherical particles. On the contrary, the HAT nanoassemblies were found to “stick” to the cell membrane and “trigger” the release of spherical cSCKs templated onto their surfaces intracellularly, while the cylindrical part of the HAT nanostructures were remained near the cell membrane. Combinations of paclitaxel and cell-death siRNA (siRNA that induces cell death) into the HAT nanostructures resulted in greater

reduction in cell viability than siRNA complexed with Lipofectamine and the assemblies loaded with the individual drugs. In addition, a shape-dependent immunotoxicity was observed for both spherical and cylindrical nanoparticles, with the latter being highly immunotoxic, even at lower concentrations than HATs. Combinations of cylindrical and spherical nanoparticles of the opposite charges *via* controlling polymeric chemistry and supramolecular assembly significantly reduced the immunotoxicity of both individual polymer nanoparticles, while maintaining the ability of prolonged circulation of the elongated morphology, active targeting, and carrying both diagnostic and therapeutic agents, with tunable control over the ratio of incorporated drugs, and amount of spherical nanoparticles *per* cylinder.

7. Limitations, conclusions and perspectives

There are several limitations towards the development of efficient theranostic nanoparticles, including technical and biological limitations. Variability between batches from same or different laboratories is one of the major pharmaceutical limitations, because batch-to-batch variation is a barrier towards their clinical evaluation and development. An absence of unique or common standardized strategies, techniques and assays for evaluation and characterization of nanomaterials is another obstacle for selecting the most efficient product from a specific category of pharmaceutical preparations. Adhering to the current good manufacturing practices and regulations of FDA, and scale-up of the materials designed on small scale of milligrams are challenges towards clinical translation of nanomaterials. Biological barriers include the variability in response to same nanomaterials between different cell types or animal models. Instantaneous destabilization following *in vivo* administration of nanoparticles and premature release of the encapsulated cargoes preclude the nanoparticles from performing their tasks and reaching their target sites.

Numerous nanotherapeutics have been developed and demonstrated greater efficacy than either free drugs or commercially available alternatives, both *in vitro* and *in vivo*, however, translation of those promising pre-clinical results to successful clinical trials have not progressed as rapidly as expected.[234] Nanoparticles, when properly designed and optimized, have the ability to increase accumulation of various therapeutics and/or diagnostics into target tissues. However, unfortunately, the major part of the dose systemically administered ends up in non-targeted organs, and thus results in toxicity, lower therapeutic efficacy, and higher cost and dosage. Although improvements are often observed in comparison to free drugs, results remain inferior to the expected outcomes from the tailored properties of the injected nanomaterials. The efficacy of nanoparticles reaching the target site needs to be maximized. Improvement of drug loading efficiency and capacity can lead to increase in the amount of delivered drugs. In addition, clearance and/or degradation of the empty nanoparticles after releasing drugs is crucial, since the remaining nanoparticles may act as a physical barrier for newly administered drug carriers,[322-324] or may lead to long-term adverse effects. Intravenously-administered nanoparticles that extravasate into tumor tissues are often found near the cells adjacent to the vasculature,[323,325] for instance due to the physiological barriers of tumors, resulting in inconsistent distribution of drugs, which leads to poor therapeutic outcomes. Elevated interstitial fluid pressure (IFP) compared to surrounding tissues and dense tumor extracellular matrix (ECM)[326] impede delivery of

nanoparticles. Anticancer agents are required to be delivered deep into tumor tissues and away from the tumor vasculature in order to affect the entirety of the malignant cells, which are known to be dispersed around blood vessels (>100 μm away).[327] Thus, deep tumor penetration of nanocarriers is necessary to prevent development of drug resistance and regeneration of tumors after the treatment.[328-329] In order to accomplish improved tissue penetration, a variety of factors need to be considered including the nanoparticle size, shape, stiffness, architecture, *etc*.[327,330-332] There is evidence that smaller nanoparticles are preferable for tumor penetration and distribution.[332-338] Further challenging problems that need to be addressed are the tissue heterogeneity and dynamic nature of biological markers.[339]

The preference for using targeted over non-targeted nanomaterials remains controversial. Several reviews and perspectives raise awareness of the need to understand the limitations of nanoparticle approaches for targeted drug delivery to tumors.[324,340-343] Development of nanoparticle systems that can not only package but also release drugs exclusively to target sites is critical to reduce side effects. Ligand-receptor interactions have been shown to improve intratumoral distribution. Decorating the surface of nanomaterials has the potential to increase cellular uptake and selectivity of therapy, although cost, toxicity, immunogenicity and scalability are critical issues.[324,340-343] Nanoparticles that only release their contents at the targeted tissues under effect of internal or external stimuli might be more efficient than decorating the surface of nanomaterials with targeting ligands.

Toxicity and immunogenicity of nanomaterials and the drugs are extremely important and must be evaluated. Drugs/nanoparticles that do not induce cell or animal death are not necessarily safe, and various biomarkers should be measured to evaluate the ability of these materials to initiate inflammatory reactions.[81] Some types of nanoparticles and therapeutic agents have the ability of inducing several biochemical changes and hypersensitivity reactions at low doses after administration through what is so called “complement activation-related pseudoallergy”.[344] Long-term use and safety of nanomaterials are mainly correlated to the degradability of these materials and ability of the body to clear them shortly after performing their desired pharmacological effects. The challenges for nanostructure-based diagnostic and therapeutic clinical applications might be handled by iterative adjustment of synthetic design of nanostructures with rigorous biological studies to maximize the existing capabilities after understanding their limitations.[345]

There is an urgent need for the collaboration between scientists from different disciplines for development of nanopharmaceuticals viable for clinical use due to the several challenges related to the clinical applications, starting from the complexity of synthetic chemistry, to the formulation processes, to the harsh environment following *in vivo* administration into humans and the various biological barriers that have been discussed in this review.

Acknowledgements

We gratefully acknowledge financial support from the National Heart Lung and Blood Institute of the National Institutes of Health as a Program of Excellence in Nanotechnology (HHSN268201000046C) and the National Institute of Diabetes and Digestive and Kidney Diseases of the National Institutes of Health (R01-DK082546). The Welch Foundation is gratefully acknowledged for support through the W. T. Doherty-Welch Chair in Chemistry, Grant No. A-0001. Financial support from the Egyptian Ministry of Scientific Research – Science and Technology

Development Fund (Demand-driven Project 5688 and Reintegration Grant 5362), and the Ministry of Higher Education (CEP2-007-ASSU) are gratefully acknowledged (M.E.).

References

(1). Toumey C. Plenty of room, plenty of history. Nat. Nanotechnol. 2009; 4:783–784. [PubMed: 19966818]

(2). Taniguchi, N. On the basic concept of nano-technology; Proc. Intl. Conf. Prod. Eng. Tokyo, Part II, Japan Society of Precision Engineering; 1974;

(3). Devadasu VR, Bhardwaj V, Kumar MN. Can controversial nanotechnology promise drug delivery? Chem. Rev. 2013; 113:1686–1735. [PubMed: 23276295]

(4). Brambilla D, Luciani P, Leroux JC. Breakthrough discoveries in drug delivery technologies: the next 30 years. J. Control. Release. 2014; 190:9–14. [PubMed: 24794899]

(5). Pahlm, O.; Wagner, G. Multimodal Cardiovascular Imaging: Principles and Clinical Applications. McGraw-Hill; New York: 2011.

(6). Yao J, Yang M, Duan Y. Chemistry, biology, and medicine of fluorescent nanomaterials and related systems: new insights into biosensing, bioimaging, genomics, diagnostics, and therapy. Chem. Rev. 2014; 114:6130–6178. [PubMed: 24779710]

(7). Ding J, Wang Y, Ma M, Zhang Y, Lu S, Jiang Y, Qi C, Luo S, Dong G, Wen S. CT/fluorescence dual-modal nanoemulsion platform for investigating atherosclerotic plaques. Biomaterials. 2013; 34:209–216. [PubMed: 23069709]

(8). Owens B. Scans: Enhanced medical vision. Nature. 2013; 502:S82–S83. [PubMed: 24187699]

(9). Lusic H, Grinstaff MW. X-ray-Computed Tomography Contrast Agents. Chem. Rev. 2013; 113:1641–1666. [PubMed: 23210836]

(10). Nystrom, AM.; Zeng, X.; Zhang, Y.; Regberg, J. Update on Polymer Based Nanomedicine. Smithers Rapra Technology Ltd; Shawbury, Shrews, Shropshire, SY4 4NR, UK: 2012.

(11). Al Zaki A, Joh D, Cheng Z, De Barros AL, Kao G, Dorsey J, Tsourkas A. Gold-loaded polymeric micelles for computed tomography-guided radiation therapy treatment and radiosensitization. ACS Nano. 2014; 8:104–112. [PubMed: 24377302]

(12). Cormode DP, Naha PC, Fayad ZA. Nanoparticle contrast agents for computed tomography: a focus on micelles. Contrast Media Mol. Imaging. 2014; 9:37–52. [PubMed: 24470293]

(13). Cunningham CH, Arai T, Yang PC, McConnell MV, Pauly JM, Conolly SM. Positive contrast magnetic resonance imaging of cells labeled with magnetic nanoparticles. Magn. Reson. Med. 2005; 53:999–1005. [PubMed: 15844142]

(14). Zurkiya O, Hu X. Off-resonance saturation as a means of generating contrast with superparamagnetic nanoparticles. Magn. Reson. Med. 2006; 56:726–732. [PubMed: 16941618]

(15). Sitharaman, B. 1 ed.. Taylor and Francis; Hoboken: 2011.

(16). Shin J, Anisur RM, Ko MK, Im GH, Lee JH, Lee IS. Hollow manganese oxide nanoparticles as multifunctional agents for magnetic resonance imaging and drug delivery. Angew. Chem. Int. Ed. 2009; 48:321–324.

(17). Savage N. Technology: Multiple exposure. Nature. 2013; 502:S90–S91. [PubMed: 24187703]

(18). Broz, P.; Kroto, H.; O'Brien, P. Polymer-based nanostructures. Royal Society of Chemistry; 2010.

(19). Janib SM, Liu S, Park R, Pastuszka MK, Shi P, Moses AS, Orosco MM, Lin YA, Cui H, Conti PS, et al. Kinetic quantification of protein polymer nanoparticles using non-invasive imaging. Integr. Biol. 2013; 5:183–194.

(20). Xu J, Sun G, Rossin R, Hagooly A, Li Z, Fukukawa KI, Messmore BW, Moore DA, Welch MJ, Hawker CJ, et al. Labeling of Polymer Nanostructures for Medical Imaging: Importance of crosslinking extent, spacer length, and charge density. Macromolecules. 2007; 40:2971–2973. [PubMed: 18779874]

(21). Afshar-Oromieh A, Malcher A, Eder M, Eisenhut M, Linhart HG, Hadaschik BA, Holland-Letz T, Giesel FL, Kratochwil C, Haufe S, et al. PET imaging with a Ga-68 gallium-labelled PSMA ligand for the diagnosis of prostate cancer: biodistribution in humans and first evaluation of tumour lesions. Eur. J. Nucl. Med. Mol. Imaging. 2013; 40:486–495. [PubMed: 23179945]

(22). Welch MJ, Hawker CJ, Wooley KL. The advantages of nanoparticles for PET. J. Nucl. Med. 2009; 50:1743–1746. [PubMed: 19837751]

(23). Phillips E, Penate-Medina O, Zanzonico PB, Carvajal RD, Mohan P, Ye Y, Humm J, Gonen M, Kalaigian H, Schoder H, et al. Clinical translation of an ultrasmall inorganic optical-PET imaging nanoparticle probe. Sci. Transl. Med. 2014; 6:260ra149.

(24). Magalotti S, Gustafson TP, Cao Q, Abendschein DR, Pierce RA, Berezin MY, Akers WJ. Evaluation of Inflammatory Response to Acute Ischemia Using Near-Infrared Fluorescent Reactive Oxygen Sensors. Mol. Imaging Biol. 2013; 15:423–430. [PubMed: 23378226]

(25). Wang ST, Zhegalova NG, Gustafson TP, Zhou A, Sher J, Achilefu S, Berezin OY, Berezin MY. Sensitivity of activatable reactive oxygen species probes by fluorescence spectroelectrochemistry. Analyst. 2013; 138:4363–4369. [PubMed: 23736882]

(26). Yeung K, Schmid KM, Phillips ST. A thermally-stable enzyme detection assay that amplifies signal autonomously in water without assistance from biological reagents. Chem. Commun. 2013; 49:394–396.

(27). Bao G, Mitragotri S, Tong S. Multifunctional nanoparticles for drug delivery and molecular imaging. Annu. Rev. Biomed. Eng. 2013; 15:253–282. [PubMed: 23642243]

(28). Weissleder R. A clearer vision for in vivo imaging. Nat. Biotechnol. 2001; 19:316–316. [PubMed: 11283581]

(29). Marshall MV, Rasmussen JC, Tan IC, Aldrich MB, Adams KE, Wang X, Fife CE, Maus EA, Smith LA, Sevick-Muraca EM. Near-Infrared Fluorescence Imaging in Humans with Indocyanine Green: A Review and Update. Open Surg. Oncol. J. 2010; 2:12–25. [PubMed: 22924087]

(30). Cui SS, Yin DY, Chen YQ, Di YF, Chen HY, Ma YX, Achilefu S, Gu YQ. In Vivo Targeted Deep-Tissue Photodynamic Therapy Based on Near-Infrared Light Triggered Upconversion Nanoconstruct. Acs Nano. 2013; 7:676–688. [PubMed: 23252747]

(31). Carling C, Viger ML, Nguyen Huu VA, Garcia AV, Almutairi A. In vivo visible light-triggered drug release from an implanted depot. Chem. Sci. 2015; 6:335–341. [PubMed: 25598962]

(32). Pu KY, Shuhendler AJ, Jokerst JV, Mei JG, Gambhir SS, Bao ZN, Rao JH. Semiconducting polymer nanoparticles as photoacoustic molecular imaging probes in living mice. Nat. Nanotechnol. 2014; 9:233–239. [PubMed: 24463363]

(33). Wang D, Lin B, Ai H. Theranostic Nanoparticles for Cancer and Cardiovascular Applications. Pharm. Res. 2014; 31:1390–1406. [PubMed: 24595494]

(34). Janib SM, Moses AS, MacKay JA. Imaging and drug delivery using theranostic nanoparticles. Adv. Drug Deliv. Rev. 2010; 62:1052–1063. [PubMed: 20709124]

(35). Elsabahy M, Wooley KL. Design of polymeric nanoparticles for biomedical delivery applications. Chem. Soc. Rev. 2012; 41:2545–2561. [PubMed: 22334259]

(36). Ensign LM, Cone R, Hanes J. Oral drug delivery with polymeric nanoparticles: the gastrointestinal mucus barriers. Adv. Drug Deliv. Rev. 2012; 64:557–570. [PubMed: 22212900]

(37). Minko T, Rodriguez-Rodriguez L, Pozharov V. Nanotechnology approaches for personalized treatment of multidrug resistant cancers. Adv. Drug Deliv. Rev. 2013; 65:1880–1895. [PubMed: 24120655]

(38). Minko T. Nanotechnology and drug resistance. Adv. Drug Deliv. Rev. 2013; 65:1665–1666. [PubMed: 24177352]

(39). Prausnitz MR, Langer R. Transdermal drug delivery. Nat. Biotechnol. 2008; 26:1261–1268. [PubMed: 18997767]

(40). Lai SK, Wang YY, Hanes J. Mucus-penetrating nanoparticles for drug and gene delivery to mucosal tissues. Adv. Drug Deliv. Rev. 2009; 61:158–171. [PubMed: 19133304]

(41). Dobrovolskaia MA, McNeil SE. Immunological properties of engineered nanomaterials. Nat. Nanotechnol. 2007; 2:469–478. [PubMed: 18654343]

(42). Patel LN, Zaro JL, Shen WC. Cell penetrating peptides: intracellular pathways and pharmaceutical perspectives. Pharm. Res. 2007; 24:1977–1992. [PubMed: 17443399]

(43). Verma A, Uzun O, Hu Y, Han HS, Watson N, Chen S, Irvine DJ, Stellacci F. Surface-structure-regulated cell-membrane penetration by monolayer-protected nanoparticles. Nat. Mater. 2008; 7:588–595. [PubMed: 18500347]

(44). World Health Organization. [accessed Feb 11, 2015] http://www.who.int/mediacentre/factsheets/fs310/en/

(45). Go AS, Mozaffarian D, Roger VL, Benjamin EJ, Berry JD, Blaha MJ, Dai SF, Ford ES, Fox CS, Franco S, et al. Heart Disease and Stroke Statistics-2014 Update A Report From the American Heart Association. Circulation. 2014; 129:E28–E292. [PubMed: 24352519]

(46). Libby P, Ridker PM, Hansson GK. Progress and challenges in translating the biology of atherosclerosis. Nature. 2011; 473:317–325. [PubMed: 21593864]

(47). Shi C, Pamer EG. Monocyte recruitment during infection and inflammation. Nat. Rev. Immunol. 2011; 11:762–774. [PubMed: 21984070]

(48). Hoshi S, Goto M, Koyama N, Nomoto K, Tanaka H. Regulation of vascular smooth muscle cell proliferation by nuclear factor-kappa B and its inhibitor, I-kappa B. J. Biol. Chem. 2000; 275:883–889. [PubMed: 10625622]

(49). de Winther MPJ, Kanters E, Kraal G, Hofker MH. Nuclear factor kappa B signaling in atherogenesis. Arterioscler. Thromb. Vasc. Biol. 2005; 25:904–914. [PubMed: 15731497]

(50). White GE, Iqbal AJ, Greaves DR. CC Chemokine Receptors and Chronic Inflammation-Therapeutic Opportunities and Pharmacological Challenges. Pharmacol. Rev. 2013; 65:47–89. [PubMed: 23300131]

(51). Liu J, Huang W, Pang Y, Zhu X, Zhou Y, Yan D. Hyperbranched polyphosphates for drug delivery application: design, synthesis, and in vitro evaluation. Biomacromolecules. 2010; 11:1564–1570. [PubMed: 20364861]

(52). Liu Y, Pressly ED, Abendschein DR, Hawker CJ, Woodard GE, Woodard PK, Welch MJ. Targeting angiogenesis using a C-type atrial natriuretic factor-conjugated nanoprobe and PET. J. Nucl. Med. 2011; 52:1956–1963. [PubMed: 22049461]

(53). Schiener M, Hossann M, Viola JR, Ortega-Gomez A, Weber C, Lauber K, Lindner LH, Soehnlein O. Nanomedicine-based strategies for treatment of atherosclerosis. Trends in Molecular Medicine. 2014; 20:271–281. [PubMed: 24594264]

(54). Hanahan D, Weinberg RA. Hallmarks of cancer: the next generation. Cell. 2011; 144:646–674. [PubMed: 21376230]

(55). Masaki T, Okada M, Shiratori Y, Rengifo W, Matsumoto K, Maeda S, Kato N, Kanai F, Komatsu Y, Nishioka M, et al. pp60c-src activation in hepatocellular carcinoma of humans and LEC rats. Hepatology. 1998; 27:1257–1264. [PubMed: 9581679]

(56). Harada K, Shiota G, Kawasaki H. Transforming growth factor-alpha and epidermal growth factor receptor in chronic liver disease and hepatocellular carcinoma. Liver. 1999; 19:318–325. [PubMed: 10459631]

(57). Giles RH, van EJ, Clevers H. Caught up in a Wnt storm: Wnt signaling in cancer. Biochim. Biophys. Acta. 2003; 1653:1–24. [PubMed: 12781368]

(58). Hu TH, Huang CC, Lin PR, Chang HW, Ger LP, Lin YW, Changchien CS, Lee CM, Tai MH. Expression and prognostic role of tumor suppressor gene PTEN/MMAC1/TEP1 in hepatocellular carcinoma. Cancer. 2013; 97:1929–1940. [PubMed: 12673720]

(59). Pikarsky E, Porat RM, Stein I, Abramovitch R, Amit S, Kasem S, Gutkovich-Pyest E, Urieli-Shoval S, Galun E, Ben-Neriah Y. NF-kappaB functions as a tumour promoter in inflammation-associated cancer. Nature. 2004; 431:461–466. [PubMed: 15329734]

(60). Sahin F, Kannangai R, Adegbola O, Wang J, Su G, Torbenson M. mTOR and P70 S6 kinase expression in primary liver neoplasms. Clin. Cancer Res. 2004; 10:8421–8425. [PubMed: 15623621]

(61). Arsura M, Cavin LG. Nuclear factor-kappaB and liver carcinogenesis. Cancer Lett. 2005; 229:157–169. [PubMed: 16125305]

(62). Chiang DY, Villanueva A, Hoshida Y, Peix J, Newell P, Minguez B, LeBlanc AC, Donovan DJ, Thung SN, Solé M, et al. Focal gains of Vascular Endothelial Growth Factor A and Molecular Classification of Hepatocellular Carcinoma. Cancer Res. 2008; 68:6779–6788. [PubMed: 18701503]

(63). Eskens FA. Angiogenesis inhibitors in clinical development; where are we now and where are we going? Br. J. Cancer. 2004; 90:1–7. [PubMed: 14710197]

(64). Zacharoulis D, Hatzitheofilou C, Athanasiou E, Zacharoulis S. Antiangiogenic strategies in hepatocellular carcinoma: current status. Expert Rev. Anticancer Ther. 2005; 5:645–656. [PubMed: 16111465]

(65). Li Y, Huang G, Diakur J, Wiebe LI. Targeted delivery of macromolecular drugs: asialoglycoprotein receptor (ASGPR) expression by selected hepatoma cell lines used in antiviral drug development. Curr. Drug Deliv. 2008; 5:299–302. [PubMed: 18855599]

(66). Zhou X, Zhang M, Yung B, Li H, Zhou C, Lee LJ, Lee RJ. Lactosylated liposomes for targeted delivery of doxorubicin to hepatocellular carcinoma. Int. J. Nanomedicine. 2012; 7:5465–5474. [PubMed: 23093902]

(67). Shi B, Abrams M, Sepp-Lorenzino L. Expression of asialoglycoprotein receptor 1 in human hepatocellular carcinoma. J. Histochem. Cytochem. 2013; 61:901–909. [PubMed: 23979840]

(68). Negishi M, Irie A, Nagata N, Ichikawa A. Specific binding of glycyrrhetinic acid to the rat liver membrane. Biochim. Biophys. Acta. 1991; 1066:77–82. [PubMed: 2065071]

(69). Ismair MG, Stanca C, Ha HR, Renner EL, Meier PJ, Kullak-Ublick GA. Interactions of glycyrrhizin with organic anion transporting polypeptides of rat and human liver. J. Hepatol. Res. 2003; 26:343–347.

(70). Matsumura Y, Maeda H. A new concept for macromolecular therapeutics in cancer chemotherapy: mechanism of tumoritropic accumulation of proteins and the antitumor agent smancs. Cancer Res. 1986; 46:6387–6392. [PubMed: 2946403]

(71). Cheng Z, Al Zaki A, Hui JZ, Muzykantov VR, Tsourkas A. Multifunctional nanoparticles: cost versus benefit of adding targeting and imaging capabilities. Science. 2012; 338:903–910. [PubMed: 23161990]

(72). Zhong Y, Meng F, Deng C, Zhong Z. Ligand-directed active tumor-targeting polymeric nanoparticles for cancer chemotherapy. Biomacromolecules. 2014; 15:1955–1969. [PubMed: 24798476]

(73). Allen TM. Ligand-targeted therapeutics in anticancer therapy. Nat. Rev. Cancer. 2002; 2:750–763. [PubMed: 12360278]

(74). Tatem AJ, Rogers DJ, Hay S. Global transport networks and infectious disease spread. Adv. Parasitol. 2006; 62:293–343. [PubMed: 16647974]

(75). Hindi KM, Ditto AJ, Panzner MJ, Medvetz DA, Han DS, Hovis CE, Hilliard JK, Taylor JB, Yun YH, Cannon CL, et al. The antimicrobial efficacy of sustained release silver-carbene complex-loaded L-tyrosine polyphosphate nanoparticles: characterization, in vitro and in vivo studies. Biomaterials. 2009; 30:3771–3779. [PubMed: 19395021]

(76). Marier JF, Brazier JL, Lavigne J, Ducharme MP. Liposomal tobramycin against pulmonary infections of Pseudomonas aeruginosa: a pharmacokinetic and efficacy study following single and multiple intratracheal administrations in rats. J. Antimicrob. Chemother. 2003; 52:247–252. [PubMed: 12837733]

(77). Beaulac C, Clément-Major S, Hawari J, Lagacé J. Eradication of mucoid Pseudomonas aeruginosa with fluid liposome-encapsulated tobramycin in an animal model of chronic pulmonary infection. Antimicrob. Agents Chemother. 1996; 40:665–669. [PubMed: 8851590]

(78). Lai S, Wang Y, Wirtz D, Hanes J. Micro- and macrorheology of mucus. Adv. Drug Deliv. Rev. 2009; 61:86–100. [PubMed: 19166889]

(79). Dawson M, Wirtz D, Hanes J. Enhanced viscoelasticity of human cystic fibrotic sputum correlates with increasing microheterogeneity in particle transport. J. Biol. Chem. 2003; 278:50393–50401. [PubMed: 13679362]

(80). Henke MO, Ratjen F. Mucolytics in cystic fibrosis. Paediatr. Respir. Rev. 2007; 8:24–29. [PubMed: 17419975]

(81). Elsabahy M, Wooley KL. Cytokines as biomarkers of nanoparticle immunotoxicity. Chem. Soc. Rev. 2013; 42:5552–5576. [PubMed: 23549679]

(82). Le Garrec D, Gori S, Luo L, Lessard D, Smith DC, Yessine MA, Ranger M, Leroux JC. Poly(N-vinylpyrrolidone)-block-poly(D,L-lactide) as a new polymeric solubilizer for hydrophobic anticancer drugs: in vitro and in vivo evaluation. J. Control. Release. 2004; 99:83–101. [PubMed: 15342183]

(83). Lin LY, Lee NS, Zhu J, Nystrom AM, Pochan DJ, Dorshow RB, Wooley KL. Tuning core vs. shell dimensions to adjust the performance of nanoscopic containers for the loading and release of doxorubicin. J. Control. Release. 2011; 152:37–48. [PubMed: 21241750]

(84). Ma Q, Remsen EE, Clark CG Jr. Kowalewski T, Wooley KL. Chemically induced supramolecular reorganization of triblock copolymer assemblies: trapping of intermediate states via a shell-crosslinking methodology. Proc. Natl. Acad. Sci. U. S. A. 2002; 99:5058–5063. [PubMed: 11929963]

(85). Carr LR, Zhou Y, Krause JE, Xue H, Jiang S. Uniform zwitterionic polymer hydrogels with a nonfouling and functionalizable crosslinker using photopolymerization. Biomaterials. 2011; 32:6893–6899. [PubMed: 21704366]

(86). Jiang S, Cao Z. Ultralow-fouling, functionalizable, and hydrolyzable zwitterionic materials and their derivatives for biological applications. Adv. Mater. 2010; 22:920–932. [PubMed: 20217815]

(87). Keefe AJ, Jiang S. Poly(zwitterionic)protein conjugates offer increased stability without sacrificing binding affinity or bioactivity. Nat. Chem. 2012; 4:59–63. [PubMed: 22169873]

(88). Li A, Luehmann HP, Sun G, Samarajeewa S, Zou J, Zhang S, Zhang F, Welch MJ, Liu Y, Wooley KL. Synthesis and in vivo pharmacokinetic evaluation of degradable shell cross-linked polymer nanoparticles with poly(carboxybetaine) versus poly(ethylene glycol) surface-grafted coatings. ACS Nano. 2012; 6:8970–8982. [PubMed: 23043240]

(89). Elsabahy M, Li A, Zhang F, Sultan D, Liu Y, Wooley KL. Differential immunotoxicities of poly(ethylene glycol)- vs. poly(carboxybetaine)-coated nanoparticles. J. Control. Release. 2013; 172:641–652. [PubMed: 24056145]

(90). Elsabahy M, Wooley KL. Strategies toward Well-Defined Polymer Nanoparticles Inspired by Nature: Chemistry versus Versatility. J. Polym. Sci. Part A: Polym. Chem. 2012; 50:1869–1880.

(91). Nystrom AM, Wooley KL. The Importance of Chemistry in Creating Well-Defined Nanoscopic Embedded Therapeutics: Devices Capable of the Dual Functions of Imaging and Therapy. Acc. Chem. Res. 2011; 44:969–978. [PubMed: 21675721]

(92). Klyachko NL, Manickam DS, Brynskikh AM, Uglanova SV, Li S, Higginbotham SM, Bronich TK, Batrakova EV, Kabanov AV. Cross-linked antioxidant nanozymes for improved delivery to CNS. Nanomedicine. 2012; 8:119–129. [PubMed: 21703990]

(93). Kakizawa Y, Harada A, Kataoka K. Glutathione-sensitive stabilization of block copolymer micelles composed of antisense DNA and thiolated poly(ethylene glycol)-block-poly(L-lysine): a potential carrier for systemic delivery of antisense DNA. Biomacromolecules. 2001; 2:491–497. [PubMed: 11749211]

(94). Miyata K, Kakizawa Y, Nishiyama N, Yamasaki Y, Watanabe T, Kohara M, Kataoka K. Freeze-dried formulations for in vivo gene delivery of PEGylated polyplex micelles with disulfide crosslinked cores to the liver. J. Control. Release. 2005; 109:15–23. [PubMed: 16298011]

(95). Navath RS, Menjoge AR, Dai H, Romero R, Kannan S, Kannan RM. Injectable PAMAM dendrimer-PEG hydrogels for the treatment of genital infections: formulation and in vitro and in vivo evaluation. Mol. Pharm. 2011; 8:1209–1223. [PubMed: 21615144]

(96). Moughton AO, O'Reilly RK. Noncovalently connected micelles, nanoparticles, and metal-functionalized nanocages using supramolecular self-assembly. J. Am. Chem. Soc. 2008; 130:8714–8725. [PubMed: 18549205]

(97). Fuhrmann K, Schulz JD, Gauthier MA, Leroux JC. PEG Nanocages as Non-sheddable Stabilizers for Drug Nanocrystals. ACS Nano. 2012; 6:1667–1676. [PubMed: 22296103]

(98). Thurmond KB, Kowalewski T, Wooley KL. Water-Soluble Knedel-like Structures: The Preparation of Shell-Cross-Linked Small Particles. J. Am. Chem. Soc. 1996; 118:7239–7240.

(99). Thurmond KB, Remsen EE, Kowalewski T, Wooley KL. Shell Cross-Linked Knedels: A Synthetic Study of the Factors Affecting the Dimensions and Properties of Amphiphilic Core-Shell Nanospheres. J. Am. Chem. Soc. 1997; 119:6656–6665.

(100). Huang H, Kowalewski T, Remsen EE, Gertzmann R, Wooley KL. Hydrogel-Coated Glassy Nanospheres: A Novel Method for the Synthesis of Shell Cross-Linked Knedels. J. Am. Chem. Soc. 1997; 119:11653–11659.

(101). Sun G, Xu J, Hagooly A, Rossin R, Li Z, Moore DA, Hawker CJ, Welch MJ, Wooley KL. Strategies for Optimized Radiolabeling of Nanoparticles for in vivo PET Imaging. Adv. Mater. 2007; 19:3157–3162.

(102). Sun G, Hagooly A, Xu J, Nyström AM, Li Z, Rossin R, Moore DA, Wooley KL, Welch MJ. Facile, Efficient Approach to Accomplish Tunable Chemistries and Variable Biodistributions for Shell Cross-Linked Nanoparticles. Biomacromolecules. 2008; 9:1997–2006. [PubMed: 18510359]

(103). Ishida T, Wang X, Shimizu T, Nawata K, Kiwada H. PEGylated liposomes elicit an anti-PEG IgM response in a T cell-independent manner. J. Control. Release. 2007; 122:349–355. [PubMed: 17610982]

(104). Wang X, Ishida T, Kiwada H. Anti-PEG IgM elicited by injection of liposomes is involved in the enhanced blood clearance of a subsequent dose of PEGylated liposomes. J. Control. Release. 2007; 119:236–244. [PubMed: 17399838]

(105). Garay RP, El-Gewely R, Armstrong JK, Garratty G, Richette P. Antibodies against polyethylene glycol in healthy subjects and in patients treated with PEG-conjugated agents. Expert Opin. Drug Deliv. 2012; 9:1319–1323. [PubMed: 22931049]

(106). Lundberg P, Lee BF, van den Berg SA, Pressly ED, Lee A, Hawker CJ, Lynd NA. Poly[(ethylene oxide)-co-(methylene ethylene oxide)]: A hydrolytically-degradable poly(ethylene oxide) platform. ACS Macro Lett. 2012; 1:1240–1243. [PubMed: 23205320]

(107). Singer JW. Paclitaxel poliglumex (XYOTAX, CT-2103): a macromolecular taxane. J. Control. Release. 2005; 109:120–126. [PubMed: 16297482]

(108). Singer JW, Shaffer S, Baker B, Bernareggi A, Stromatt S, Nienstedt D, Besman M. Paclitaxel poliglumex (XYOTAX; CT-2103): an intracellularly targeted taxane. Anticancer Drugs. 2005; 16:243–254. [PubMed: 15711176]

(109). Stanberry LR, Simon JK, Johnson C, Robinson PL, Morry J, Flack MR, Gracon S, Myc A, Hamouda T, Baker JR Jr. Safety and immunogenicity of a novel nanoemulsion mucosal adjuvant W(80)5EC combined with approved seasonal influenza antigens. Vaccine. 2012; 30:307–316. [PubMed: 22079079]

(110). Gianella A, Jarzyna PA, Mani V, Ramachandran S, Calcagno C, Tang J, Kann B, Dijk WJ, Thijssen VL, Griffioen AW, et al. Multifunctional nanoemulsion platform for imaging guided therapy evaluated in experimental cancer. ACS Nano. 2011; 5:4422–4433. [PubMed: 21557611]

(111). Kataoka K, Harada A, Nagasaki Y. Block copolymer micelles for drug delivery: design, characterization and biological significance. Adv. Drug Deliv. Rev. 2001; 47:113–131. [PubMed: 11251249]

(112). Torchilin VP. Micellar nanocarriers: pharmaceutical perspectives. Pharm. Res. 2007; 24:1–16. [PubMed: 17109211]

(113). Gaucher G, Dufresne MH, Sant VP, Kang N, Maysinger D, Leroux JC. Block copolymer micelles: preparation, characterization and application in drug delivery. J. Control. Release. 2005; 109:169–188. [PubMed: 16289422]

(114). Hawkins MJ, Soon-Shiong P, Desai N. Protein nanoparticles as drug carriers in clinical medicine. Adv. Drug Deliv. Rev. 2008; 60:876–885. [PubMed: 18423779]

(115). Shi J, Xiao Z, Kamaly N, Farokhzad OC. Self-Assembled Targeted Nanoparticles: Evolution of Technologies and Bench to Bedside Translation. Acc. Chem. Res. 2011; 44:1123–1134. [PubMed: 21692448]

(116). Li C, Wallace S. Polymer-drug conjugates: recent development in clinical oncology. Adv. Drug Deliv. Rev. 2008; 60:886–898. [PubMed: 18374448]

(117). Wolfrum C, Shi S, Jayaprakash KN, Jayaraman M, Wang G, Pandey RK, Rajeev KG, Nakayama T, Charrise K, Ndungo EM, et al. Mechanisms and optimization of in vivo delivery of lipophilic siRNAs. Nat. Biotechnol. 2007; 25:1149–1157. [PubMed: 17873866]

(118). Simard P, Leroux JC. In vivo evaluation of pH-sensitive polymer-based immunoliposomes targeting the CD33 antigen. Mol. Pharm. 2010; 7:1098–1107. [PubMed: 20476756]

(119). Movassaghian S, Moghimi HR, Shirazi FH, Torchilin VP. Dendrosome-dendriplex inside liposomes: as a gene delivery system. J. Drug Target. 2011; 19:925–932. [PubMed: 22023509]

(120). Bedi D, Musacchio T, Fagbohun OA, Gillespie JW, Deinnocentes P, Bird RC, Bookbinder L, Torchilin VP, Petrenko VA. Delivery of siRNA into breast cancer cells via phage fusion protein-targeted liposomes. Nanomedicine. 2011; 7:315–323. [PubMed: 21050894]

(121). Nishiyama N, Kataoka K. Current state, achievements, and future prospects of polymeric micelles as nanocarriers for drug and gene delivery. Pharmacol. Ther. 2006; 112:630–648. [PubMed: 16815554]

(122). Wolff JA, Rozema DB. Breaking the bonds: non-viral vectors become chemically dynamic. Mol. Ther. 2008; 16:8–15. [PubMed: 17955026]

(123). Elsabahy M, Wazen N, Puxan N, Deleavey G, Servant M, Damha MJ, Leroux JC. Delivery of nucleic acids through the controlled disassembly of multifunctional nanocomplexes. Adv. Funct. Mater. 2009; 19:3862–3867.

(124). Elsabahy, M.; Dufresne, MH.; Leroux, JC. Materials for Nanomedicine. Torchilin, V.; Amiji, M., editors. Pan Stanford Publishing; Hackensack: 2010.

(125). Semple SC, Akinc A, Chen J, Sandhu AP, Mui BL, Cho CK, Sah DW, Stebbing D, Crosley EJ, Yaworski E, et al. Rational design of cationic lipids for siRNA delivery. Nat. Biotechnol. 2010; 28:172–176. [PubMed: 20081866]

(126). Judge AD, Robbins M, Tavakoli I, Levi J, Hu L, Fronda A, Ambegia E, McClintock K, MacLachlan I. Confirming the RNAi-mediated mechanism of action of siRNA-based cancer therapeutics in mice. J. Clin. Invest. 2009; 119:661–673. [PubMed: 19229107]

(127). Dreaden EC, Mackey MA, Huang X, Kang B, El-Sayed MA. Beating cancer in multiple ways using nanogold. Chem. Soc. Rev. 2011; 40:3391–3404. [PubMed: 21629885]

(128). Lee JH, Lee K, Moon SH, Lee Y, Park TG, Cheon J. All-in-one target-cell-specific magnetic nanoparticles for simultaneous molecular imaging and siRNA delivery. Angew. Chem. Int. Ed. 2009; 48:4174–4179.

(129). Huang HC, Barua S, Sharma G, Dey SK, Rege K. Inorganic nanoparticles for cancer imaging and therapy. J. Control. Release. 2011; 155:344–357. [PubMed: 21723891]

(130). Prato M, Kostarelos K, Bianco A. Functionalized carbon nanotubes in drug design and discovery. Acc. Chem. Res. 2008; 41:60–68. [PubMed: 17867649]

(131). Liu Z, Davis C, Cai W, He L, Chen X, Dai H. Circulation and long-term fate of functionalized, biocompatible single-walled carbon nanotubes in mice probed by Raman spectroscopy. Proc. Natl. Acad. Sci. U. S. A. 2008; 105:1410–1415. [PubMed: 18230737]

(132). Lux F, Mignot A, Mowat P, Louis C, Dufort S, Bernhard C, Denat F, Boschetti F, Brunet C, Antoine R, et al. Ultrasmall Rigid Particles as Multimodal Probes for Medical Applications. Angew. Chem. Int. Ed. 2011; 50:12299–12303.

(133). Zhao Y, Sultan D, Detering L, Luehmann H, Liu Y. Facile synthesis, pharmacokinetic and systemic clearance evaluation, and positron emission tomography cancer imaging of 64Cu-Au alloy nanoclusters. Nanoscale. 2014; 6:13501–13509. [PubMed: 25266128]

(134). Kang N, Perron ME, Prud'homme RE, Zhang Y, Gaucher G, Leroux JC. Stereocomplex block copolymer micelles: core-shell nanostructures with enhanced stability. Nano Lett. 2005; 5:315–319. [PubMed: 15794618]

(135). Cui H, Chen Z, Zhong S, Wooley KL, Pochan DJ. Block copolymer assembly via kinetic control. Science. 2007; 317:647–650. [PubMed: 17673657]

(136). Yang C, Tan JPK, Cheng W, Attia ABE, Ting CTY, Nelson A, Hedrick JL, Yang YY. Supramolecular nanostructures designed for high cargo loading capacity and kinetic stability. Nano Today. 2010; 5:515–523.

(137). O'Reilly RK, Hawker CJ, Wooley KL. Cross-linked block copolymer micelles: functional nanostructures of great potential and versatility. Chem. Soc. Rev. 2006; 35:1068–1083. [PubMed: 17057836]

(138). van Nostrum CF. Covalently cross-linked amphiphilic block copolymer micelles. Soft Matter. 2011; 7:3246–3259.

(139). Read ES, Armes SP. Recent advances in shell cross-linked micelles. Chem. Commun. 2007:3021–3035.

(140). Zhang F, Zhang S, Pollack SF, Li R, Gonzalez A, Fan J, Zou J, Leininger SE, Pavía-Sanders A, Johnson R, et al. Improving Paclitaxel Delivery: In vitro and in vivo characteri-zation of ultra-

high loaded PEGylated polyphosphoester-based nanocarriers. J. Am. Chem. Soc. 2015; 137:2056–2066. [PubMed: 25629952]

(141). Kim JO, Sahay G, Kabanov AV, Bronich TK. Polymeric micelles with ionic cores containing biodegradable cross-links for delivery of chemotherapeutic agents. Biomacromolecules. 2010; 11:919–926. [PubMed: 20307096]

(142). Abdelwahed W, Degobert G, Stainmesse S, Fessi H. Freeze-drying of nanoparticles: formulation, process and storage considerations. Adv. Drug Deliv. Rev. 2006; 58:1688–1713. [PubMed: 17118485]

(143). Jeon SI, Andrade JD. Protein-surface interactions in the presence of polyethylene oxide: II. effect of protein size. J. Colloid Interface Sci. 1991; 142:159–166.

(144). Jeon SI, Lee JH, Andrade JD, De Gennes PG. Protein-surface interactions in the presence of polyethylene oxide: I. simplified theory. J. Colloid Interface Sci. 1991; 142:149–158.

(145). Elsabahy M, Zhang S, Zhang F, Deng ZJ, Lim YH, Wang H, Parsamian P, Hammond PT, Wooley KL. Surface Charges and Shell Crosslinks Each Play Significant Roles in Mediating Degradation, Biofouling, Cytotoxicity and Immunotoxicity for Polyphosphoester-based Nanoparticles. Sci. Rep. 2013; 3:3313. [PubMed: 24264796]

(146). Elsabahy M, Samarajeewa S, Raymond JE, Clark C, Wooley KL. Shell-crosslinked knedel-like nanoparticles induce lower immunotoxicity than their non-crosslinked analogs. J. Mater. Chem. 2013; 1:5241–5255.

(147). Sun G, Berezin MY, Fan J, Lee H, Ma J, Zhang K, Wooley KL, Achilefu S. Bright fluorescent nanoparticles for developing potential optical imaging contrast agents. Nanoscale. 2010; 2:548–558. [PubMed: 20644758]

(148). Lee NS, Sun G, Neumann WL, Freskos JN, Shieh JJ, Dorshow RB, Wooley KL. Photonic Shell-Crosslinked Nanoparticle Probes for Optical Imaging and Monitoring. Adv. Mater. 2009; 21:1344–1348. [PubMed: 22058610]

(149). Sun G, Cui H, Lin LY, Lee NS, Yang C, Neumann WL, Freskos JN, Shieh JJ, Dorshow RB, Wooley KL. Multicompartment polymer nanostructures with ratiometric dual-emission pH-sensitivity. J. Am. Chem. Soc. 2011; 133:8534–8543. [PubMed: 21574617]

(150). Lee NS, Sun G, Lin LY, Neumann WL, Freskos JN, Karwa A, Shieh JJ, Dorshow RB, Wooley KL. Tunable dual-emitting shell-crosslinked nano-objects as single-component ratiometric pH-sensing materials. J. Mater. Chem. 2011; 21:14193–14202. [PubMed: 25506129]

(151). Li Y, Du W, Sun GL,WK. pH-Responsive Shell Cross-Linked Nanoparticles with Hydrolytically Labile Cross-Links. Macromolecules. 2008; 41:6605–6607.

(152). Lin YA, Ou YC, Cheetham AG, Cui H. Rational design of MMP degradable peptide-based supramolecular filaments. Biomacromolecules. 2014; 15:1419–1427. [PubMed: 24611531]

(153). Jones MC, Tewari P, Blei C, Hales K, Pochan DJ, Leroux JC. Self-assembled nanocages for hydrophilic guest molecules. J. Am. Chem. Soc. 2006; 128:14599–14605. [PubMed: 17090044]

(154). Huang H, Remsen EE, Kowalewski T, Wooley KL. Nanocages derived from shell cross-linked micelle templates. J. Am. Chem. Soc. 1999; 121:3805–3806.

(155). Turner JL, Chen Z, Wooley KL. Regiochemical functionalization of a nanoscale cage-like structure: robust core-shell nanostructures crafted as vessels for selective uptake and release of small and large guests. J. Control. Release. 2005; 109:189–202. [PubMed: 16278031]

(156). Turner JL, Wooley KL. Nanoscale cage-like structures derived from polyisoprene-containing shell cross-linked nanoparticle templates. Nano Lett. 2004; 4:683–688.

(157). Cheng C, Qi K, Khoshdel E, Wooley KL. Tandem synthesis of core-shell brush copolymers and their transformation to peripherally cross-linked and hollowed nanostructures. J. Am. Chem. Soc. 2006; 128:6808–6809. [PubMed: 16719459]

(158). Huang K, Jacobs A, Rzayev J. De novo synthesis and cellular uptake of organic nanocapsules with tunable surface chemistry. Biomacromolecules. 2011; 12:2327–2334. [PubMed: 21563757]

(159). Chen CK, Wang Q, Jones CH, Yu Y, Zhang H, Law WC, Lai CK, Zeng Q, Prasad PN, Pfeifer BA, et al. Synthesis of pH-responsive chitosan nanocapsules for the controlled delivery of doxorubicin. Langmuir. 2014; 30:4111–4119. [PubMed: 24665861]

(160). Chen CK, Law WC, Aalinkeel R, Yu Y, Nair B, Wu J, Mahajan S, Reynolds JL, Li Y, Lai CK, et al. Biodegradable cationic polymeric nanocapsules for overcoming multidrug resistance and

enabling drug-gene co-delivery to cancer cells. Nanoscale. 2014; 6:1567–1572. [PubMed: 24326457]

(161). Samarajeewa S, Shrestha R, Li Y, Wooley KL. Degradability of poly(Lactic Acid)-containing nanoparticles: Enzymatic access through a cross-linked shell barrier. J. Am. Chem. Soc. 2012; 134:1235–1242. [PubMed: 22257265]

(162). Zhang Q, Remsen EE, Wooley KL. Shell Crosslinked Nanoparticles Containing Hydrolytically-degradable Crystalline Core Domains. J. Am. Chem. Soc. 2000; 122:3642–3651.

(163). Li Y, Themistou E, Das BP, Christian-Tabak L, Zou J, Tsianou M, Cheng C. Polyelectrolyte nanocages via crystallized miniemulsion droplets. Chem. Commun. 2011; 47:11697–11699.

(164). Sun G, Lee NS, Neumann WL, Freskos JN, Shieh JJ, Dorshow RB, Wooley KL. A Fundamental Investigation of Cross-linking Efficiencies within Discrete Nanostructures, Using the Cross-linker as a Reporting Molecule. Soft Matter. 2009; 5:3422–3429.

(165). Shilo M, Reuveni T, Motiei M, Popovtzer R. Nanoparticles as computed tomography contrast agents: current status and future perspectives. Nanomedicine. 2012; 7:257–269. [PubMed: 22339135]

(166). Xi D, Dong S, Meng XX, Lu QH, Meng LJ, Ye J. Gold nanoparticles as computerized tomography (CT) contrast agents. Rsc Advances. 2012; 2:12515–12524.

(167). NIH. Molecular Imaging and Contrast Agent Database (MICAD). 2013.

(168). Srikar R, Upendran A, Kannan R. Polymeric nanoparticles for molecular imaging. Wiley Interdiscip. Rev. Nanomed. Nanobiotechnol. 2014; 6:245–267. [PubMed: 24616442]

(169). Lee N, Choi SH, Hyeon T. Nano-Sized CT Contrast Agents. Adv. Mater. 2013; 25:2641–2660. [PubMed: 23553799]

(170). Anton N, Vandamme TF. Nanotechnology for Computed Tomography: A Real Potential Recently Disclosed. Pharm. Res. 2014; 31:20–34. [PubMed: 23896738]

(171). Hallouard F, Briancon S, Anton N, Li X, Vandamme T, Fessi H. Influence of Diblock Copolymer PCL-mPEG and of Various Iodinated Oils on the Formulation by the Emulsion-Solvent Diffusion Process of Radiopaque Polymeric Nanoparticles. J. Pharm. Sci. 2013; 102:4150–4158. [PubMed: 24018705]

(172). Jost G, Pietsch H, Grenacher L. Dynamic Contrast-Enhanced Computed Tomography to Assess Antitumor Treatment Effects Comparison of Two Contrast Agents With Different Pharmacokinetics. Invest. Radiol. 2013; 48:715–721. [PubMed: 23666093]

(173). Mieszawska AJ, Mulder WJM, Fayad ZA, Cormode DP. Multifunctional Gold Nanoparticles for Diagnosis and Therapy of Disease. Mol. Pharm. 2013; 10:831–847. [PubMed: 23360440]

(174). Chen H, Moore T, Qi B, Colvin DC, Jelen EK, Hitchcock DA, He J, Mefford OT, Gore JC, Alexis F, et al. Monitoring pH-Triggered Drug Release from Radioluminescent Nanocapsules with X-ray Excited Optical Luminescence. Acs Nano. 2013; 7:1178–1187. [PubMed: 23281651]

(175). Liu Z, Pu F, Liu J, Jiang L, Yuan Q, Li Z, Ren J, Qu X. PEGylated hybrid ytterbia nanoparticles as high-performance diagnostic probes for in vivo magnetic resonance and X-ray computed tomography imaging with low systemic toxicity. Nanoscale. 2013; 5:4252–4261. [PubMed: 23546530]

(176). Jin Y, Li Y, Ma X, Zha Z, Shi L, Tian J, Dai Z. Encapsulating tantalum oxide into polypyrrole nanoparticles for X-ray CT/photoacoustic bimodal imaging-guided photothermal ablation of cancer. Biomaterials. 2014; 35:5795–5804. [PubMed: 24746966]

(177). Kandanapitiye MS, Gao M, Molter J, Flask CA, Huang SD. Synthesis, Characterization, and X-ray Attenuation Properties of Ultrasmall BiOI Nanoparticles: Toward Renal Clearable Particulate CT Contrast Agents. Inorg. Chem. 2014; 53:10189–10194. [PubMed: 25283335]

(178). Chen J, Yang X, Meng Y, Huang H, Qin M, Yan D, Zhao Y, Ma Z. In vitro and in vivo CT imaging using bismuth sulfide modified with a highly biocompatible Pluronic F127. Nanotechnology. 2014; 25:295103. [PubMed: 24990410]

(179). Brown AL, Naha PC, Benavides-Montes V, Litt HI, Goforth AM, Cormode DP. Synthesis, X-ray Opacity, and Biological Compatibility of Ultra-High Payload Elemental Bismuth Nanoparticle X-ray Contrast Agents. Chem. Mater. 2014; 26:2266–2274. [PubMed: 24803727]

(180). Hallouard F, Briancon S, Anton N, Li X, Vandamme T, Fessi H. Poly(ethylene glycol)-poly(epsilon-caprolactone) Iodinated Nanocapsules as Contrast Agents for X-ray Imaging. Pharm. Res. 2013; 30:2023–2035. [PubMed: 23619594]

(181). Sosna J, Havivi E, Khan W, Appelbaum L, Nyska A, Domb AJ. Computed tomography of Lipiodol-loaded biodegradable pasty polymer for implant visualization. Contrast Media Mol. Imaging. 2014; 9:246–251. [PubMed: 24700752]

(182). Liu YJ, Feng LX, Liu TX, Zhang L, Yao Y, Yu DX, Wang LL, Zhang N. Multifunctional pH-sensitive polymeric nanoparticles for theranostics evaluated experimentally in cancer. Nanoscale. 2014; 6:3231–3242. [PubMed: 24500240]

(183). Cheng D, Hong G, Wang W, Yuan R, Ai H, Shen J, Liang B, Gao J, Shuai X. Nonclustered magnetite nanoparticle encapsulated biodegradable polymeric micelles with enhanced properties for in vivo tumor imaging. J. Mater. Chem. 2011; 21:4796–4804.

(184). Karagoz B, Yeow J, Esser L, Prakash SM, Kuchel RP, Davis TP, Boyer C. An Efficient and Highly Versatile Synthetic Route to Prepare Iron Oxide Nanoparticles/Nanocomposites with Tunable Morphologies. Langmuir. 2014; 30:10493–10502. [PubMed: 25137176]

(185). Weissleder R, Nahrendorf M, Pittet MJ. Imaging macrophages with nanoparticles. Nat. Mater. 2014; 13:125–138. [PubMed: 24452356]

(186). Fukukawa KI, Rossin R, Hagooly A, Pressly ED, Hunt JN, Messmore BW, Wooley KL, Welch MJ, Hawker CJ. Synthesis and characterization of core-shell star copolymers for in vivo PET imaging applications. Biomacromolecules. 2008; 9:1329–1339. [PubMed: 18338840]

(187). Pressly ED, Rossin R, Hagooly A, Fukukawa KI, Messmore BW, Welch MJ, Wooley KL, Lamm MS, Hule RA, Pochan DJ, et al. Structural effects on the biodistribution and positron emission tomography (PET) imaging of well-defined Cu-64-labeled nanoparticles comprised of amphiphilic block graft copolymers. Biomacromolecules. 2007; 8:3126–3134. [PubMed: 17880180]

(188). Tu C, Ma X, House A, Kauzlarich SM, Louie AY. PET imaging and biodistribution of silicon quantum dots in mice. AACS Med. Chem. Lett. 2011; 2:285–288.

(189). Jensen AI, Binderup T, Kumar PEK, Kjaer A, Rasmussen PH, Andresen TL. Positron Emission Tomography Based Analysis of Long-Circulating Cross-Linked Triblock Polymeric Micelles in a U87MG Mouse Xenograft Model and Comparison of DOTA and CB-TE2A as Chelators of Copper-64. Biomacromolecules. 2014; 15:1625–1633. [PubMed: 24645913]

(190). Tarkin JM, Joshi FR, Rudd JHF. PET imaging of inflammation in atherosclerosis. Nat. Rev. Cardiol. 2014; 11:443–457. [PubMed: 24913061]

(191). Devaraj NK, Keliher EJ, Thurber GM, Nahrendorf M, Weissleder R. 18F Labeled Nanoparticles for in Vivo PET-CT Imaging. Bioconjug. Chem. 2009; 20:397–401. [PubMed: 19138113]

(192). Zeng D, Lee NS, Liu Y, Zhou D, Dence CS, Wooley KL, Katzenellenbogen JA, Welch MJ. 64Cu Core-Labeled Nanoparticles with High Specific Activity via Metal-Free Click Chemistry. ACS Nano. 2012; 6:5209–5219. [PubMed: 22548282]

(193). Hooker JM, O'Neil JP, Romanini DW, Taylor SE, Francis MB. Genome-free Viral Capsids as Carriers for Positron Emission Tomography Radiolabels. Mol. Imaging Biol. 2008; 10:182–191. [PubMed: 18437498]

(194). Campbell MG, Ritter T. Modern Carbon–Fluorine Bond Forming Reactions for Aryl Fluoride Synthesis. Chem. Rev. 2015; 115:612–633. [PubMed: 25474722]

(195). Tredwell M, Gouverneur V. 18F Labeling of Arenes. Angew. Chem. Int. Ed. 2012; 51:11426–11437.

(196). Cheung ENM, Alvares RDA, Oakden W, Chaudhary R, Hill ML, Pichaandi J, Mo GCH, Yip C, Macdonald PM, Stanisz GJ, et al. Polymer-Stabilized Lanthanide Fluoride Nanoparticle Aggregates as Contrast Agents for Magnetic Resonance Imaging and Computed Tomography. Chem. Mater. 2010; 22:4728–4739.

(197). Wen S, Li K, Cai H, Chen Q, Shen M, Huang Y, Peng C, Hou W, Zhu M, Zhang G, et al. Multifunctional dendrimer-entrapped gold nanoparticles for dual mode CT/MR imaging applications. Biomaterials. 2013; 34:1570–1580. [PubMed: 23199745]

(198). Li K, Wen S, Larson AC, Shen M, Zhang Z, Chen Q, Shi X, Zhang G. Multifunctional dendrimer-based nanoparticles for in vivo MR/CT dual-modal molecular imaging of breast cancer. Int. J. Nanomedicine. 2013; 8:2589–2600. [PubMed: 23888113]

(199). Majmudar MD, Yoo J, Keliher EJ, Truelove JJ, Iwamoto Y, Sena B, Dutta P, Borodovsky A, Fitzgerald K, Di Carli MF, et al. Polymeric nanoparticle PET/MR imaging allows macrophage detection in atherosclerotic plaques. Circ. Res. 2013; 112:755–761. [PubMed: 23300273]

(200). Boase NRB, Blakey I, Rolfe BE, Mardon K, Thurecht KJ. Synthesis of a multimodal molecular imaging probe based on a hyperbranched polymer architecture. Polym. Chem. 2014; 5:4450–4458.

(201). Harrison J, Bartlett CA, Cowin G, Nicholls PK, Evans CW, Clemons TD, Zdyrko B, Luzinov IA, Harvey AR, Iyer KS, et al. In vivo Imaging and Biodistribution of Multimodal Polymeric Nanoparticles Delivered to the Optic Nerve. Small. 2012; 8:1579–1589. [PubMed: 22411702]

(202). Rolfe BE, Blakey I, Squires O, Peng H, Boase NRB, Alexander C, Parsons PG, Boyle GM, Whittaker AK, Thurecht KJ. Multimodal Polymer Nanoparticles with Combined F-19 Magnetic Resonance and Optical Detection for Tunable, Targeted, Multimodal Imaging in Vivo. J. Am. Chem. Soc. 2014; 136:2413–2419. [PubMed: 24437730]

(203). Tan YF, Chandrasekharan P, Maity D, Yong CX, Chuang KH, Zhao Y, Wang S, Ding J, Feng SS. Multimodal tumor imaging by iron oxides and quantum dots formulated in poly (lactic acid)-D-alpha-tocopheryl polyethylene glycol 1000 succinate nanoparticles. Biomaterials. 2011; 32:2969–2978. [PubMed: 21257200]

(204). Miki K, Inoue T, Kobayashi Y, Nakano K, Matsuoka H, Yamauchi F, Yano T, Ohe K. Near-Infrared Dye-Conjugated Amphiphilic Hyaluronic Acid Derivatives as a Dual Contrast Agent for In Vivo Optical and Photoacoustic Tumor Imaging. Biomacromolecules. 2015; 16:219–227. [PubMed: 25402751]

(205). Fan QL, Cheng K, Yang Z, Zhang RP, Yang M, Hu X, Ma XW, Bu LH, Lu XM, Xiong XX, et al. Perylene-Diimide-Based Nanoparticles as Highly Efficient Photoacoustic Agents for Deep Brain Tumor Imaging in Living Mice. Adv. Mater. 2015; 27:843–847. [PubMed: 25376906]

(206). Nahrendorf M, Zhang H, Hembrador S, Panizzi P, Sosnovik DE, Aikawa E, Libby P, Swirski FK, Weissleder R. Nanoparticle PET-CT imaging of macrophages in inflammatory atherosclerosis. Circulation. 2008; 117:379–387. [PubMed: 18158358]

(207). Lee J, Lee TS, Ryu J, Hong S, Kang M, Im K, Kang JH, Lim SM, Park S, Song R. RGD Peptide-Conjugated Multimodal NaGdF4:Yb3+/Er3+ Nanophosphors for Upconversion Luminescence, MR, and PET Imaging of Tumor Angiogenesis. J. Nucl. Med. 2013; 54:96–103. [PubMed: 23232276]

(208). Li Y, Lin T, Luo Y, Liu Q, Xiao W, Guo W, Lac D, Zhang H, Feng C, Wachsmann-Hogiu S, et al. A smart and versatile theranostic nanomedicine platform based on nanoporphyrin. Nat. Commun. 2014; 5:4712. [PubMed: 25158161]

(209). Xing HY, Bu WB, Zhang SJ, Zheng XP, Li M, Chen F, He QJ, Zhou LP, Peng WJ, Hua YQ, et al. Multifunctional nanoprobes for upconversion fluorescence, MR and CT trimodal imaging. Biomaterials. 2012; 33:1079–1089. [PubMed: 22061493]

(210). Majmudar MD, Keliher EJ, Heidt T, Leuschner F, Truelove J, Sena BF, Gorbatov R, Iwamoto Y, Dutta P, Wojtkiewicz G, et al. Monocyte-directed RNAi targeting CCR2 improves infarct healing in atherosclerosis-prone mice. Circulation. 2013; 127:2038–2046. [PubMed: 23616627]

(211). Sowers MA, McCombs JR, Wang Y, Paletta JT, Morton SW, Dreaden EC, Boska MD, Ottaviani MF, Hammond PT, Rajca A, et al. Redox-responsive branched-bottlebrush polymers for in vivo MRI and fluorescence imaging. Nat. Commun. 2014; 5:5460–5460. [PubMed: 25403521]

(212). Sun Y, Zheng YY, Ran HT, Zhou Y, Shen HX, Chen Y, Chen HR, Krupka TM, Li A, Li P, et al. Superparamagnetic PLGA-iron oxide microcapsules for dual-modality US/MR imaging and high intensity focused US breast cancer ablation. Biomaterials. 2012; 33:5854–5864. [PubMed: 22617321]

(213). Zheng YY, Zhang YP, Ao M, Zhang P, Zhang H, Li P, Qing L, Wang ZG, Ran HT. Hematoporphyrin encapsulated PLGA microbubble for contrast enhanced ultrasound imaging and sonodynamic therapy. J. Microencapsul. 2012; 29:437–444. [PubMed: 22299595]

(214). Li K, Liu B. Polymer-encapsulated organic nanoparticles for fluorescence and photoacoustic imaging. Chem. Soc. Rev. 2014; 43:6570–6597. [PubMed: 24792930]

(215). Gong H, Dong ZL, Liu YM, Yin SN, Cheng L, Xi WY, Xiang J, Liu K, Li YG, Liu Z. Engineering of Multifunctional Nano-Micelles for Combined Photothermal and Photodynamic Therapy Under the Guidance of Multimodal Imaging. Adv. Funct. Mater. 2014; 24:6492–6502.

(216). Liu Y, Yin JJ, Nie ZH. Harnessing the collective properties of nanoparticle ensembles for cancer theranostics. Nano Res. 2014; 7:1719–1730.

(217). Rhee JW, Wu JC. Advances in nanotechnology for the management of coronary artery disease. Trends Cardiovasc. Med. 2013; 23:39–45. [PubMed: 23245913]

(218). Wickline SA, Neubauer AM, Winter P, Caruthers S, Lanza G. Applications of nanotechnology to atherosclerosis, thrombosis, and vascular biology. Arterioscler. Thromb. Vasc. Biol. 2006; 26:435–441. [PubMed: 16373609]

(219). Mulder WJM, Jaffer FA, Fayad ZA, Nahrendorf M. Imaging and Nanomedicine in Inflammatory Atherosclerosis. Sci. Transl. Med. 2014; 6:239sr231.

(220). You DG, Sarayanakumar G, Son S, Han HS, Heo R, Kim K, Kwon IC, Lee JY, Park JH. Dextran sulfate-coated superparamagnetic iron oxide nanoparticles as a contrast agent for atherosclerosis imaging. Carbohydr. Polym. 2014; 101:1225–1233. [PubMed: 24299895]

(221). Wang YQ, Wang F, Deng XQ, Sheng J, Chen SY, Su J. Delivery of Therapeutic AGT shRNA by PEG-Bu for Hypertension Therapy. Plos One. 2013; 8:e68651. [PubMed: 23894329]

(222). Du AW, Stenzel MH. Drug Carriers for the Delivery of Therapeutic Peptides. Biomacromolecules. 2014; 15:1097–1114. [PubMed: 24661025]

(223). Chan JM, Rhee J, Drum CL, Bronson RT, Golomb G, Langer R, Farokhzad OC. In vivo prevention of arterial restenosis with paclitaxel-encapsulated targeted lipid–polymeric nanoparticles. Proc. Natl. Acad. Sci. U. S. A. 2011; 108:19347–19352. [PubMed: 22087004]

(224). Karagkiozaki V. Nanomedicine highlights in atherosclerosis. J. Nanopart. Res. 2013; 15:1–17.

(225). Chan JM, Zhang LF, Tong R, Ghosh D, Gao WW, Liao G, Yuet KP, Gray D, Rhee JW, Cheng JJ, et al. Spatiotemporal controlled delivery of nanoparticles to injured vasculature. Proc. Natl. Acad. Sci. U. S. A. 2010; 107:2213–2218. [PubMed: 20133865]

(226). Kamaly N, Fredman G, Subramanian M, Gadde S, Pesic A, Cheung L, Fayad ZA, Langer R, Tabas I, Farokhzad OC. Development and in vivo efficacy of targeted polymeric inflammation-resolving nanoparticles. Proc. Natl. Acad. Sci. U. S. A. 2013; 110:6506–6511. [PubMed: 23533277]

(227). Gundogan B, Tan A, Farhatnia Y, Alavijeh MS, Cui Z, Seifalian AM. Bioabsorbable stent quo vadis: a case for nano-theranostics. Theranostics. 2014; 4:514–533. [PubMed: 24672583]

(228). Jeewandara TM, Wise SG, Ng MKC. Biocompatibility of Coronary Stents. Materials. 2014; 7:769–786.

(229). Oh B, Lee CH. Advanced Cardiovascular Stent Coated with Nanofiber. Mol. Pharm. 2013; 10:4432–4442. [PubMed: 24050259]

(230). Bigdeli AK, Lyer S, Detsch R, Boccaccini AR, Beier JP, Kneser U, Horch RE, Arkudas A. Nanotechnologies in tissue engineering. Nanotechnol. Rev. 2013; 2:411–425.

(231). Lupi A, Secco GG, Rognoni A, Lazzero M, Fattori R, Sheiban I, Bongo AS, Bolognese L, Agostoni P, Porto I. Meta-analysis of bioabsorbable versus durable polymer drug-eluting stents in 20,005 patients with coronary artery disease: An update. Catheter. Cardiovasc. Interv. 2014; 83:E193–E206. [PubMed: 24478247]

(232). [accessed Feb 11, 2015] The clinical trial database service of the U.S. National Institutes of Health. https://clinicaltrials.gov

(233). Lee J, Jun I, Park HJ, Kang TJ, Shin H, Cho SW. Genetically Engineered Myoblast Sheet for Therapeutic Angiogenesis. Biomacromolecules. 2014; 15:361–372. [PubMed: 24304175]

(234). Venditto VJ, Szoka FC Jr. Cancer nanomedicines: so many papers and so few drugs! Adv. Drug Deliv. Rev. 2013; 65:80–88. [PubMed: 23036224]

(235). The National Library of Medicine. [accessed Feb 11, 2015] https://www.nlm.nih.gov

(236). Wicki A, Witzigmann D, Balasubramanian V, Huwyler J. Nanomedicine in cancer therapy: challenges, opportunities, and clinical applications. J. Control. Release. 2015; 200:138–157. [PubMed: 25545217]

(237). Garbuzenko OB, Mainelis G, Taratula O, Minko T. Inhalation treatment of lung cancer: the influence of composition, size and shape of nanocarriers on their lung accumulation and retention. Cancer Biol. Med. 2014; 11:44–55. [PubMed: 24738038]

(238). Taratula O, Garbuzenko OB, Chen AM, Minko T. Innovative strategy for treatment of lung cancer: targeted nanotechnology-based inhalation co-delivery of anticancer drugs and siRNA. J. Drug Target. 2011; 19:900–914. [PubMed: 21981718]

(239). Zhang S, Zou J, Elsabahy M, Karwa A, Li A, Moore DA, Dorshow RB, Wooley KL. Poly (ethylene oxide)-block-polyphosphester-based paclitaxel conjugates as a platform for ultra-high paclitaxel-loaded multifunctional nanoparticles. Chem. Sci. 2013; 4:2122–2126. [PubMed: 25152808]

(240). Zou J, Zhang F, Zhang S, Pollack SF, Elsabahy M, Fan J, Wooley KL. Poly(ethylene oxide)-block-polyphosphoester-graft-paclitaxel conjugates with acid-labile linkages as a pH-sensitive and functional nanoscopic platform for paclitaxel delivery. Adv. Healthc. Mater. 2014; 3:441–448. [PubMed: 23997013]

(241). Dhar S, Kolishetti N, Lippard SJ, Farokhzad OC. Targeted delivery of a cisplatin prodrug for safer and more effective prostate cancer therapy in vivo. Proc. Natl. Acad. Sci. U. S. A. 2011; 108:1850–1855. [PubMed: 21233423]

(242). Dhar S, Gu FX, Langer R, Farokhzad OC, Lippard SJ. Targeted delivery of cisplatin to prostate cancer cells by aptamer functionalized Pt(IV) prodrug-PLGA-PEG nanoparticles. Proc. Natl. Acad. Sci. U. S. A. 2008; 105:17356–17361. [PubMed: 18978032]

(243). Graf N, Bielenberg DR, Kolishetti N, Muus C, Banyard J, Farokhzad OC, Lippard SJ. αVβ3 Integrin-Targeted PLGA-PEG Nanoparticles for Enhanced Anti-tumor Efficacy of a Pt(IV) Prodrug. ACS Nano. 2012; 6:4530–4539. [PubMed: 22584163]

(244). Kolishetti N, Dhar S, Valencia PM, Lin LQ, Karnik R, Lippard SJ, Langer R, Farokhzad OC. Engineering of self-assembled nanoparticle platform for precisely controlled combination drug therapy. Proc. Natl. Acad. Sci. U. S. A. 2010; 107:17939–17944. [PubMed: 20921363]

(245). Johnstone TC, Kulak N, Pridgen EM, Farokhzad OC, Langer R, Lippard SJ. Nanoparticle encapsulation of mitaplatin and the effect thereof on in vivo properties. ACS Nano. 2013; 7:5675–5683. [PubMed: 23697579]

(246). Dhar S, Lippard SJ. Mitaplatin, a potent fusion of cisplatin and the orphan drug dichloroacetate. Proc. Natl. Acad. Sci. U. S. A. 2009; 106:22199–22204. [PubMed: 20007777]

(247). Bonnet S, Archer SL, Allalunis-Turner J, Haromy A, Beaulieu C, Thompson R, Lee CT, Lopaschuk GD, Puttagunta L, Bonnet S, et al. A Mitochondria-K+ Channel Axis Is Suppressed in Cancer and Its Normalization Promotes Apoptosis and Inhibits Cancer Growth. Cancer Cell. 2007; 11:37–51. [PubMed: 17222789]

(248). Marrache S, Pathak RK, Dhar S. Detouring of cisplatin to access mitochondrial genome for overcoming resistance. Proc. Natl. Acad. Sci. U. S. A. 2014; 111:10444–10449. [PubMed: 25002500]

(249). Dahlman JE, Barnes C, Khan OF, Thiriot A, Jhunjunwala S, Shaw TE, Xing YP, Sager HB, Sahay G, Speciner L, et al. In vivo endothelial siRNA delivery using polymeric nanoparticles with low molecular weight. Nat. Nanotechnol. 2014; 9:648–655. [PubMed: 24813696]

(250). Hasan W, Chu K, Gullapalli A, Dunn SS, Enlow EM, Luft JC, Tian S, Napier ME, Pohlhaus PD, Rolland JP, et al. Delivery of Multiple siRNAs Using Lipid-Coated PLGA Nanoparticles for Treatment of Prostate Cancer. Nano Lett. 2011; 12:287–292. [PubMed: 22165988]

(251). Rolland JP, Maynor BW, Euliss LE, Exner AE, Denison GM, DeSimone JM. Direct fabrication and harvesting of monodisperse, shape-specific nanobiomaterials. J. Am. Chem. Soc. 2005; 127:10096–100100. [PubMed: 16011375]

(252). Euliss LE, DuPont JA, Gratton S, DeSimone J. Imparting size, shape, and composition control of materials for nanomedicine. Chem. Soc. Rev. 2006; 35:1095–1104. [PubMed: 17057838]

(253). Wang J, Byrne JD, Napier ME, DeSimone JM. More effective nanomedicines through particle design. Small. 2011; 7:1919–1931. [PubMed: 21695781]

(254). Gratton SEA, Ropp PA, Pohlhaus PD, Luft JC, Madden VJ, Napier ME, DeSimone JM. The effect of particle design on cellular internalization pathways. Proc. Natl. Acad. Sci. U. S. A. 2008; 105:11613–11618. [PubMed: 18697944]

(255). Chu KS, Hasan W, Rawal S, Walsh MD, Enlow EM, Luft JC, Bridges AS, Kuijer JL, Napier ME, Zamboni WC. Plasma, tumor and tissue pharmacokinetics of Docetaxel delivered via nanoparticles of different sizes and shapes in mice bearing SKOV-3 human ovarian carcinoma xenograft. Nanomedicine. 2013; 9:686–693. [PubMed: 23219874]

(256). Lehar J, Krueger AS, Avery W, Heilbut AM, Johansen LM, Price ER, Rickles RJ, Short GF Iii, Staunton JE, Jin X, et al. Synergistic drug combinations tend to improve therapeutically relevant selectivity. Nat. Biotechnol. 2009; 27:659–666. [PubMed: 19581876]

(257). Al-Lazikani B, Banerji U, Workman P. Combinatorial drug therapy for cancer in the post-genomic era. Nat. Biotechnol. 2012; 30:679–692. [PubMed: 22781697]

(258). Alexis F. Nano-Polypharmacy to Treat Tumors: Coencapsulation of Drug Combinations Using Nanoparticle Technology. Mol. Ther. 2014; 22:1239–1240. [PubMed: 24981439]

(259). Mayer LD, Janoff AS. Optimizing combination chemotherapy by controlling drug ratios. Mol. Interv. 2007; 7:216–223. [PubMed: 17827442]

(260). Aryal S, Hu CM, Zhang L. Combinatorial drug conjugation enables nanoparticle dual-drug delivery. Small. 2010; 6:1442–1448. [PubMed: 20564488]

(261). Ma L, Kohli M, Smith A. Nanoparticles for combination drug therapy. ACS Nano. 2013; 7:9518–9525. [PubMed: 24274814]

(262). Cho H, Lai TC, Tomoda K, Kwon GS. Polymeric micelles for multi-drug delivery in cancer. AAPS PharmSciTech. 2015; 16:10–20. [PubMed: 25501872]

(263). Mignani S, Bryszewska M, Klajnert-Maculewicz B, Zablocka M, Majoral JP. Advances in combination therapies based on nanoparticles for efficacious cancer treatment: an analytical report. Biomacromolecules. 2015; 16:1–27. [PubMed: 25426779]

(264). Saraswathy M, Gong S. Recent developments in the co-delivery of siRNA and small molecule anticancer drugs for cancer treatment. Mater. Today. 2014; 17:298–306.

(265). Blanco E, Sangai T, Wu S, Hsiao A, Ruiz-Esparza G,U, Gonzalez-Delgado CA, Cara FE, Granados-Principal S, Evans KW, Akcakanat A, et al. Colocalized Delivery of Rapamycin and Paclitaxel to Tumors Enhances Synergistic Targeting of the PI3K/Akt/mTOR Pathway. Mol. Ther. 2014; 22:1310–1319. [PubMed: 24569835]

(266). Chou T. Theoretical basis, experimental design, and computerized simulation of synergism and antagonism in drug combination studies. Pharmacol. Rev. 2006; 58:621–681. [PubMed: 16968952]

(267). Chou T. Drug combination studies and their synergy quantification using the Chou-Talalay method. Cancer Res. 2010; 70:440–446. [PubMed: 20068163]

(268). Liao LY, Liu J, Dreaden EC, Morton SW, Shopsowitz KE, Hammond PT, Johnson JA. A Convergent Synthetic Platform for Single-Nanoparticle Combination Cancer Therapy: Ratiometric Loading and Controlled Release of Cisplatin, Doxorubicin, and Camptothecin. J. Am. Chem. Soc. 2014; 136:5896–5899. [PubMed: 24724706]

(269). Lutz J, Laschewsky A. Multicompartment Micelles: Has the Long-Standing Dream Become a Reality? Macromol. Chem. Phys. 2005; 206:813–817.

(270). Moughton AO, Hillmyer MA, Lodge TP. Multicompartment block polymer micelles. Macromolecules. 2011; 45:2–19.

(271). Nomoto T, Fukushima S, Kumagai M, Machitani K, Arnida, Matsumoto Y, Oba M, Miyata K, Osada K, Nishiyama N, et al. Three-layered polyplex micelle as a multifunctional nanocarrier platform for light-induced systemic gene transfer. Nat. Commun. 2014; 5:3545. [PubMed: 24694458]

(272). Synatschke CV, Nomoto T, Cabral H, Förtsch M, Toh K, Matsumoto Y, Miyazaki K, Hanisch A, Schacher FH, Kishimura A, et al. Multicompartment Micelles with Adjustable Poly(ethylene glycol) Shell for Efficient in Vivo Photodynamic Therapy. ACS Nano. 2014; 8:1161–1172. [PubMed: 24386876]

(273). Yuan Y, Mao C, Du X, Du J, Wang F, Wang J. Surface charge switchable nanoparticles based on zwitterionic polymer for enhanced drug delivery to tumor. Adv. Mater. 2012; 24:5476–5480. [PubMed: 22886872]

(274). Yang XZ, Du JZ, Dou S, Mao CQ, Long HY, Wang J. Sheddable ternary nanoparticles for tumor acidity-targeted siRNA delivery. ACS Nano. 2012; 6:771–781. [PubMed: 22136582]

(275). Zhu L, Wang T, Perche F, Taigind A, Torchilin VP. Enhanced anticancer activity of nanopreparation containing an MMP2-sensitive PEG-drug conjugate and cell-penetrating moiety. Proc. Natl. Acad. Sci. U. S. A. 2013; 110:17047–17052. [PubMed: 24062440]

(276). Huang R, Mocherla S, Heslinga M, Charoenphol P, Eniola Adefeso O. Dynamic and cellular interactions of nanoparticles in vascular-targeted drug delivery. Mol. Membr. Biol. 2010; 27:312–327. [PubMed: 21028938]

(277). Zhao F, Zhao Y, Liu Y, Chang X, Chen C. Cellular uptake, intracellular trafficking, and cytotoxicity of nanomaterials. Small. 2011; 7:1322–1337. [PubMed: 21520409]

(278). Davis SS. Biomedical applications of nanotechnology--implications for drug targeting and gene therapy. Trends Biotechnol. 1997; 15:217–224. [PubMed: 9183864]

(279). Niven RW. Delivery of biotherapeutics by inhalation aerosol. Crit. Rev. Ther. Drug Carrier Syst. 1995; 12:151–231. [PubMed: 9501969]

(280). Tsapis N, Bennett D, Jackson B, Weitz DA, Edwards DA. Trojan particles: large porous carriers of nanoparticles for drug delivery. Proc. Natl. Acad. Sci. U. S. A. 2002; 99:12001–12005. [PubMed: 12200546]

(281). Sung JC, Pulliam BL, Edwards DA. Nanoparticles for drug delivery to the lungs. Trends Biotechnol. 2007; 25:563–570. [PubMed: 17997181]

(282). Gelperina S, Kisich K, Iseman MD, Heifets L. The potential advantages of nanoparticle drug delivery systems in chemotherapy of tuberculosis. Am. J. Respir. Crit. Care Med. 2005; 172:1487–1490. [PubMed: 16151040]

(283). Andrade F, Rafael D, Videira M, Ferreira D, Sosnik A, Sarmento B. Nanotechnology and pulmonary delivery to overcome resistance in infectious diseases. Adv. Drug Deliv. Rev. 2013; 65:1816–1827. [PubMed: 23932923]

(284). Engler AC, Wiradharma N, Ong ZY, Coady DJ, Hedrick JL, Yang Y. Emerging trends in macromolecular antimicrobials to fight multi-drug-resistant infections. Nano Today. 2012; 7:201–222.

(285). Chen J, Wang F, Liu Q, Du J. Antibacterial polymeric nanostructures for biomedical applications. Chem. Commun. 2014; 50:14482–14493.

(286). Nederberg F, Zhang Y, Tan JPK, Xu K, Wang H, Yang C, Gao S, Guo XD, Fukushima K, Li L. Biodegradable nanostructures with selective lysis of microbial membranes. Nat. chem. 2011; 3:409–414. [PubMed: 21505501]

(287). Qiao Y, Yang C, Coady DJ, Ong ZY, Hedrick JL, Yang Y. Highly dynamic biodegradable micelles capable of lysing Gram-positive and Gram-negative bacterial membrane. Biomaterials. 2012; 33:1146–1153. [PubMed: 22061492]

(288). Zhang J, Chen YP, Miller KP, Ganewatta MS, Bam M, Yan Y, Nagarkatti M, Decho AW, Tang C. Antimicrobial Metallopolymers and Their Bioconjugates with Conventional Antibiotics against Multidrug-Resistant Bacteria. J. Am. Chem. Soc. 2014; 136:4873–4876. [PubMed: 24628053]

(289). Shah PN, Lin LY, Smolen JA, Tagaev JA, Gunsten SP, Han DS, Heo GS, Li Y, Zhang F, Zhang S, et al. Synthesis, characterization, and in vivo efficacy of shell cross-linked nanoparticle formulations carrying silver antimicrobials as aerosolized therapeutics. ACS Nano. 2013; 7:4977–4987. [PubMed: 23718195]

(290). Lim YH, Tiemann KM, Heo GS, Wagers PO, Rezenom YH, Zhang S, Zhang F, Youngs WJ, Hunstad DA, Wooley KL. Preparation and in Vitro Antimicrobial Activity of Silver-Bearing Degradable Polymeric Nanoparticles of Polyphosphoester-block-Poly(l-lactide). ACS Nano. 2015; 9:1995–2008. [PubMed: 25621868]

(291). Zhang F, Smolen JA, Zhang S, Li R, Shah PN, Cho S, Wang H, Raymond JE, Cannon CL, Wooley KL. Degradable polyphosphoester-based silver-loaded nanoparticles as therapeutics for bacterial lung infections. Nanoscale. 2015; 7:2265–2270. [PubMed: 25573163]

(292). Suk JS, Kim AJ, Trehan K, Schneider CS, Cebotaru L, Woodward OM, Boylan NJ, Boyle MP, Lai SK, Guggino WB, et al. Lung gene therapy with highly compacted DNA nanoparticles that overcome the mucus barrier. J. Control. Release. 2014; 178:8–17. [PubMed: 24440664]

(293). Boylan NJ, Kim AJ, Suk JS, Adstamongkonkul P, Simons BW, Lai SK, Cooper MJ, Hanes J. Enhancement of airway gene transfer by DNA nanoparticles using a pH-responsive block copolymer of polyethylene glycol and poly-L-lysine. Biomaterials. 2012; 33:2361–2371. [PubMed: 22182747]

(294). Radovic-Moreno AF, Lu TK, Puscasu VA, Yoon CJ, Langer R, Farokhzad OC. Surface charge-switching polymeric nanoparticles for bacterial cell wall-targeted delivery of antibiotics. ACS nano. 2012; 6:4279–4287. [PubMed: 22471841]

(295). Xiong M, Bao Y, Yang X, Wang Y, Sun B, Wang J. Lipase-sensitive polymeric triple-layered nanogel for “on-demand” drug delivery. J. Am. Chem. Soc. 2012; 134:4355–4362. [PubMed: 22304702]

(296). Xiong M, Li Y, Bao Y, Yang X, Hu B, Wang J. Bacteria-Responsive Multifunctional Nanogel for Targeted Antibiotic Delivery. Adv. Mater. 2012; 24:6175–6180. [PubMed: 22961974]

(297). Wang Z, Niu G, Chen X. Polymeric materials for theranostic applications. Pharm. Res. 2014; 31:1358–1376. [PubMed: 23765400]

(298). Chen Q, Wang C, Cheng L, He W, Cheng Z, Liu Z. Protein modified upconversion nanoparticles for imaging-guided combined photothermal and photodynamic therapy. Biomaterials. 2014; 35:2915–2923. [PubMed: 24412081]

(299). Idris NM, Gnanasammandhan MK, Zhang J, Ho PC, Mahendran R, Zhang Y. In vivo photodynamic therapy using upconversion nanoparticles as remote-controlled nanotransducers. Nat. Med. 2012; 18:1580–1585. [PubMed: 22983397]

(300). Liu K, Liu X, Zeng Q, Zhang Y, Tu L, Liu T, Kong X, Wang Y, Cao F, Lambrechts SA, et al. Covalently assembled NIR nanoplatform for simultaneous fluorescence imaging and photodynamic therapy of cancer cells. ACS Nano. 2012; 6:4054–4062. [PubMed: 22463487]

(301). Wang C, Tao H, Cheng L, Liu Z. Near-infrared light induced in vivo photodynamic therapy of cancer based on upconversion nanoparticles. Biomaterials. 2011; 32:6145–6154. [PubMed: 21616529]

(302). Park YI, Kim HM, Kim JH, Moon KC, Yoo B, Lee KT, Lee N, Choi Y, Park W, Ling D, et al. Theranostic probe based on lanthanide-doped nanoparticles for simultaneous in vivo dual-modal imaging and photodynamic therapy. Adv. Mater. 2012; 24:5755–5761. [PubMed: 22915170]

(303). Cheng L, Yang K, Li Y, Chen J, Wang C, Shao M, Lee ST, Liu Z. Facile preparation of multifunctional upconversion nanoprobes for multimodal imaging and dual-targeted photothermal therapy. Angew. Chem. Int. Ed. 2011; 50:7385–7390.

(304). Chen H, Kim S, He W, Wang H, Low PS, Park K, Cheng JX. Fast release of lipophilic agents from circulating PEG-PDLLA micelles revealed by in vivo forster resonance energy transfer imaging. Langmuir. 2008; 24:5213–5217. [PubMed: 18257595]

(305). Savic R, Azzam T, Eisenberg A, Maysinger D. Assessment of the integrity of poly(caprolactone)-b-poly(ethylene oxide) micelles under biological conditions: a fluorogenic-based approach. Langmuir. 2006; 22:3570–3578. [PubMed: 16584228]

(306). Lee SJ, Koo H, Lee DE, Min S, Lee S, Chen X, Choi Y, Leary JF, Park K, Jeong SY, et al. Tumor-homing photosensitizer-conjugated glycol chitosan nanoparticles for synchronous photodynamic imaging and therapy based on cellular on/off system. Biomaterials. 2011; 32:4021–4029. [PubMed: 21376388]

(307). Lovell JF, Chen J, Jarvi MT, Cao WG, Allen AD, Liu Y, Tidwell TT, Wilson BC, Zheng G. FRET quenching of photosensitizer singlet oxygen generation. J. Phys. Chem. B. 2009; 113:3203–3211. [PubMed: 19708269]

(308). Koo H, Lee H, Lee S, Min KH, Kim MS, Lee DS, Choi Y, Kwon IC, Kim K, Jeong SY. In vivo tumor diagnosis and photodynamic therapy via tumoral pH-responsive polymeric micelles. Chem. Commun. 2010; 46:5668–5670.

(309). Choi Y, Weissleder R, Tung CH. Selective antitumor effect of novel protease-mediated photodynamic agent. Cancer Res. 2006; 66:7225–7229. [PubMed: 16849570]

(310). Huang P, Lin J, Li W, Rong P, Wang Z, Wang S, Wang X, Sun X, Aronova M, Niu G, et al. Biodegradable gold nanovesicles with an ultrastrong plasmonic coupling effect for photoacoustic imaging and photothermal therapy. Angew. Chem. Int. Ed. 2013; 52:13958–13964.

(311). Cheng L, Yang K, Chen Q, Liu Z. Organic stealth nanoparticles for highly effective in vivo near-infrared photothermal therapy of cancer. ACS Nano. 2012; 6:5605–5613. [PubMed: 22616847]

(312). Yang HW, Liu HL, Li ML, Hsi IW, Fan CT, Huang CY, Lu YJ, Hua MY, Chou HY, Liaw JW, et al. Magnetic gold-nanorod/ PNIPAAmMA nanoparticles for dual magnetic resonance and photoacoustic imaging and targeted photothermal therapy. Biomaterials. 2013; 34:5651–5660. [PubMed: 23602366]

(313). Shen JM, Gao FY, Yin T, Zhang HX, Ma M, Yang YJ, Yue F. cRGD-functionalized polymeric magnetic nanoparticles as a dual-drug delivery system for safe targeted cancer therapy. Pharmacol. Res. 2013; 70:102–115. [PubMed: 23376353]

(314). Ling D, Park W, Park S, Lu Y, Kim KS, Hackett MJ, Kim BH, Yim H, Jeon YS, Na K. Multifunctional Tumor pH-Sensitive Self-Assembled Nanoparticles for Bimodal Imaging and Treatment of Resistant Heterogeneous Tumors. J. Am. Chem. Soc. 2014; 136:5647–5655. [PubMed: 24689550]

(315). Park W, Yang HN, Ling D, Yim H, Kim KS, Hyeon T, Na K, Park KH. Multi-modal transfection agent based on monodisperse magnetic nanoparticles for stem cell gene delivery and tracking. Biomaterials. 2014; 35:7239–7247. [PubMed: 24881029]

(316). Agyare EK, Jaruszewski KM, Curran GL, Rosenberg JT, Grant SC, Lowe VJ, Ramakrishnan S, Paravastu AK, Poduslo JF, Kandimalla KK. Engineering theranostic nanovehicles capable of targeting cerebrovascular amyloid deposits. J. Control. Release. 2014; 185:121–129. [PubMed: 24735640]

(317). Lee JY, Choi DY, Cho MY, Park KE, Lee SH, Hun Cho S, Hong KS, Lim YT. Targeted theranostic nanoparticles: receptor-mediated entry into cells, pH-induced signal generation and cytosolic delivery. Small. 2014; 10:901–906. [PubMed: 24106164]

(318). Guo Y, Chen W, Wang W, Shen J, Guo R, Gong F, Lin S, Cheng D, Chen G, Shuai X. Simultaneous diagnosis and gene therapy of immuno-rejection in rat allogeneic heart transplantation model using a T-cell-targeted theranostic nanosystem. ACS Nano. 2012; 6:10646–10657. [PubMed: 23189971]

(319). Shrestha R, Elsabahy M, Luehmann H, Samarajeewa S, Florez-Malaver S, Lee NS, Welch MJ, Liu Y, Wooley KL. Hierarchically Assembled Theranostic Nanostructures for siRNA Delivery and Imaging Applications. J. Am. Chem. Soc. 2012; 134:17362–17365. [PubMed: 23050597]

(320). Elsabahy M, Shrestha R, Clark C, Taylor S, Leonard J, Wooley KL. Multifunctional hierarchically assembled nanostructures as complex stage-wise dual-delivery systems for coincidental yet differential trafficking of siRNA and paclitaxel. Nano Lett. 2013; 13:2172–2181. [PubMed: 23574430]

(321). Samarajeewa S, Ibricevic A, Gunsten SP, Shrestha R, Elsabahy M, Brody SL, Wooley KL. Degradable cationic shell cross-linked knedel-like nanoparticles: synthesis, degradation, nucleic acid binding, and in vitro evaluation. Biomacromolecules. 2013; 14:1018–1027. [PubMed: 23510389]

(322). Mohammad AK, Reineke JJ. Quantitative Detection of PLGA Nanoparticle Degradation in Tissues following Intravenous Administration. Mol. Pharm. 2013; 10:2183–2189. [PubMed: 23510239]

(323). Yuan F, Leunig M, Huang SK, Berk DA, Papahadjopoulos D, Jain RK. Mirovascular permeability and interstitial penetration of sterically stabilized (stealth) liposomes in a human tumor xenograft. Cancer Res. 1994; 54:3352–3356. [PubMed: 8012948]

(324). Park K. Facing the truth about nanotechnology in drug delivery. ACS Nano. 2013; 7:7442–7447. [PubMed: 24490875]

(325). Campbell RB, Fukumura D, Brown EB, Mazzola LM, Izumi Y, Jain RK, Torchilin VP, Munn LL. Cationic charge determines the distribution of liposomes between the vascular and extravascular compartments of tumors. Cancer Res. 2002; 62:6831–6836. [PubMed: 12460895]

(326). Jain RK. Delivery of molecular and cellular medicine to solid tumors. Adv. Drug Deliv. Rev. 2001; 46:149–168. [PubMed: 11259838]

(327). Minchinton AI, Tannock IF. Drug penetration in solid tumours. Nat. Rev. Cancer. 2006; 6:583–592. [PubMed: 16862189]

(328). Dean M, Fojo T, Bates S. Tumour stem cells and drug resistance. Nat. Rev. Cancer. 2005; 5:275–284. [PubMed: 15803154]

(329). Visvader JE, Lindeman GJ. Cancer stem cells in solid tumours: accumulating evidence and unresolved questions. Nat. Rev. Cancer. 2008; 8:755–768. [PubMed: 18784658]

(330). Fox ME, Szoka FC, Fréchet JMJ. Soluble Polymer Carriers for the Treatment of Cancer: The Importance of Molecular Architecture. Acc. Chem. Res. 2009; 42:1141–1151. [PubMed: 19555070]

(331). Nasongkla N, Chen B, Macaraeg N, Fox ME, Fréchet JMJ, Szoka FC. Dependence of Pharmacokinetics and Biodistribution on Polymer Architecture: Effect of Cyclic versus Linear Polymers. J. Am. Chem. Soc. 2009; 131:3842–3843. [PubMed: 19256497]

(332). Popović Z, Liu W, Chauhan VP, Lee J, Wong C, Greytak AB, Insin N, Nocera DG, Fukumura D, Jain RK, et al. A Nanoparticle Size Series for In Vivo Fluorescence Imaging. Angew. Chem. Int. Ed. 2010; 49:8649–8652.

(333). MacKay JA, Chen M, McDaniel JR, Liu W, Simnick AJ, Chilkoti A. Self-assembling chimeric polypeptide–doxorubicin conjugate nanoparticles that abolish tumours after a single injection. Nat. Mater. 2009; 8:993–999. [PubMed: 19898461]

(334). Sarin H, Kanevsky AS, Wu H, Sousa AA, Wilson CM, Aronova MA, Griffiths GL, Leapman RD, Vo HQ. Physiologic upper limit of pore size in the blood-tumor barrier of malignant solid tumors. J. Transl. Med. 2009; 7:51. [PubMed: 19549317]

(335). Cabral H, Matsumoto Y, Mizuno K, Chen Q, Murakami M, Kimura M, Terada Y, Kano MR, Miyazono K, Uesaka M, et al. Accumulation of sub-100 nm polymeric micelles in poorly permeable tumours depends on size. Nat. Nanotechnol. 2011; 6:815–823. [PubMed: 22020122]

(336). Wong C, Stylianopoulos T, Cui J, Martin J, Chauhan VP, Jiang W, Popovic Z, Jain RK, Bawendi MG, Fukumura D. Multistage nanoparticle delivery system for deep penetration into tumor tissue. Proc. Natl. Acad. Sci. U. S. A. 2011; 108:2426–2431. [PubMed: 21245339]

(337). Perrault SD, Walkey C, Jennings T, Fischer HC, Chan WC. Mediating tumor targeting efficiency of nanoparticles through design. Nano Lett. 2009; 9:1909–1915. [PubMed: 19344179]

(338). Tang L, Fan TM, Borst LB, Cheng J. Synthesis and biological response of size-specific, monodisperse drug-silica nanoconjugates. ACS Nano. 2012; 6:3954–3966. [PubMed: 22494403]

(339). Denison TA, Bae YH. Tumor heterogeneity and its implication for drug delivery. J. Control. Release. 2012; 164:187–191. [PubMed: 22537887]

(340). Ruenraroengsak P, Cook JM, Florence AT. Nanosystem drug targeting: Facing up to complex realities. J. Control. Release. 2010; 141:265–276. [PubMed: 19895862]

(341). Bae YH, Park K. Targeted drug delivery to tumors: myths, reality and possibility. J. Control. Release. 2011; 153:198–205. [PubMed: 21663778]

(342). Kwon IK, Lee SC, Han B, Park K. Analysis on the current status of targeted drug delivery to tumors. J. Control. Release. 2012; 164:108–114. [PubMed: 22800574]

(343). Nichols JW, Bae YH. Odyssey of a cancer nanoparticle: from injection site to site of action. Nano Today. 2012; 7:606–618. [PubMed: 23243460]

(344). Szebeni J, Bedocs P, Csukas D, Rosivall L, Bunger R, Urbanics R. A porcine model of complement-mediated infusion reactions to drug carrier nanosystems and other medicines. Adv. Drug Deliv. Rev. 2012; 64:1706–1716. [PubMed: 22820530]

(345). Elsabahy M, Wooley KL. Data mining as a guide for the construction of cross-linked nanoparticles with low immunotoxicity via control of polymer chemistry and supramolecular assembly. Acc. Chem. Res. 2015 10.1021/acs.accounts.1025b00066.

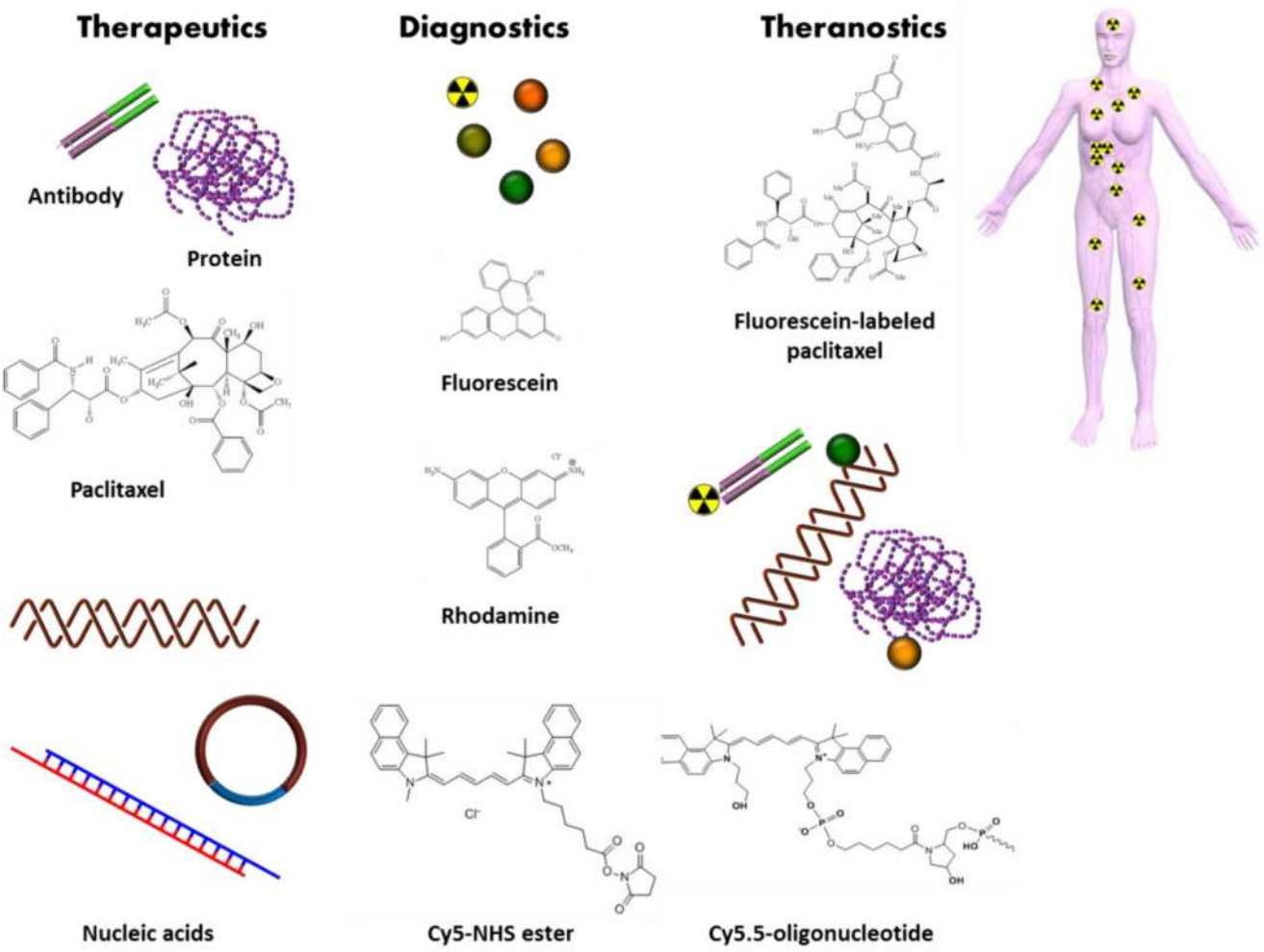

Figure 1.

Examples of therapeutics of various sizes, solubilities and structures, and diagnostics (fluorophores, radioactive probes, quantum dots, etc.), that are commonly utilized for therapy and imaging. Labeling of various therapeutics with imaging probes is also exploited for simultaneous therapy and diagnosis (theranostics). It is observed in the body inset that random biodistribution usually occurs after administration of these agents.

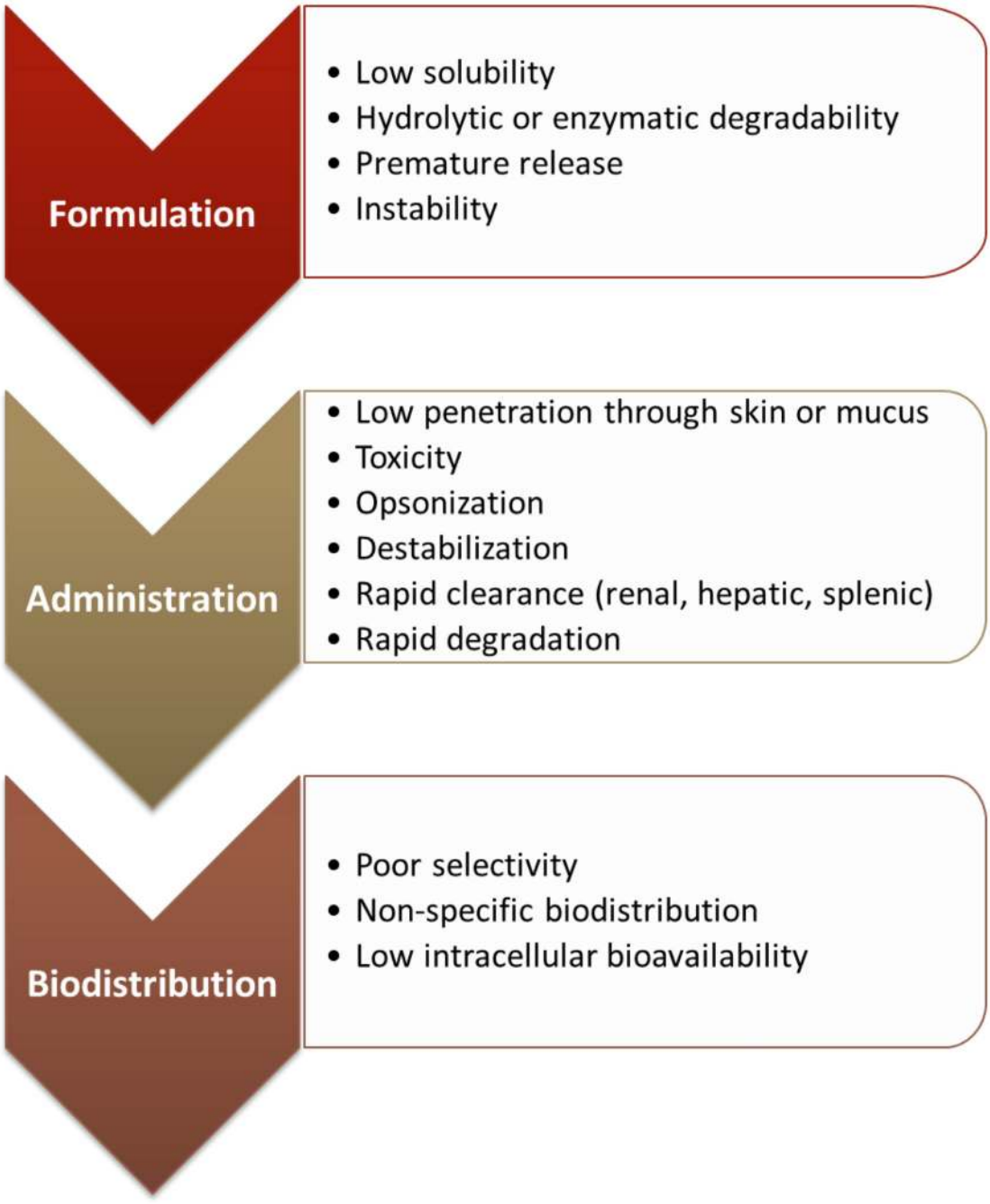

Figure 2.
The main challenges towards the use of various therapeutics, diagnostics and theranostics, during formulation, administration and the resulting biodistribution, with no control over their characteristics and navigation within the biological system.

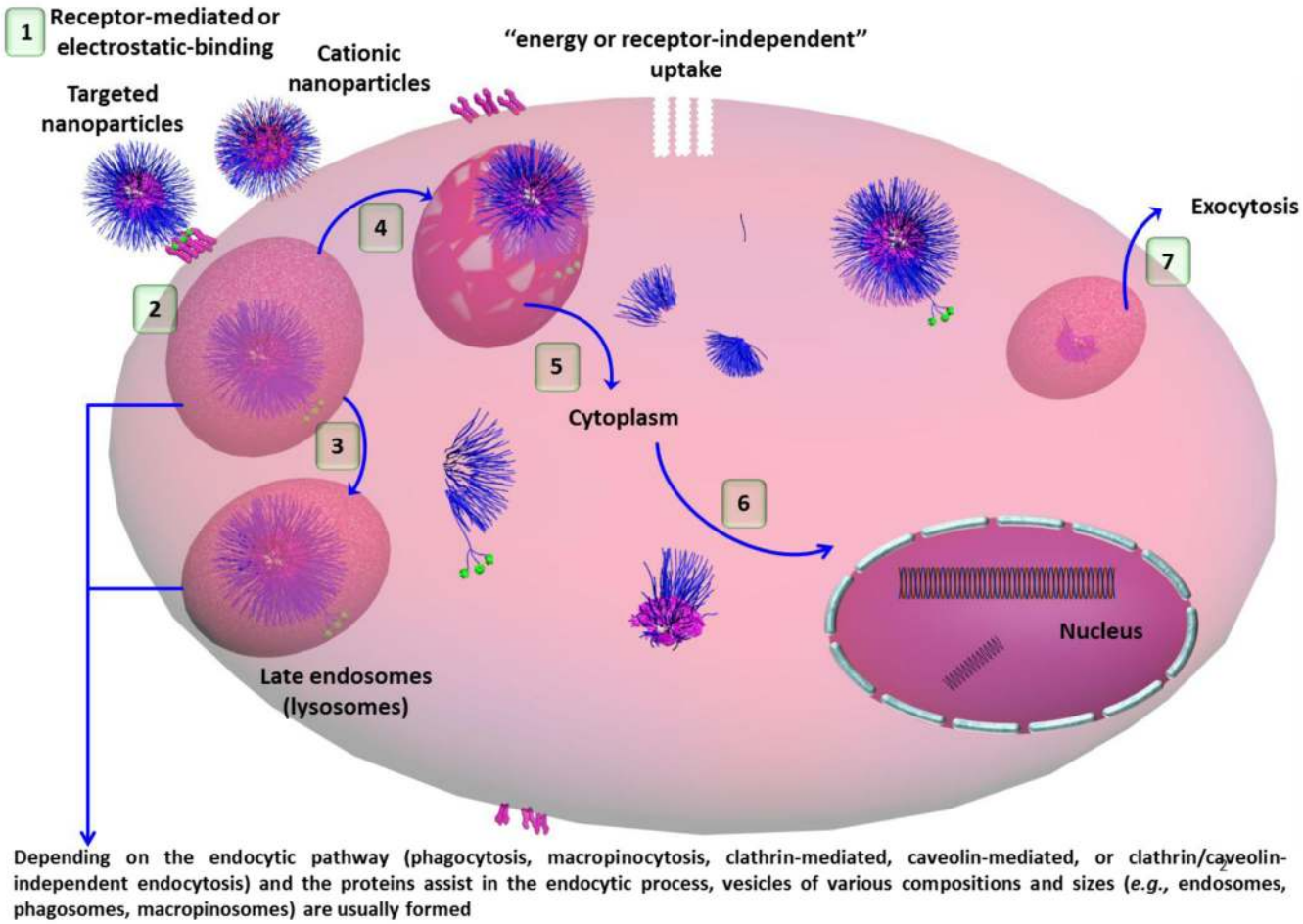

Figure 3.

Intracellular trafficking pathways: (1) Hydrophilic molecules and macromolecules usually have low cellular uptake and, thus, overall cationic charge or decoration with targeting ligands is required for efficient cellular uptake; (2) Endocytosis starts with the internalization of the nanoparticles into vesicles, that later are pinched off to form membrane-bound vesicles of different sizes, compositions and internal environments, called endosomes, phagosomes or macropinosomes, depending on the energy dependent or independent, and receptor dependent or independent internalization pathways;[42-43] (3) Degradation of nanoparticles or their cargoes usually occurs with catalysis by the acidic pH and/or enzymes found in the lysosomes; (4-6) Escape of nanoparticles or their payloads from these vesicles into the cytoplasm is essential for them to reach the targeted subcellular organelles (steps 4 and 5 represent the escape of nanoparticles or some of their components from a leaky endosomes); (7) Nanoparticles can also be cleared from the cells *via* exocytosis. Adapted with permission from Reference 35. Copyright 2012 Royal Society of Chemistry.

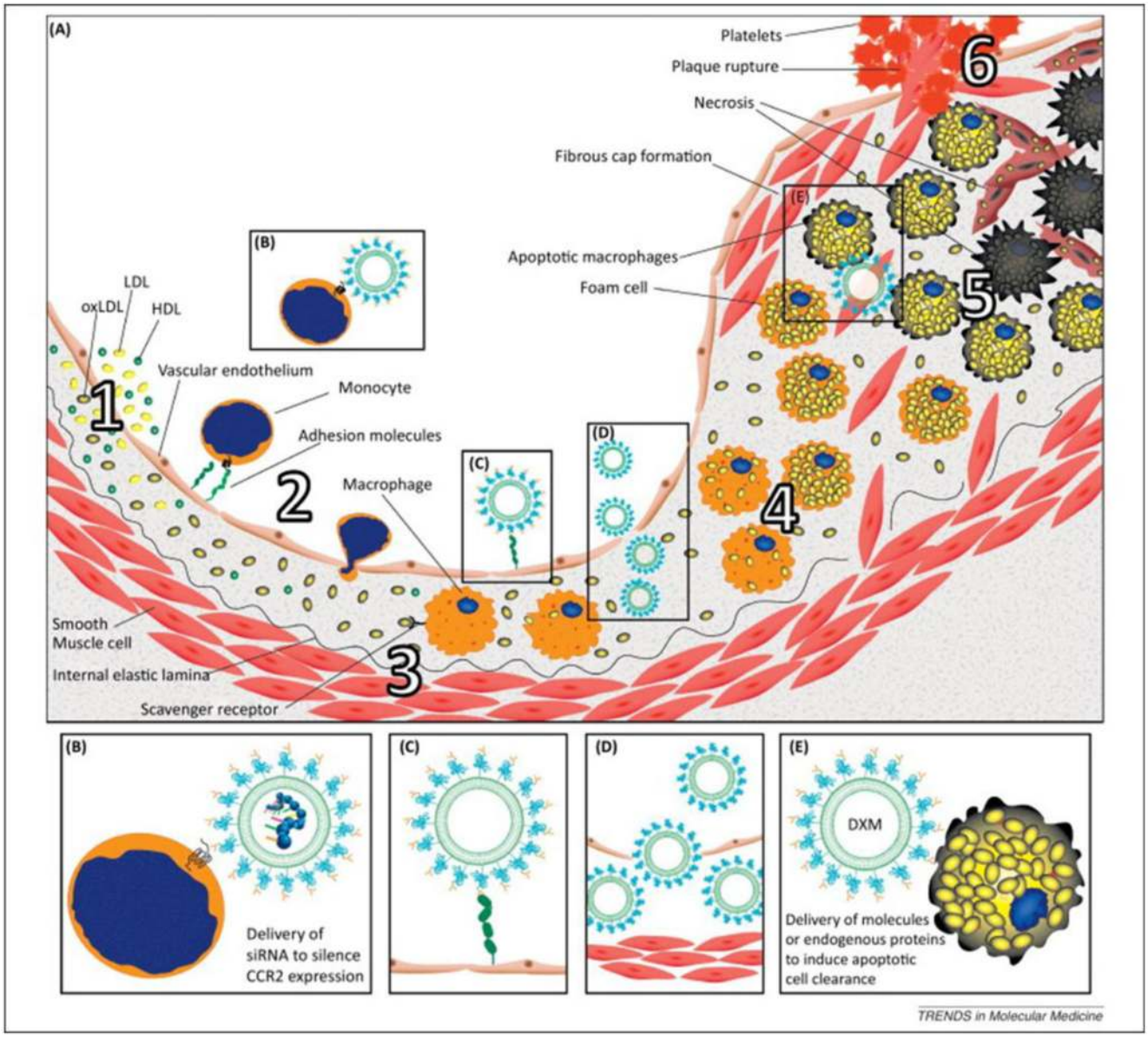

Figure 4.

Nanomedicine-based therapeutic targets in atherosclerosis. (A) Summary of mechanisms underlying atherogenesis, atheroprogression, and plaque destabilization. The leakiness of endothelial cell junctions in areas of low shear stress permits low-density lipoprotein (LDL) to enter the intima, where it is oxidized (oxLDL) (1). LDL mediates the upregulation of adhesion molecules, such as P-selectin, intercellular adhesion molecule 1 (ICAM1), and vascular cell adhesion molecule 1 (VCAM1), to recruit leukocytes, such as monocytes and neutrophils (2). Recruited macrophages engulf oxLDL *via* scavenger receptors and give rise to foam cells (3). Atheroprogression is characterized by further accumulation of leukocytes by local proliferation, ongoing recruitment, and hampered egress (4). The fate of atherosclerotic plaques is determined by the failed clearance of apoptotic cells, which leads to secondary necrosis and plaque destabilization (5). The plaque is shielded from the

bloodstream by a matrix-containing fibrous cap that is covered by endothelial cells. At late stages, the fibrous cap is weakened by matrix-degrading proteases from macrophages, leading to plaque rupture and the exposure of thrombogenic material to the bloodstream, causing platelet activation and blood clotting, which is clinically observed as myocardial infarction or stroke (6). (B) To intervene in leukocyte recruitment, circulating monocytes can be targeted to deliver nanoparticles to the lesion as 'Trojan horses' or to knock down surface receptors, such as CC-chemokine receptor 2 (CCR2), which is crucial for the adhesion to endothelial cells, by siRNA. (C) Natural ligands (as well as mimetics or antibodies) of adhesion molecules can be used as targeting entities to direct nanoparticles to atherosclerotic tissue. (D) Particles such as high-density lipoprotein (HDL) and LDL naturally home to atherosclerotic lesions, and synthetic equivalents or mimetics can be used as nanocarriers for drug delivery or as cholesterol acceptors to stimulate cholesterol efflux. The increased permeability of endothelial cells or neovessels not only allows lipoproteins to enter the lesion but also permits the entry of (untargeted, long-circulating) nanocarriers within a certain size range. (E) The fate of the stability of atherosclerotic lesion is determined by defects in the clearance of apoptotic cells. Inducing this clearance by anti-inflammatory and pro-resolving drugs [such as dexamethasone (DXM)] encapsulated into liposomes could therefore stabilize the lesion. Reprinted with permission from Reference 53.

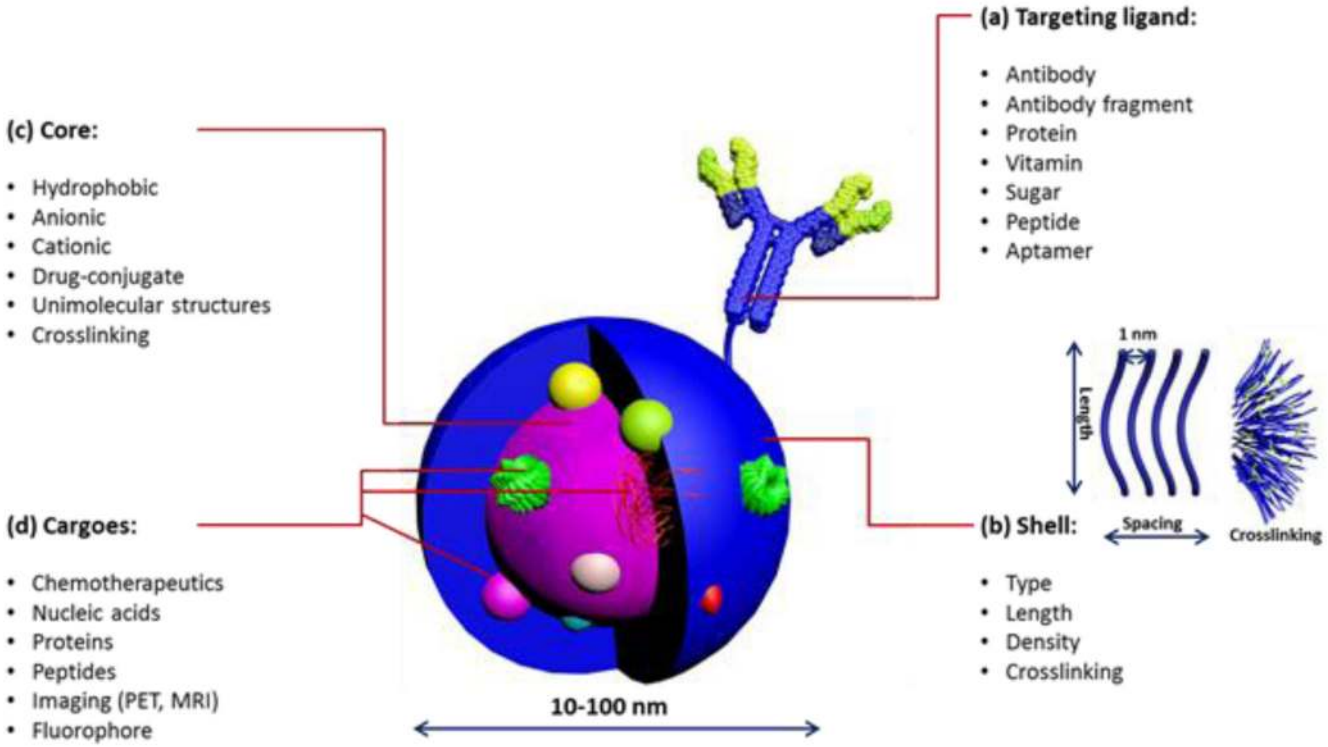

Figure 5.

Compositional versatility of multifunctional nanoparticles for biomedical delivery applications, illustrated generically for a solid core-shell polymer nanoparticle scaffold. (a) Targeting: Clusters of targeting moieties are important for multivalent binding to receptors for enhanced cellular uptake; the use of various ligands (antibody, antibody fragment, peptide, *etc*.) depends on the therapeutic application and disease type. (b) Shell: The length, spacing and crosslinking of the shell polymers are critical parameters that dictate the blood circulation time and stability of nanoparticles with ~1 nm spacing found to be efficient in preventing protein adsorption. (c) Core: The nature of the core dictates the type of the drug to be encapsulated. Crosslinking and conjugation of drugs to the core-forming polymer are common strategies for enhancing the stability of nanoparticles and drug-encapsulation efficiency, respectively. (d) Cargo: A wide range of imaging agents and/or therapeutics can be packaged, ranging from small molecules to macromolecular cargoes. Adapted with permission from References 35,81. Copyright 2012 and 2013 Royal Society of Chemistry.

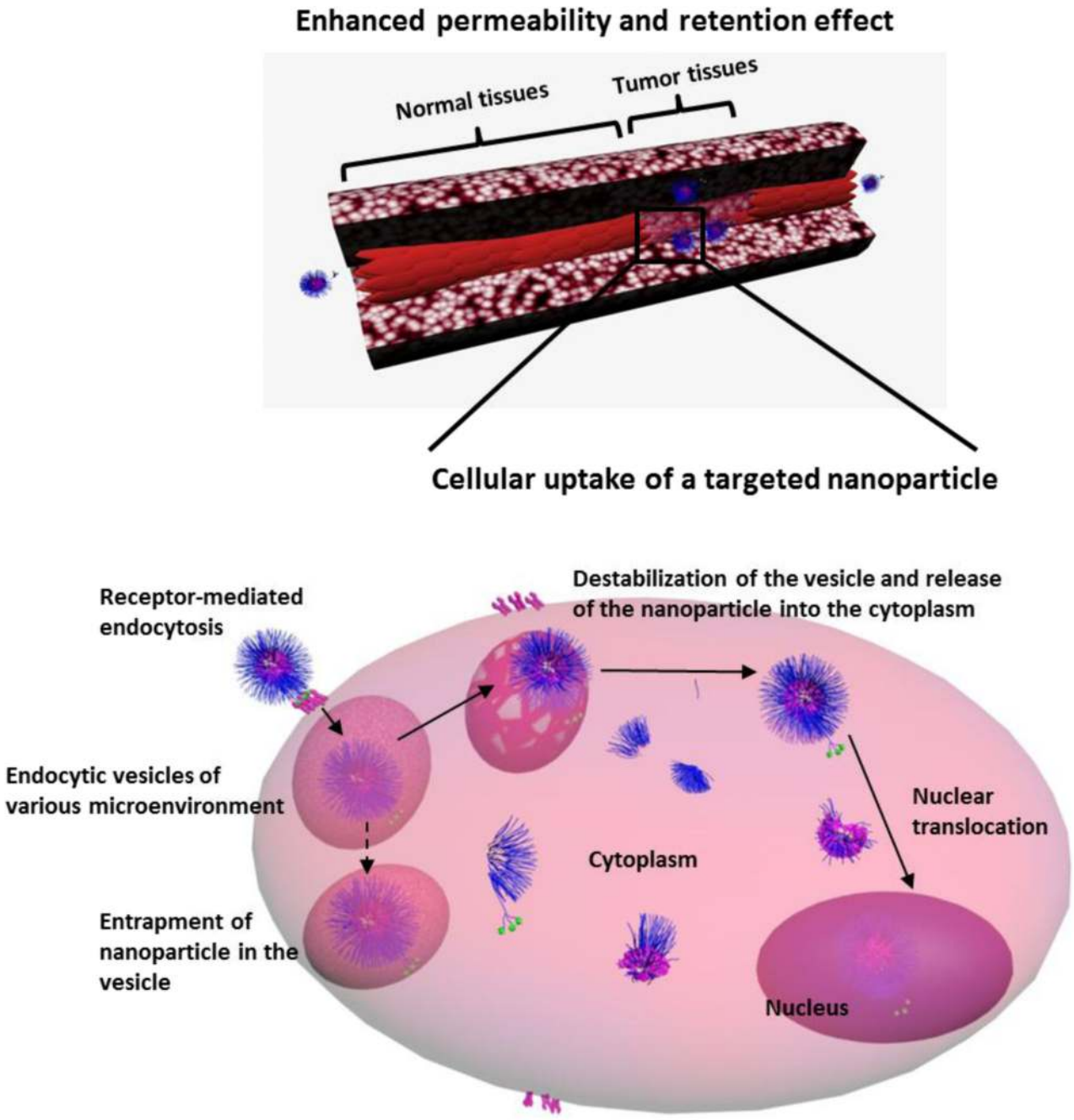

Figure 6.

Passive and active targeting features of multifunctional nanomaterials. In passive targeting, nanoparticles accumulate into pathological sites with leaky vasculature (*e.g.* tumor) due to the enhanced permeability and retention effect. In active targeting, the targeting ligands on the surface of nanoparticles enhance cellular uptake by binding to specific receptors overexpressed on the diseased cells. Targeting may also be achieved *via* facilitating escape from endosomes/lysosomes and/or enhancing nuclear translocation. Multifunctional nanoparticles have additional functionalities to deliver more than one cargo (*e.g.* more than

one type of therapeutic and/or diagnostic agent), or combine more than one targeting mechanism (*i.e.* passive and active targeting). Adapted with permission from Reference 35. Copyright 2012 Royal Society of Chemistry.

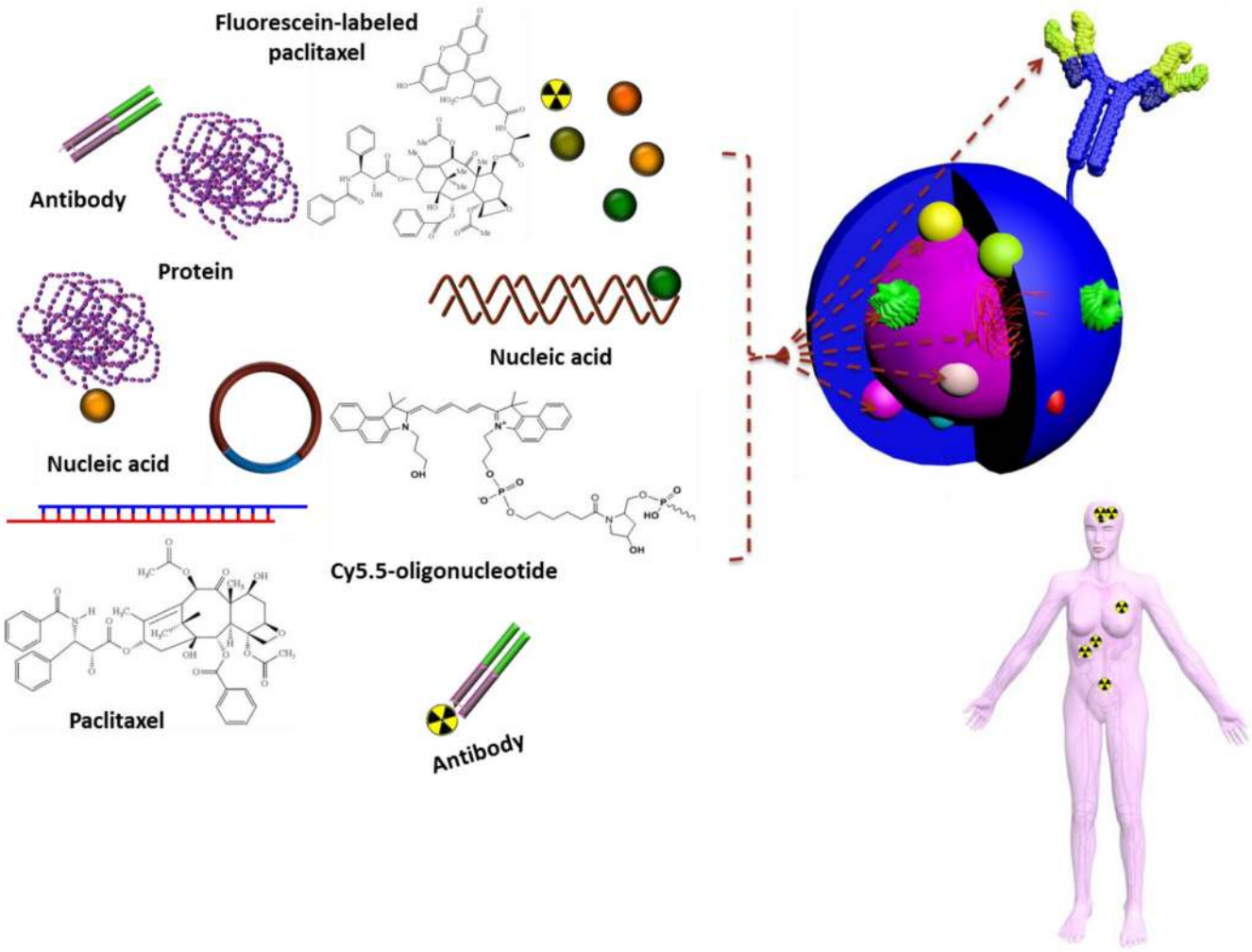

Figure 7.

Possibilities of incorporating various therapeutic and/or diagnostic agents into one set of nanomaterial. It is observed in the body inset that encapsulation of these agents into nanomaterials may re-direct their biodistribution to specific organ (brain, for example) for targeted delivery to the sites of the diseases, as compared to the free drug (*vide supra*, Figure 1).

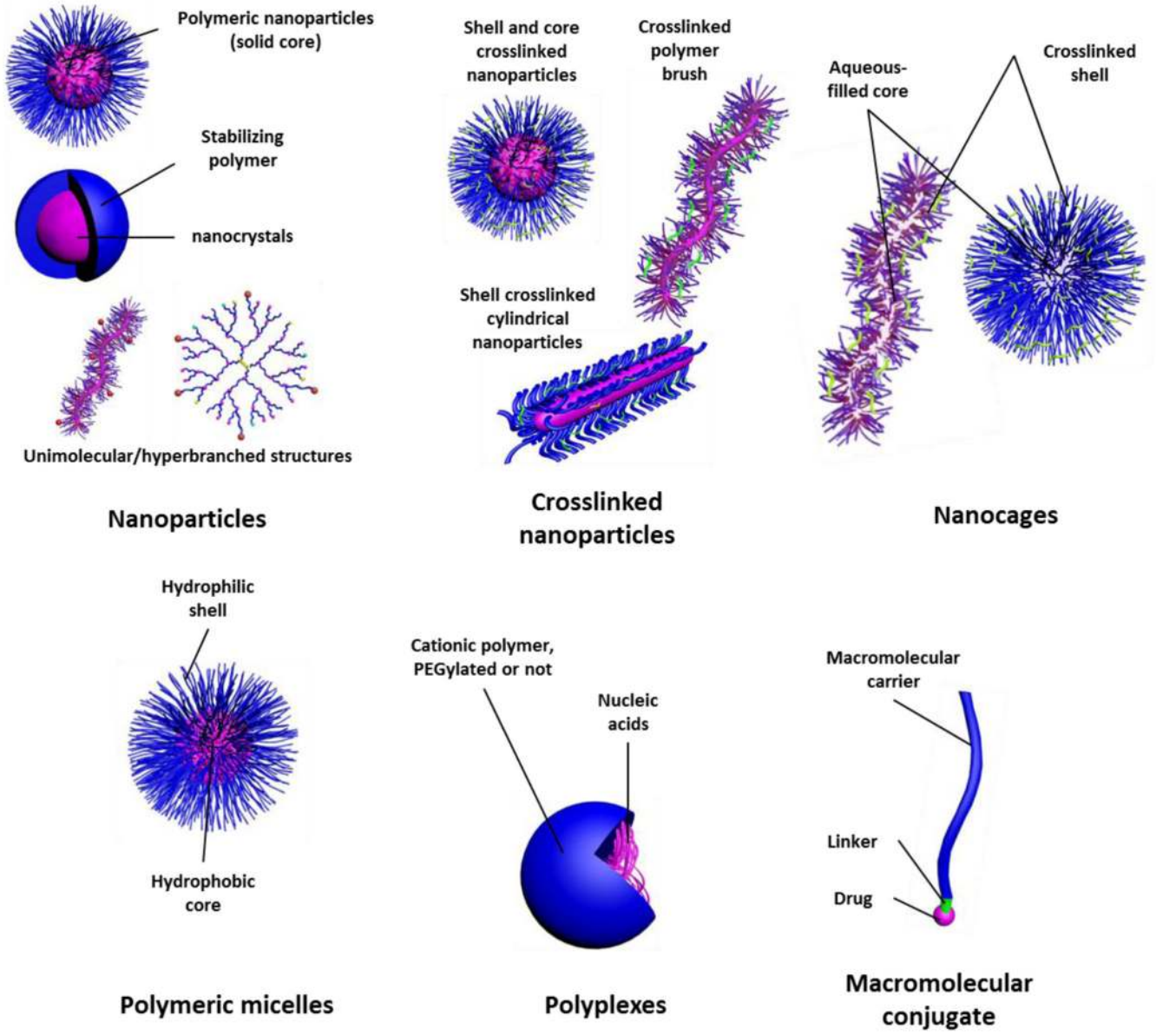

Figure 8.

Main types of polymeric nanoparticles that have been utilized for therapy and/or imaging. Adapted with permission from Reference 81. Copyright 2013 Royal Society of Chemistry.

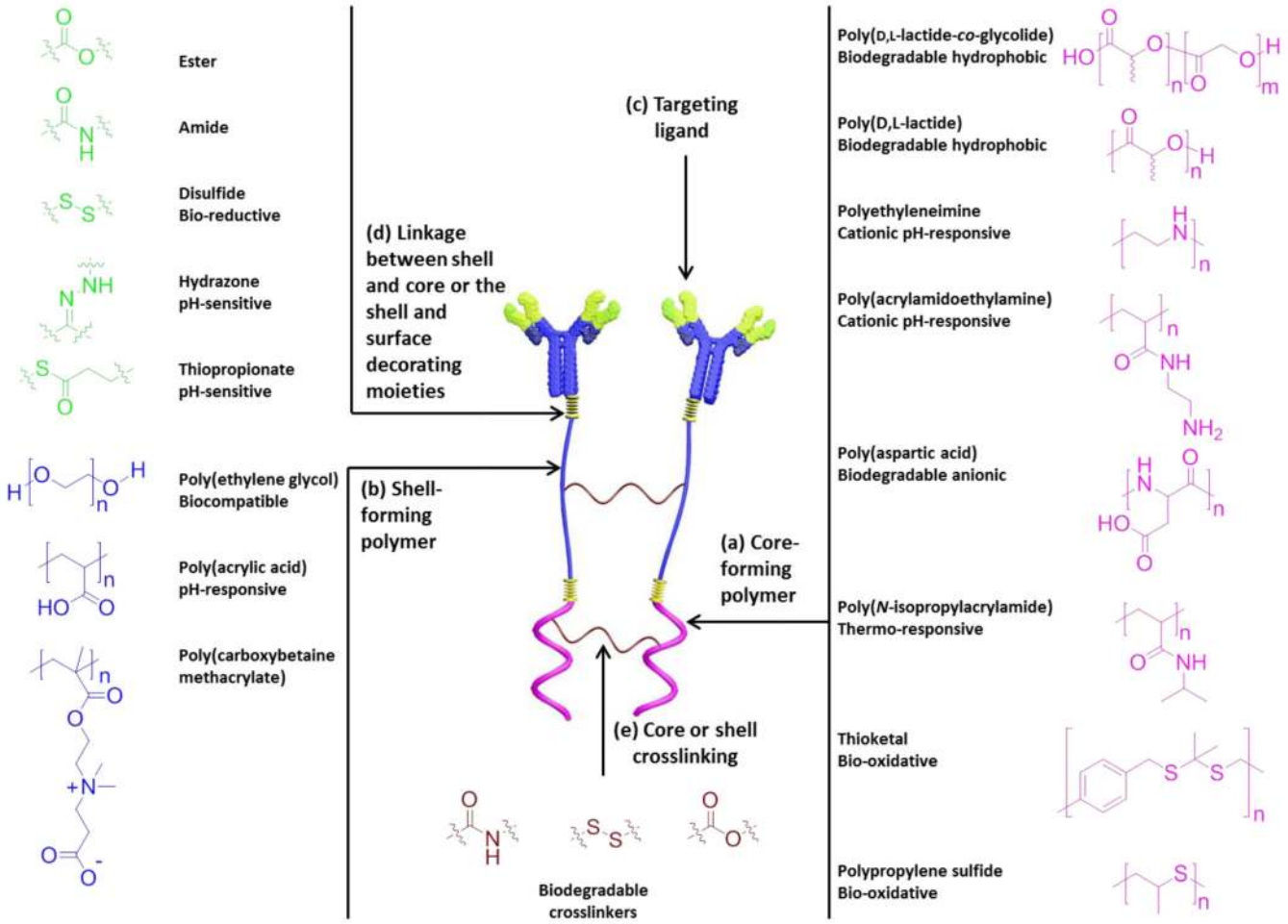

Figure 9.

Building blocks of various types of polymeric nanoparticles with examples of some commonly used polymers and linkages. The main building blocks of polymeric nanoparticles are usually comprised of core-forming polymer; hydrophobic or charged (a), shell-forming polymer; neutral, hydrophilic and flexible properties are important for stealth nanoparticles (b), targeting ligand for selective cellular uptake and accumulation at target sites (c), and linkages between the shell and core and/or targeting moieties (d). Stimuli-responsiveness (pH, temperature, enzymatic, reductive or oxidative, *etc.*) can be imparted into the core, shell and/or the linkages. Shell or core-crosslinking can be also utilized to enhance the stability of nanoparticles (e). Adapted with permission from Reference 35. Copyright 2012 Royal Society of Chemistry.

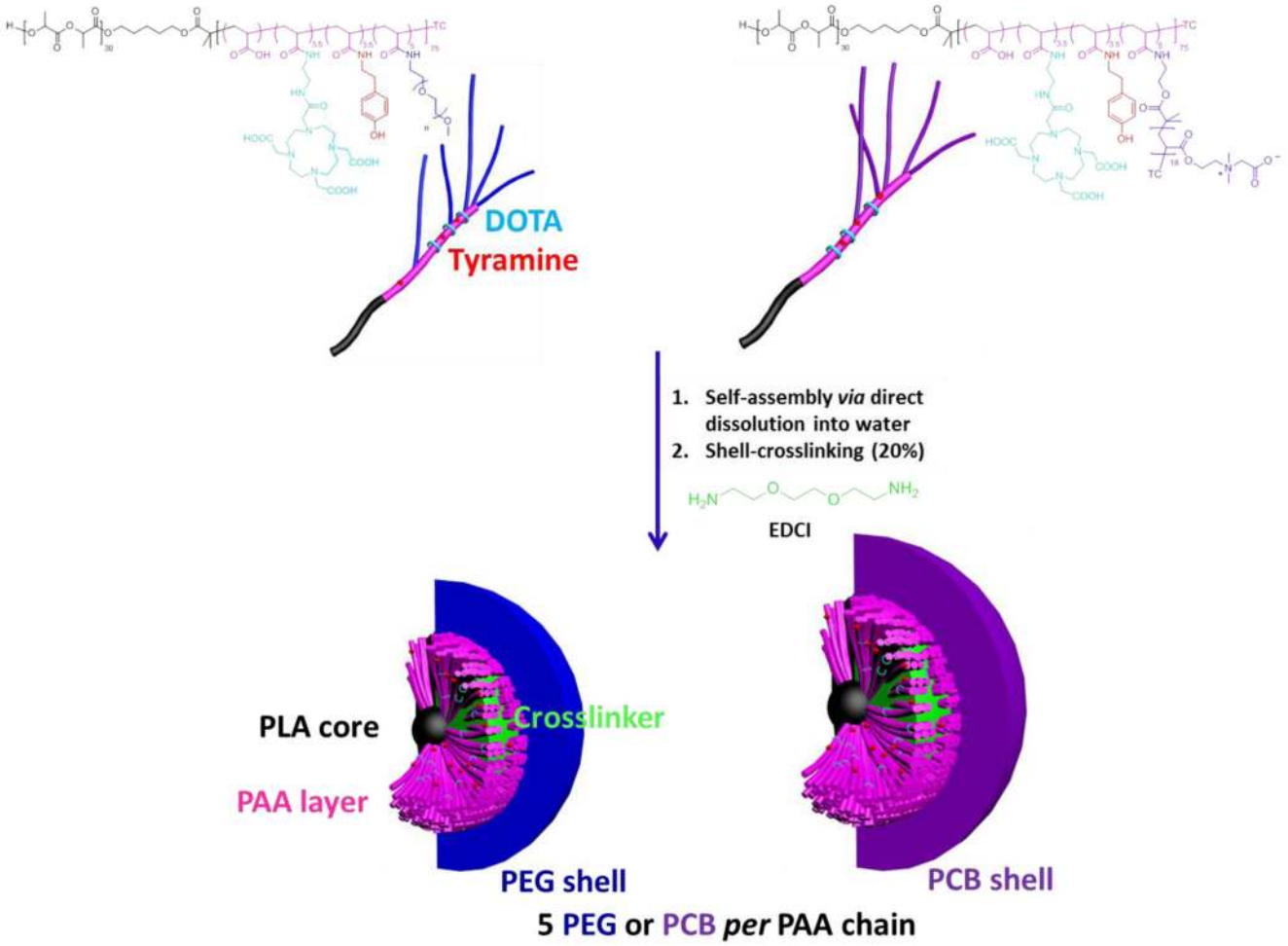

Figure 10.

Chemical structures of DOTA- and tyramine-functionalized PEG- and PCB-*g*-PAA-*b*-PLA copolymers, their self-assembly in water and crosslinking to form SCKs, with PLA degradable cores, PAA crosslinked shells, DOTA and tyramine available functionalities, and a hydrophilic shell of either PEG or PCB. TC = $SC(=S)SC_{12}H_{25}$, trithiocarbonate chain end from the RAFT polymerization chemistry. Reproduced with permission from Reference 89. Copyright 2013 Elsevier Ltd.

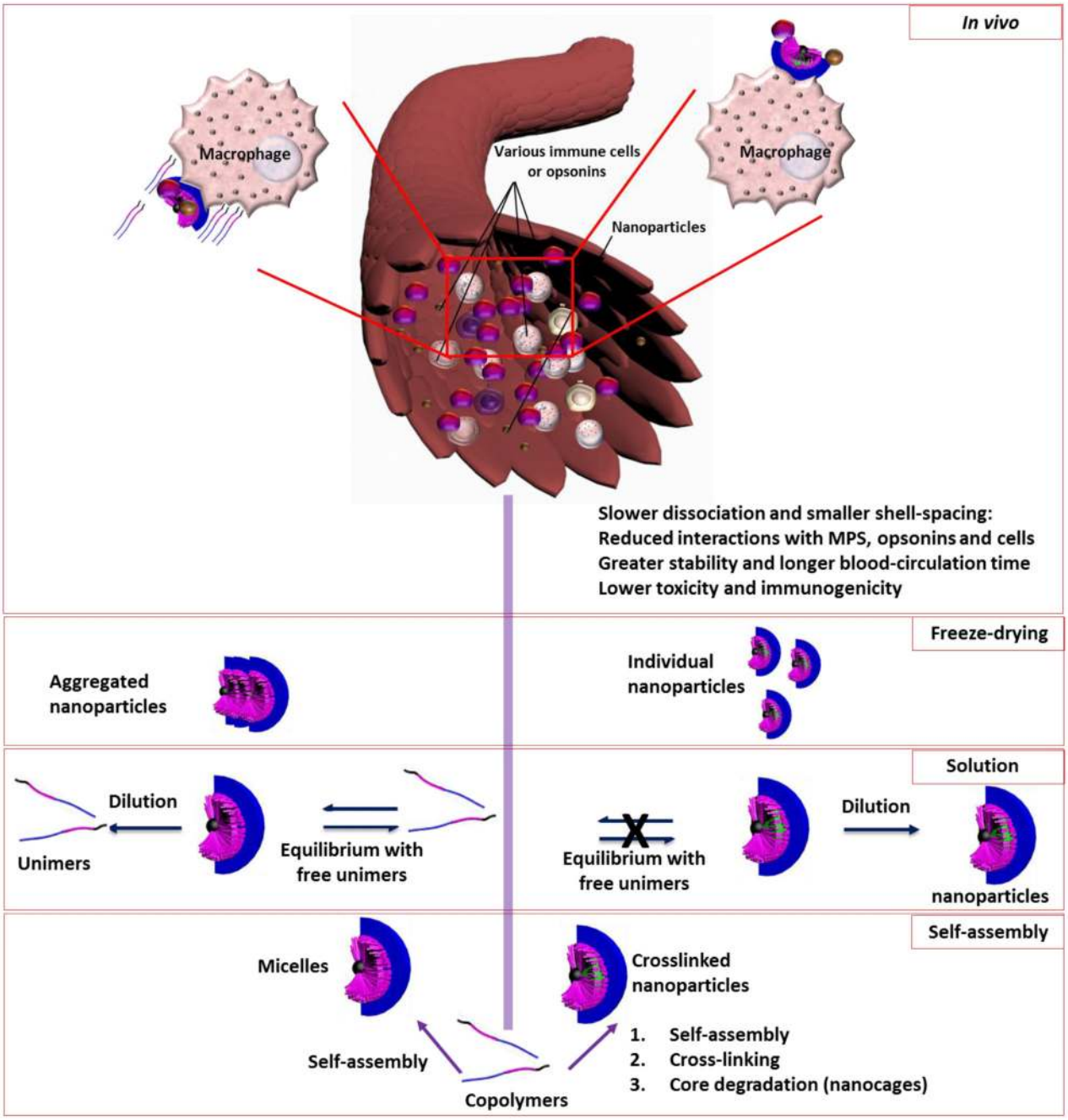

Figure 11.

Crosslinking imparts superior characteristics and features to the nanoparticles compared to the non-crosslinked ones, such as, higher stability in solution and in contact with biological interfaces, which reduces the premature cargo release and cyto/immunotoxicities, higher kinetic- and blood-stability, and resistance to aggregation during lyophilization and resuspension processes.

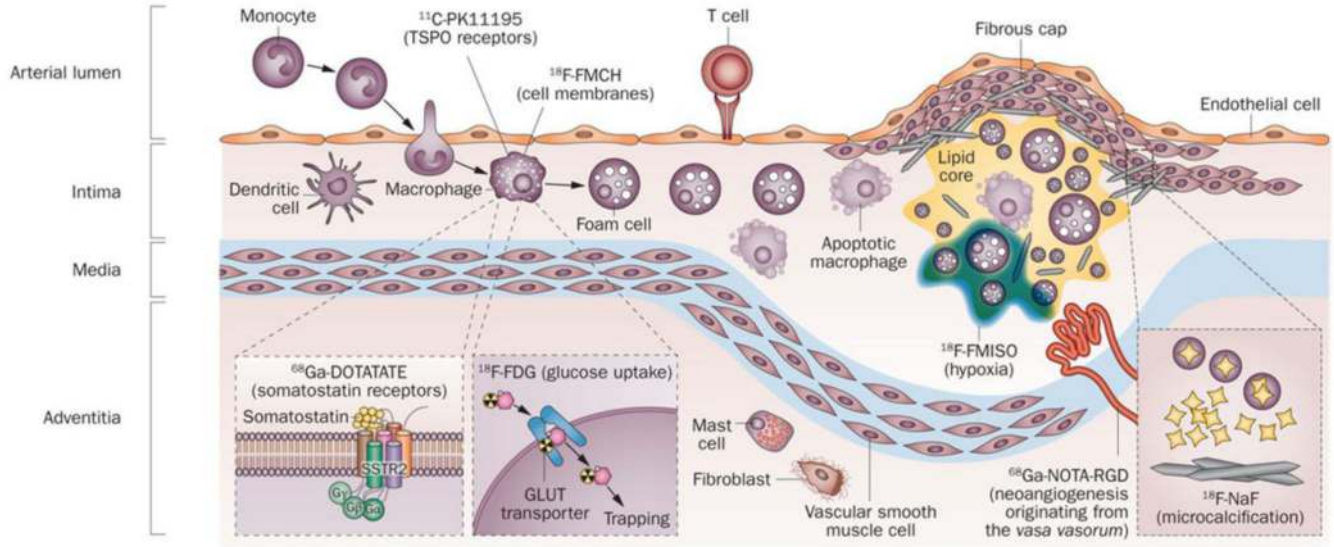

Figure 12.

The potential of scope PET atherosclerosis imaging. Inflammation and related pathogenic processes occurring within high-risk plaques can be imaged *in vivo* using specifically targeted radiolabelled PET tracers. ^{18}F-FDG is the most-widely studied and validated tracer, which is taken up by active macrophages where it is metabolically trapped and accumulates in proportion to intracellular demands. However, the ^{18}F-FDG arterial signal is also influenced by local hypoxia and uptake by other resident cell types. Alternative PET tracers, including ^{18}F-FMCH, ^{68}Ga-DOTATATE, and ^{11}C-PK11195 could be more-specific for macrophage activity (and, therefore, for inflammation) than ^{18}F-FDG. These tracers also seem to have lower background myocardial cell uptake than ^{18}F-FDG, which makes them preferable for coronary artery imaging. Within an inflamed plaque, hypoxia, neoangiogenesis, and microcalcification also contribute to plaque vulnerability; these processes can potentially be imaged with PET using novel tracers, such as ^{18}F-FMISO, ^{68}Ga-NOTA-RGD, and ^{18}F-NaF, respectively. Abbreviations: DOTATATE, [1,4,7,10-tetraazacyclododecane-*N*,*N*′,*N*″,*N*‴-tetraacetic acid]-D-Phe^{1},Tyr^{3}-octreotate; FDG, fluorodeoxyglucose; FMCH, fluoromethylcholine; FMISO, fluoromisonidazole; GLUT, solute carrier family 2, facilitated glucose transporter member; NaF, sodium fluoride; NOTA-RGD, 1,4,7-triazacyclononane-1,4,7-triacetic acid-Arg–Gly–Asp; SSTR2, somatostatin receptor type 2; TSPO, translocator protein. Reprinted with permission from Reference 190. Copyright 2014 Macmillan Publishers Ltd.

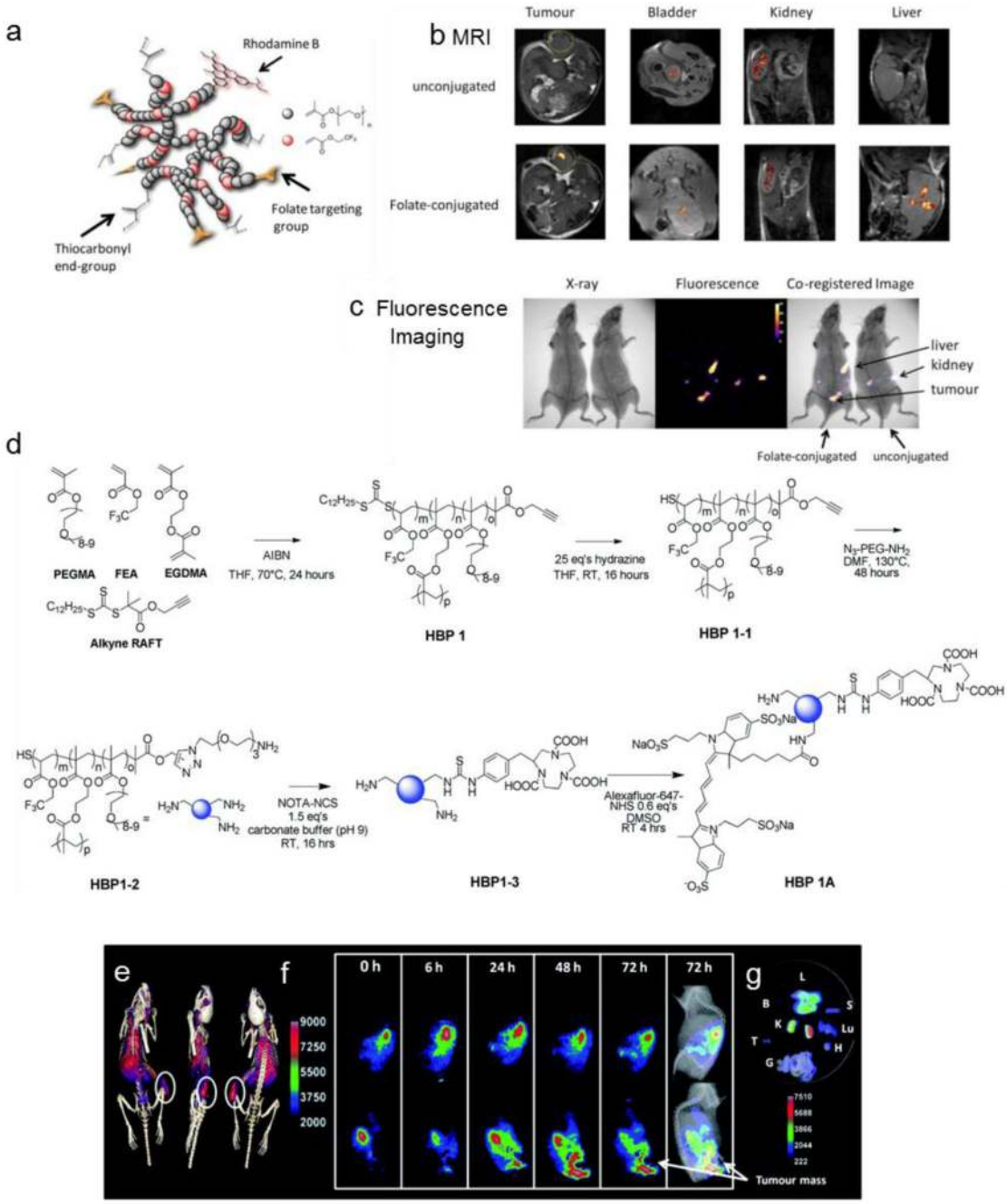

Figure 13.

(a) Schematic representation of hyperbranched polymer (HBP) used in folate-targeting experiments and MRI and optical images of the mouse subcutaneous B16 melanoma model with HBP. (b) MRI images of bladder, kidney, liver, or tumor (circled in image) in the tumor-bearing mice 1 h following intravenous injection of 100 μL of folate-conjugated or unconjugated (control) HBP (20 mg/mL in PBS). The high-resolution ^{1}H MR image is overlaid with the ^{19}F image. Experiments were performed under isofluorane. (c) Fluorescence images of mice following injection of the same two compounds at the same

concentration. The fluorescence images are co-registered with X-ray images of the mice 1 h following subcutaneous injection. (d) Synthesis of a hyperbranched polymer using RAFT mediated polymerization and subsequent end group modifications to introduce amine functionality, followed by attachment of PET ligand and optical NIR dye to synthesize multimodal imaging agent. PET/optical images of C57 Bl/6J mice with subcutaneous B16 melanoma tumor, injected with HBP 2A (e-f). (e) PET/CT image 24 h post injection, showing significant uptake in the tumor (white circle). (f) 72 h time course of optical imaging, top row: non-tumor bearing flank, bottom row: tumor bearing flank. (g) Optical imaging of excised organs (L: liver, K: kidneys, B: blood, Lu: lungs, H: heart, S: spleen, G: gut, and T: tumor). Adapted with permission from References [200,202]. Copyright 2014, Royal Society of Chemistry and American Chemical Society, respectively.

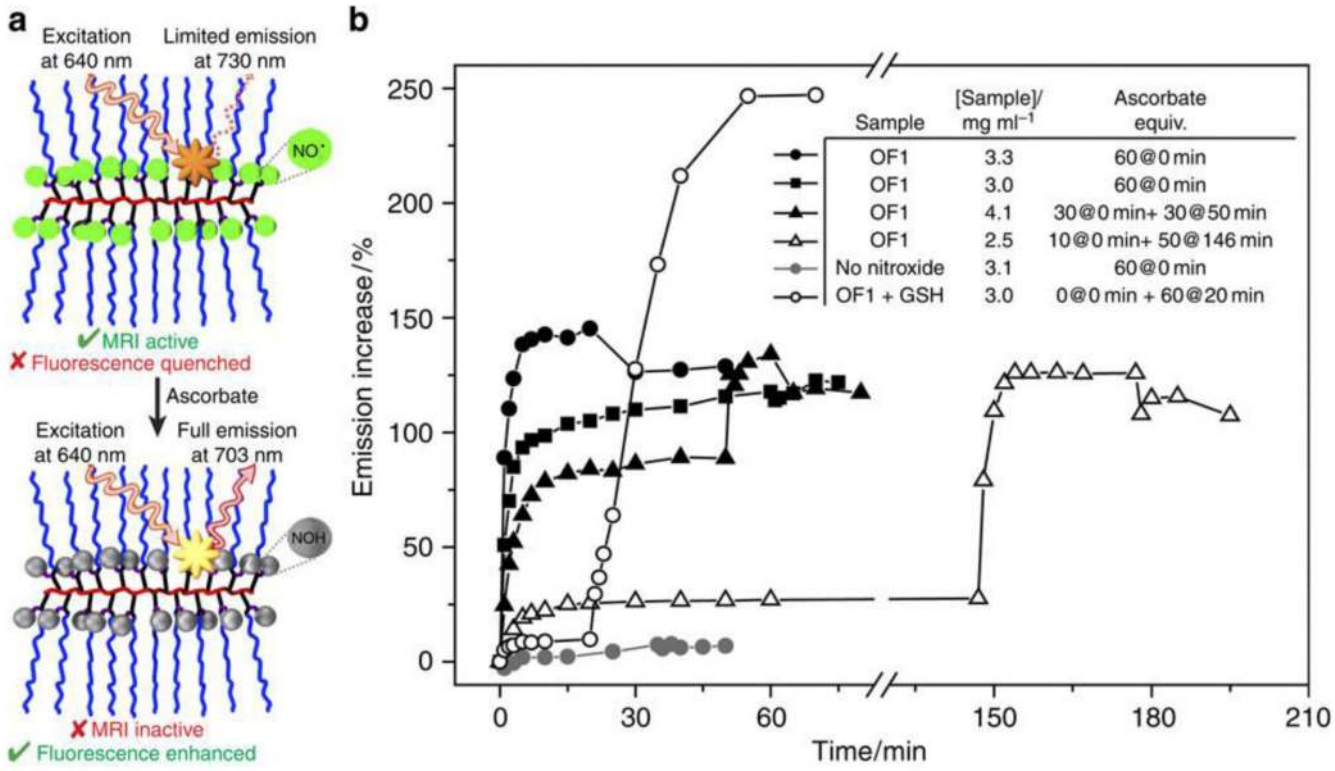

Figure 14.

Redox-sensitive dual-modality imaging mechanism. (a) Schematic for dual-modality molecular imaging in response to nitroxide reduction. (b) Emission behavior of OF1 and a control polymer with Cy5.5 and no nitroxides upon exposure to varied amounts of ascorbate or glutathione (GSH) in PBS buffer. The solution pH before and after addition of 60 equiv. ascorbic acid was 7.0 and 6.31, respectively; this pH change has no effect on Cy5.5 absorbance/emission. Reprinted with permission from Reference 211. Copyright 2014 Macmillan Publishers Ltd.

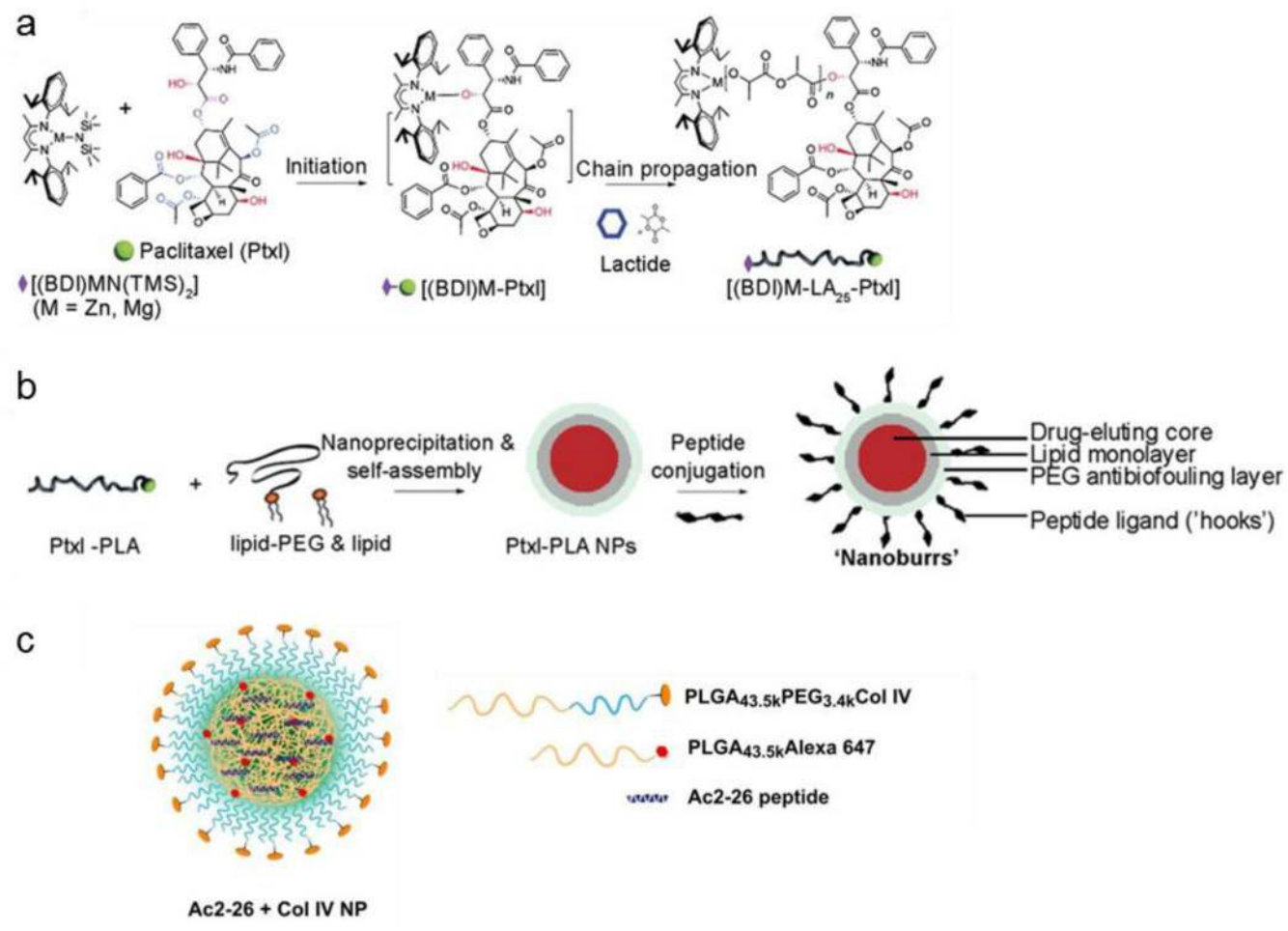

Figure 15.

Nanoparticle core-shell design and synthesis. (a) Schematic of paclitaxel-polylactide (Ptxl–PLA) biomaterial synthesis. Ptxl was mixed with equimolar amounts of $[(BDI)ZnN(TMS)_2]$; the (BDI)Zn–Ptxl complex formed *in situ* initiated and completed the polymerization of lactide. For the nanoburr core, we synthesized Ptxl–PLA_{25} drug conjugates, which have approximately 25 DL-lactide monomer units. (b) Schematic of nanoburr synthesis by nanoprecipitation and self-assembly. Ptxl–PLA in acetone was added dropwise to a heated lipid solution, vortexed vigorously, and allowed to self-assemble for 2 h to form NPs. The NPs were peptide-functionalized using maleimide-thiol chemistry. Nanoburrs have a drug-eluting polymeric core, a lipid monolayer, a PEG antibiofouling layer, and peptide ligands (hooks) to adhere to the exposed basement membrane during vascular injury. (c) Targeted (Col IV) NPs encapsulating the Ac2-26 peptide was developed using biodegradable polymers *via* a single-step nanoprecipitation method. The synthesized polymer and Ac2-26 peptide were dissolved in acetonitrile (total polymer 3 mg/mL), and 25 (*wt*/*wt*) of the fluorescent PLGA-Alexa 647 was added to the formulation. The NP sample contained 4% (*wt*/*wt*) peptide and 5% (*wt*/*wt*) of the Col IV peptide-conjugated targeting polymer. The organic mixture containing the polymers and peptide was then added dropwise to nuclease-free water (10 mL). The solution was stirred for 2-4 h, and the particles were

filtered, washed, and resuspended in water or PBS. BDI = 2-((2,6-diisopropylphenyl)amino)-4-((2,6-diisopropylphenyl)imino)-2-pentene, TMS = trimethylsilyl. Adapted with permission from References 225-226. Copyright 2010 National Academy of Sciences.

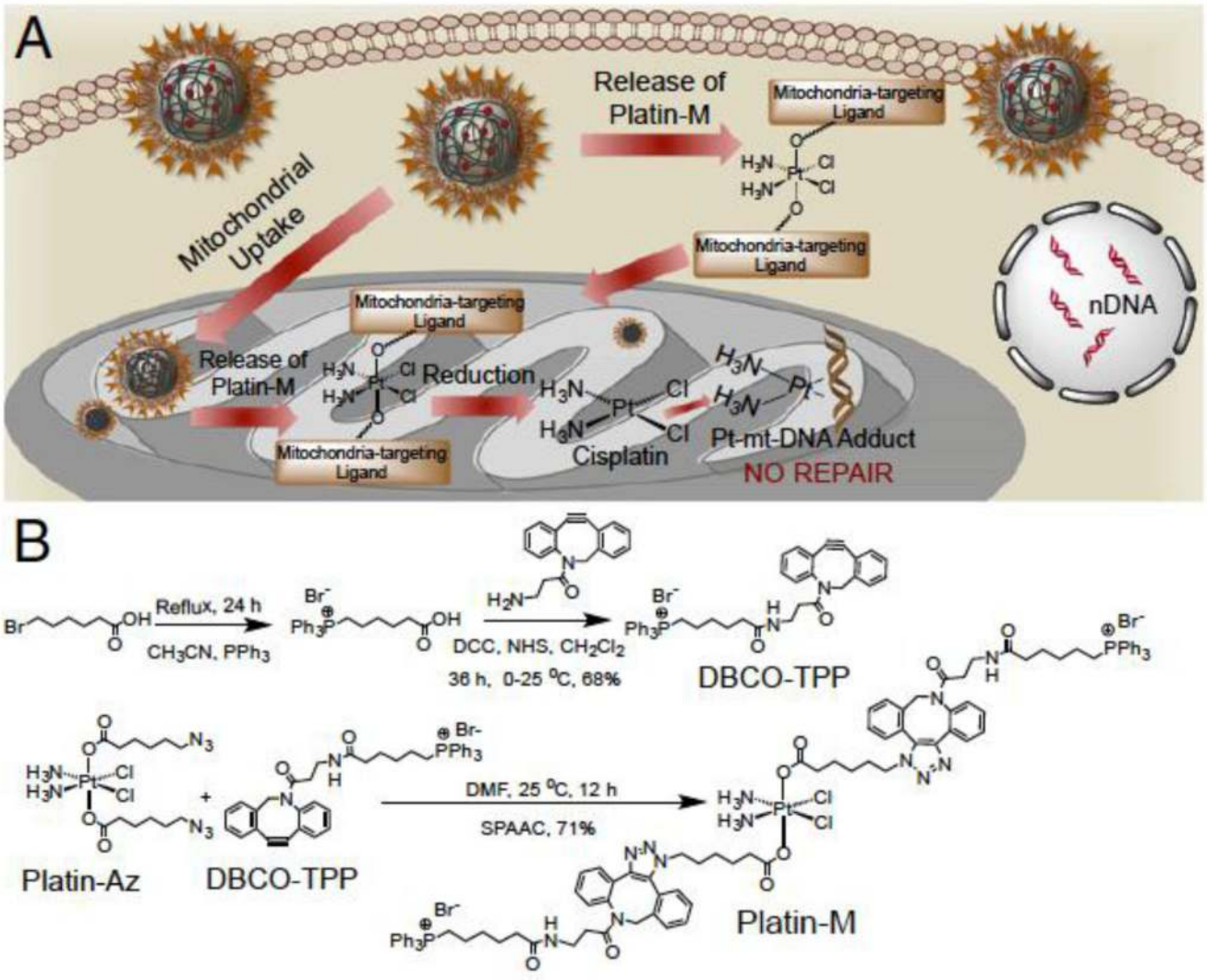

Figure 16.

(A) Schematic diagram for mitochondrial delivery of cisplatin prodrug using a targeted NP and the mechanism of action. (B) Synthesis of mitochondria-targeted Pt(IV) prodrug Platin-M. Reprinted with permission from Reference [248]. Copyright 2014 National Academy of Sciences.

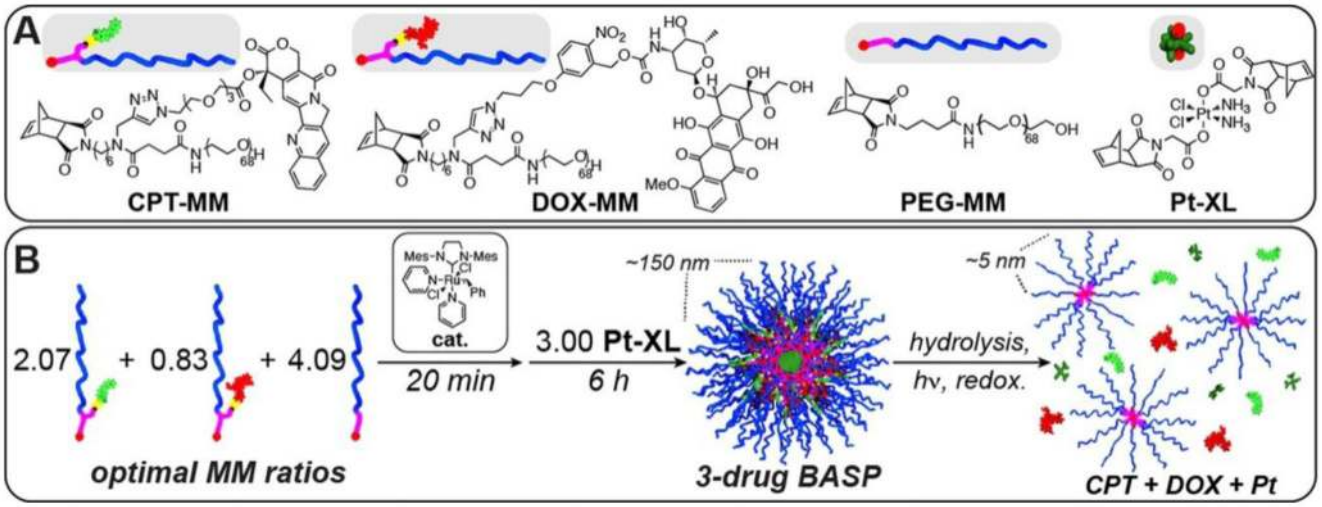

Figure 17.

(A) Structures of monomers used in the controlled loading and release of multiple anticancer drugs. (B) Schematic for synthesis of three-drug-loaded BASP. Drug release occurs in response to three distinct triggers. Reprinted with permission from Reference [268]. Copyright 2014 American Chemical Society.

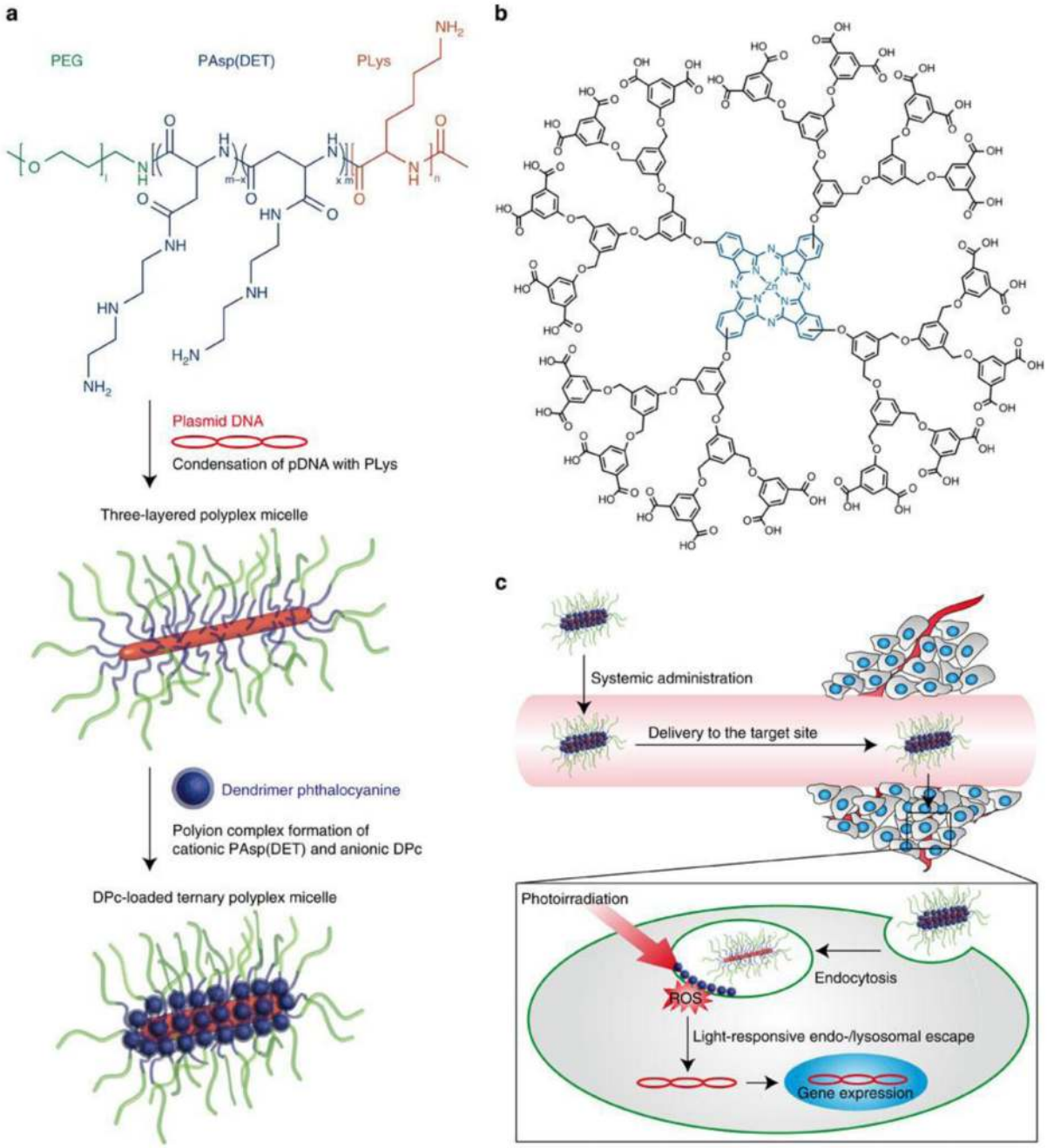

Figure 18.

Construction of the DPc-TPM and light-responsive gene transfer. (a) Design of the DPc-TPM. First, a three-layered polyplex micelle is prepared by mixing PEG-PAsp(DET)-PLys triblock copolymer and pDNA; the polyplex micelle is composed of a PEG shell, an intermediate PAsp(DET) layer and a PLys/pDNA core. The DPc-TPM is constructed by adding DPc to the PAsp(DET) intermediate layer. (b) Chemical structure of DPc. (c) Scheme showing the delivery at systemic and intracellular levels. At the systemic level, DPc-TPM circulates in the blood stream; non-specific interaction with biological

components is prevented after intravenous injection. In the target tissue (a solid tumor), DPc-TPMs are taken up by cells *via* endocytosis and entrapped in endo-/lysosomes. In response to the low pH prevalent in the endo-/lysosome, DPc is released from the DPc-TPMs owing to the protonation of the peripheral carboxyl groups and interacts with the endo-/lysosomal membrane through hydrophobic interactions. Upon photoirradiation, DPc generates ROS that destabilize the endo-/lysosomal membrane, facilitating endo-/lysosomal escape. Reprinted with permission from Reference 271. Copyright 2014 Macmillan Publishers Ltd.

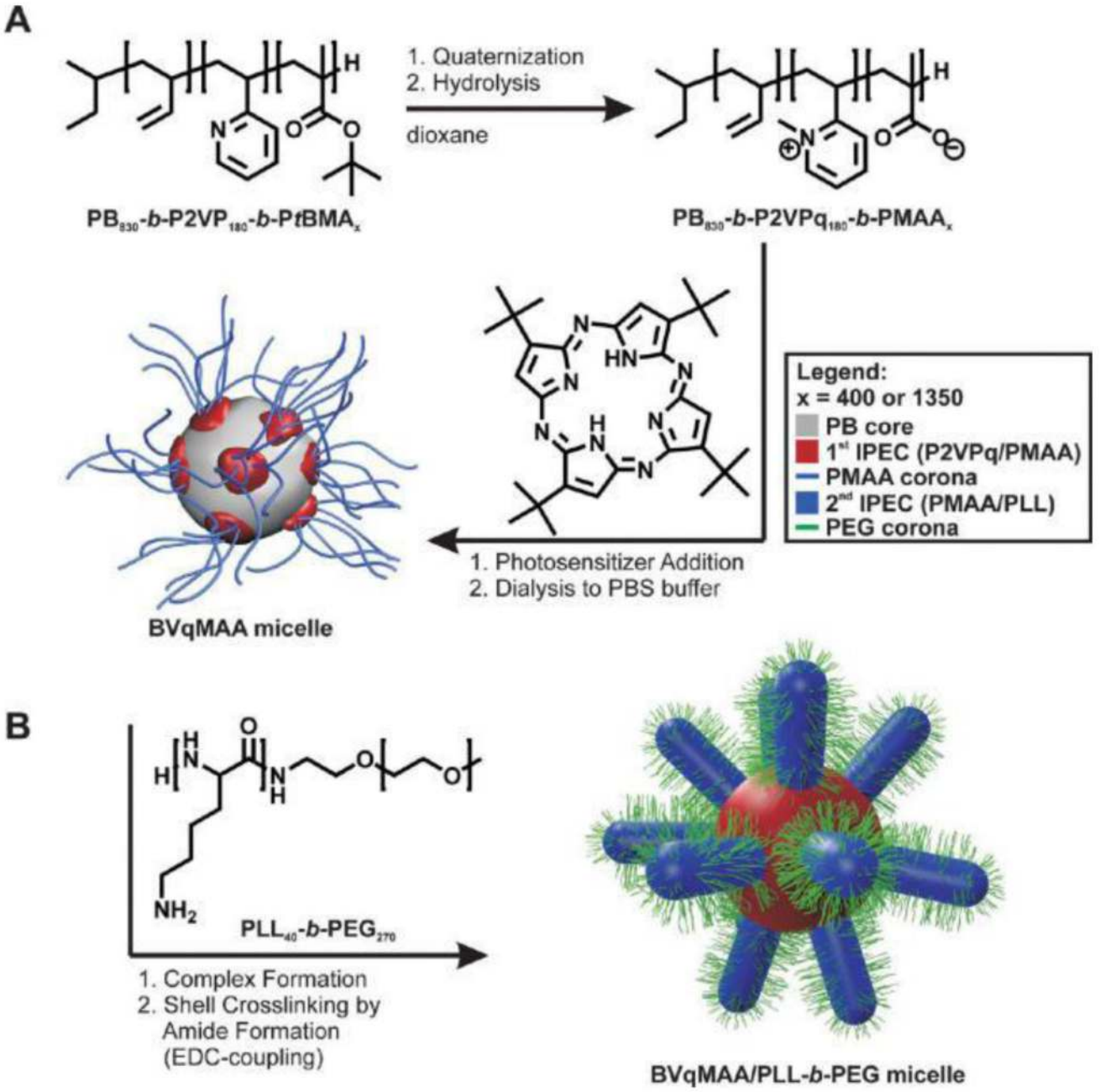

Figure 19.

(A) Preparative procedure to obtain PS-carrying BVqMAA micelles in water. A BVT triblock terpolymer is quaternized and hydrolyzed in dioxane to give amphiphilic BVqMAA. After PS addition, self-assembly to micelles takes place through the exchange of solvent from dioxane to PBS buffer. (B) Complexation with PLL-*b*-PEG diblock copolymers and subsequent crosslinking of PMAA with PLL yields PEGylated micelles (BVqMAA/PLL-*b*-PEG). Reprinted with permission from Reference 272. Copyright 2014 American Chemical Society.

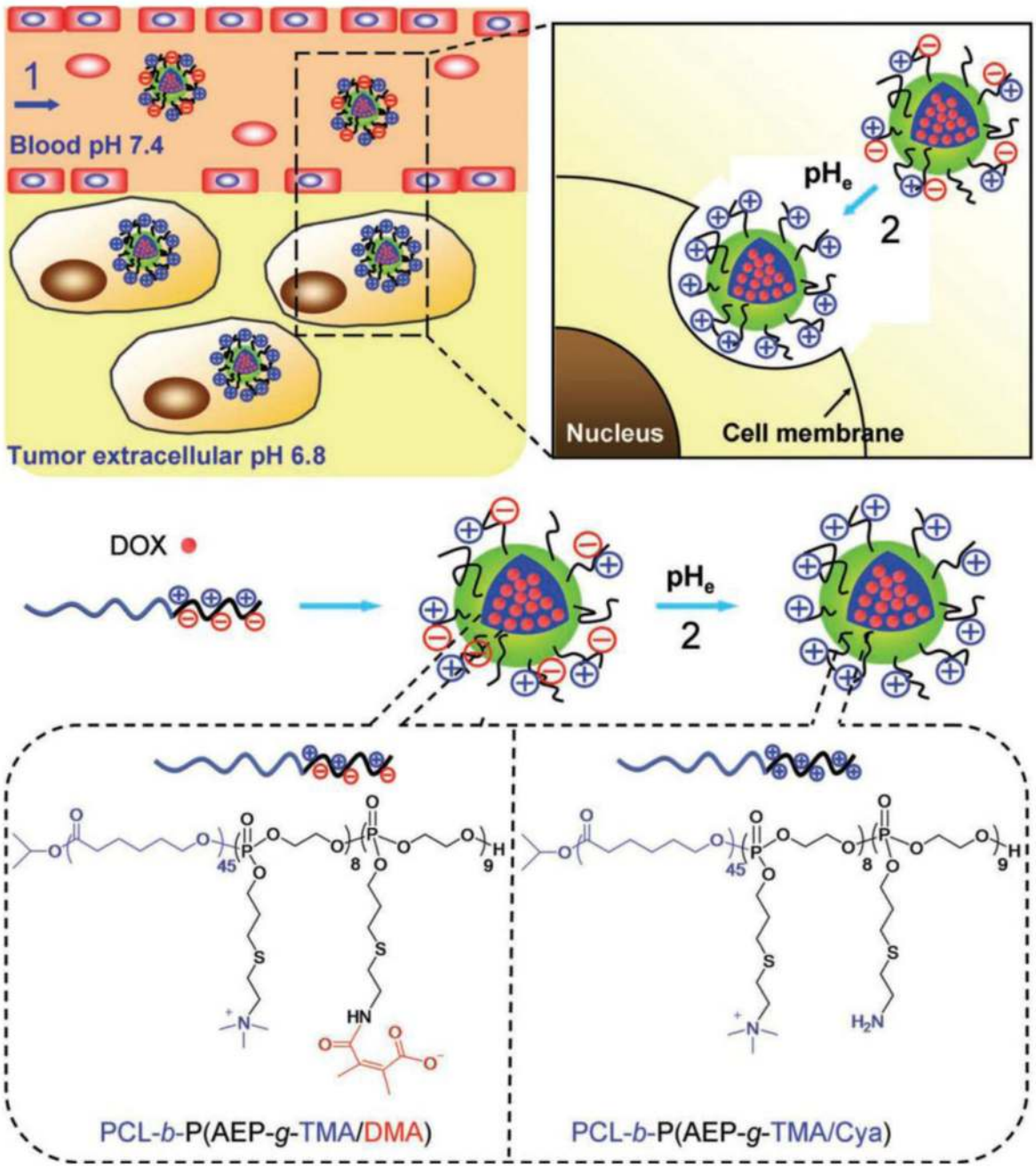

Figure 20.

Schematic illustration of doxorubicin (DOX)-loaded zwitterionic polymer-based nanoparticles and the changing of surface charge property in response to the tumor acidity (pH_e). 1) Amphiphilic zwitterionic block copolymer PCL-*b*-P(AEP-*g*-TMA/DMA) self-assembles into nanoparticles in aqueous solution with DOX encapsulation. During circulation in blood, the nanoparticles show prolonged circulation time and can leak into tumor sites through the EPR effect. 2) Responding to the pH_e, the zwitterionic polymer diminishes its anionic part, forming PCL-*b*-P(AEP-*g*-TMA/Cya), and the formed

nanoparticles are activated to be positively charged and become recognizable by tumor cells. Reprinted with permission from Reference 273. Copyright 2012 John Wiley & sons, Inc.

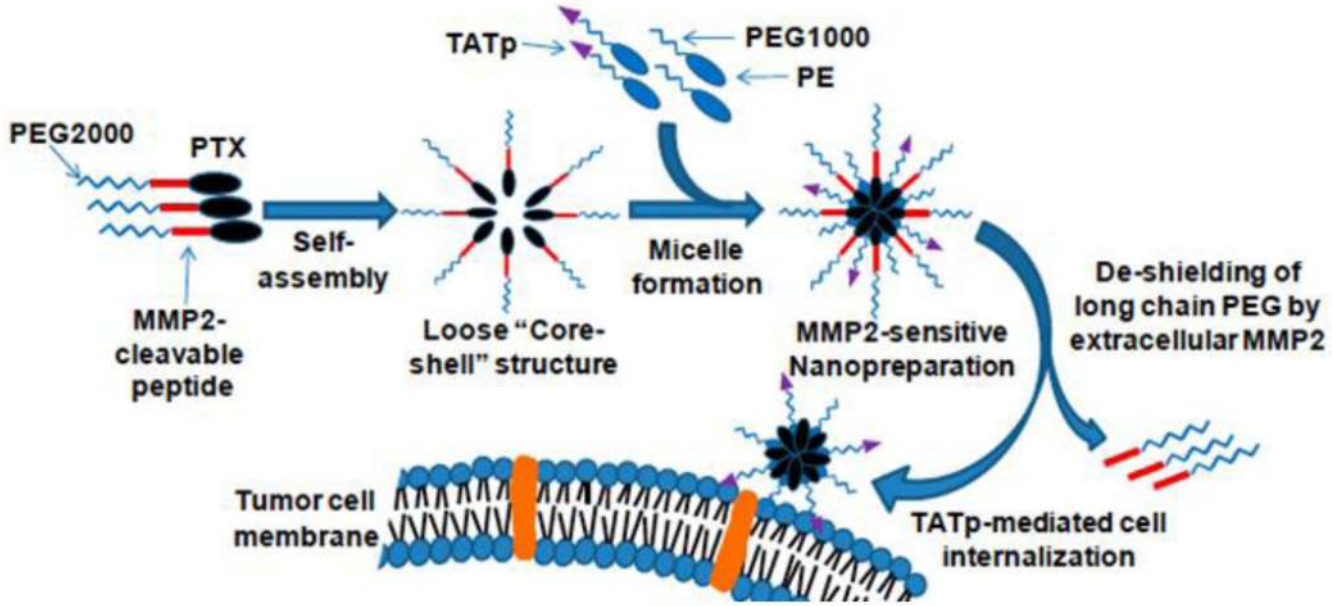

Figure 21.

Drug delivery strategy of the MMP2-sensitive nanopreparation. Adapted with permission from Reference 275. Copyright 2013 National Academy of Sciences.

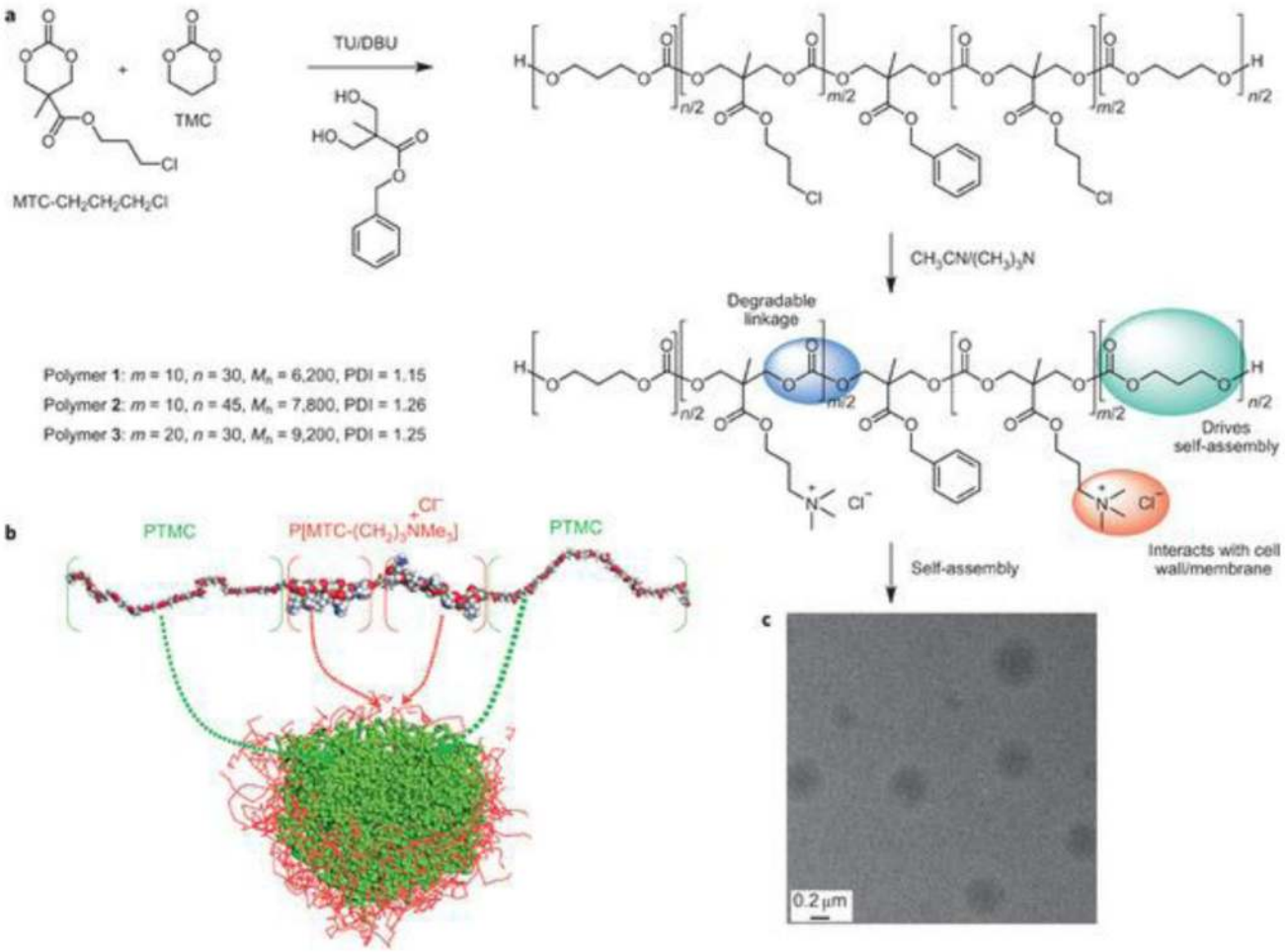

Figure 22.

Synthesis and micelle formation of cationic amphiphilic polycarbonates. a, Cationic amphiphilic polycarbonates were synthesized with a well-defined structure and narrow molecular weight distribution. Based on light scattering, zeta potential, TEM and simulation analyses, these polymers easily formed cationic micelles by direct dissolution in water. b,c, The formation of micelles was simulated through molecular modeling using Materials Studio Software (b) (in the polymer molecule: red, O; white, H; grey, C; blue, N), and was observed in a TEM image of polymer 3 (c) (scale bar, 0.2 μm). Reprinted with permission from Reference 286. Copyright 2011 Macmillan Publishers Ltd.

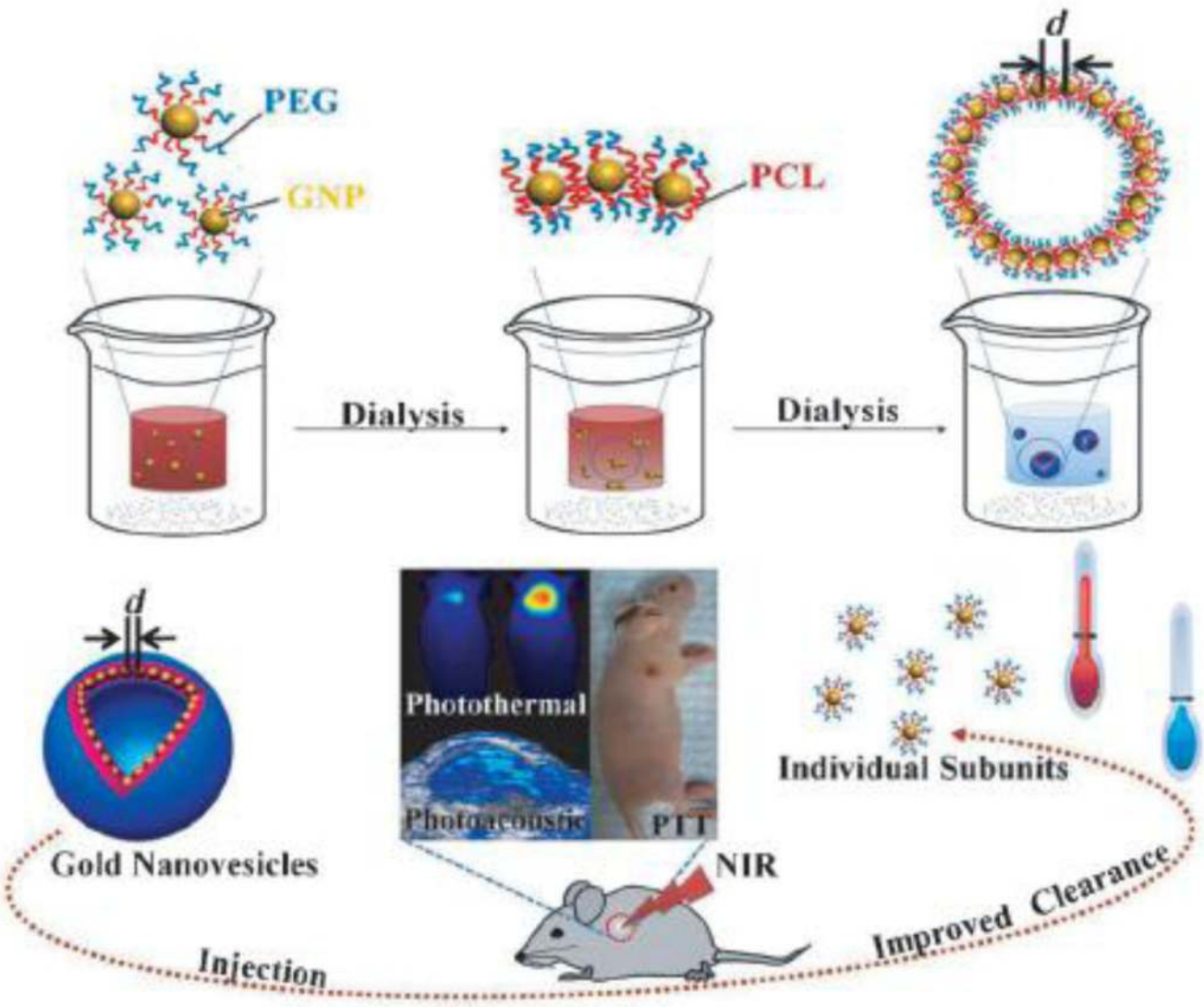

Figure 23.

Self-assembly of biodegradable gold vesicles (BGVs) composed of poly(ethylene glycol)-*b*-poly(ε-caprolactone) (PEG-*b*-PCL)-tethered GNPs through the dot–line–plane–vesicle mode during the dialysis process. BGVs with an ultrastrong plasmonic coupling effect are superior photoacoustic (PA) imaging and photothermal therapy (PTT) agents with improved clearance after the dissociation of the assemblies. The PA signal and PTT efficiency of BGVs are increased as the distance (*d*) between adjacent GNPs decreases. Reprinted with permission from Reference 310. Copyright 2014 John Wiley & Sons, Inc.

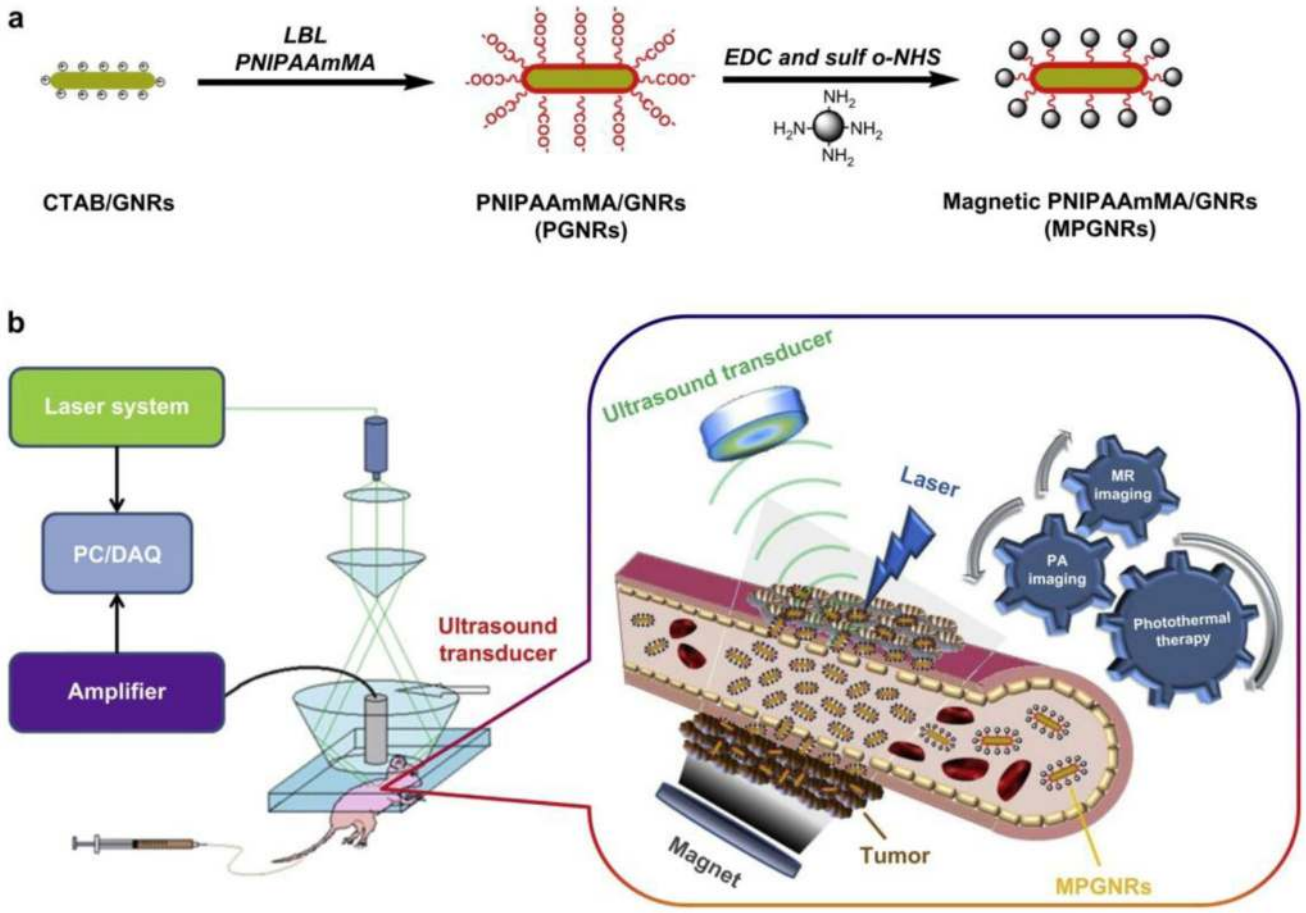

Figure 24.

(a) Schematic illustration of the synthesis and structure of PGNRs and MPGNRs. (b) The mechanism of action of MPGNRs for targeted photothermal therapy and dual MR/PA imaging. Abbreviations: PGNRs, PEGylated gold nanorods; MPGNRs, magnetic PGNRs; MR/PA imaging, magnetic resonance/photoacoustic imaging. Reprinted with permission from Reference 312. Copyright 2013 Elsevier Ltd.

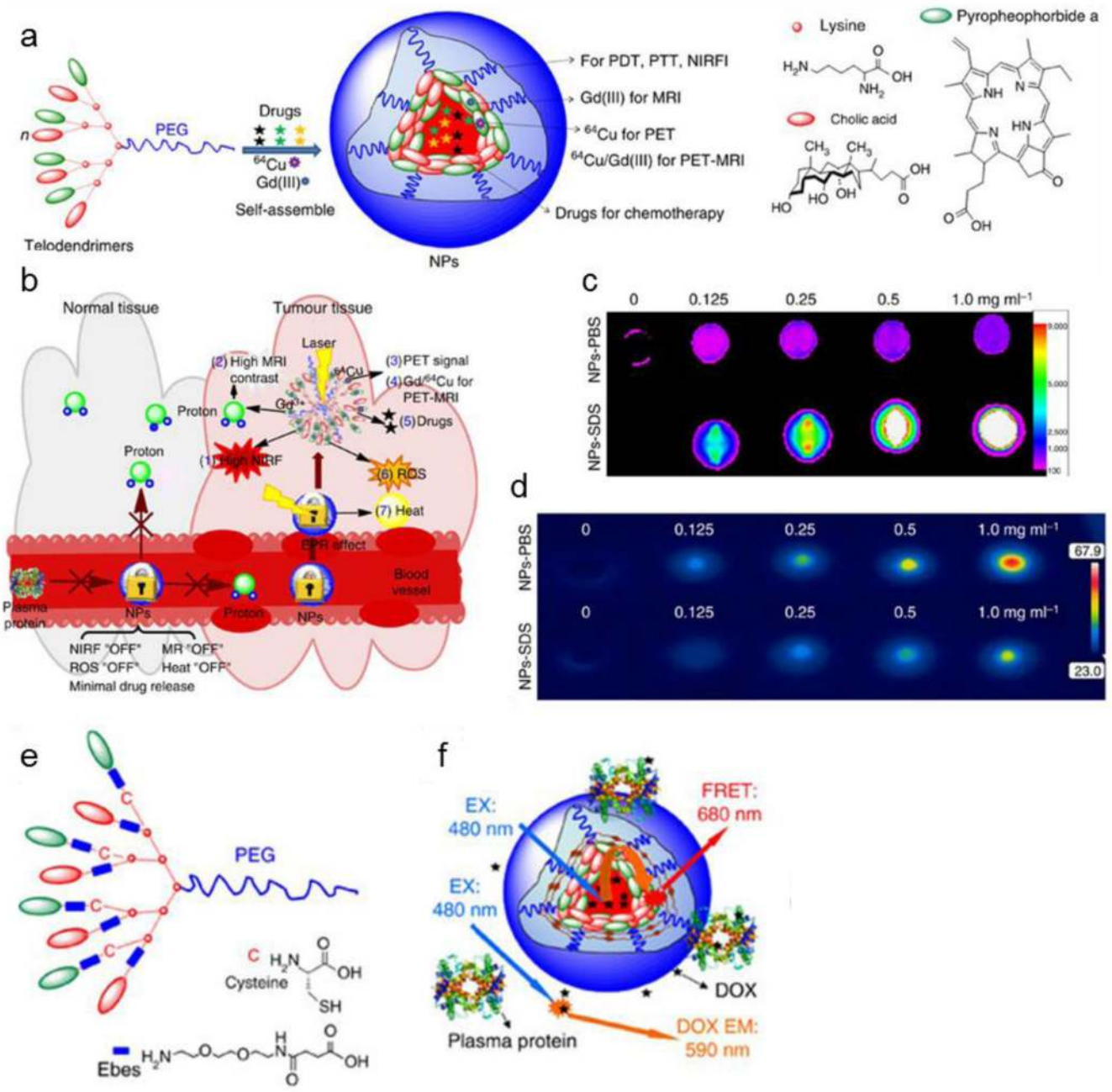

Figure 25.

Design, synthesis and characterizations of NPs and disulfide-crosslinked NPs. (**a**) Schematic illustration of a multifunctional NP self-assembled by a representative porphyrin–telodendrimer, PEG_{5k}-Por_4-CA_4, composed of four pyropheophorbide-a molecules and four cholic acids attached to the terminal end of a linear PEG chain. (**b**) Schematic illustration of NPs as a smart 'all-in-one' nanomedicine platform against cancers. (**c**) Near-infrared fluorescence imaging of NP solution (10 μL) in the absence and in the presence of SDS with an excitation bandpass filter at 625/20 nm and an emission filter at 700/35 nm. Concentration-dependent photothermal transduction of NPs: (**d**) thermal images after

irradiation with NIR laser (690 nm) at 1.25 w cm^{-2} for 20 s. (**e**) Schematic illustration of a representative crosslinkable porphyrin–telodendrimer (PEG_{5k}-Cys_4-Por_4-CA_4), composed of four cysteines, four pyropheophorbide-a molecules and four cholic acids attached to the terminal end of a linear PEG chain. (**f**) Schematic illustration of FRET-based approach for study of the real-time release of doxorubicin from nanoporphyrins in human plasma. Adapted with permission from Reference 208. Copyright 2014 Macmillan Publishers Ltd.

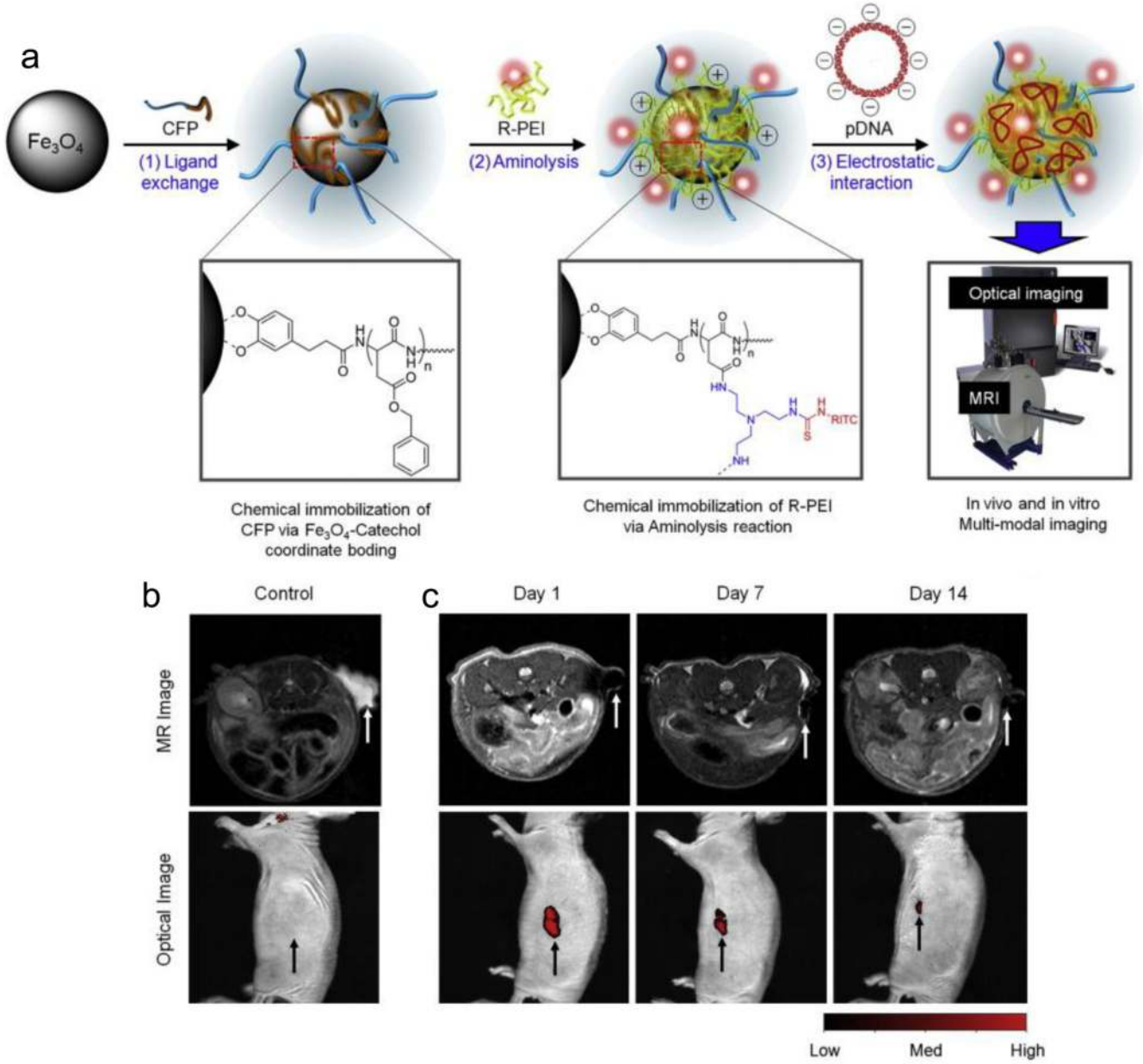

Figure 26.

(a) Fabrication process of multi-modal transfection agents (MTA) and *in vitro* and *in vivo* multi-modal imaging of MTA in hMSCs. (b) No hyperintense signal (arrow) of MR and optical fluorescence was detected in mice transplanted with MTA-untransfected hMSCs. (c) Hyperintense signals (arrows) of MR and optical fluorescence were detected in mice transplanted with MTA-transfected hMSCs and were still visible 14 days after transplantation. Adapted with permission from Reference 315. Copyright 2014 Elsevier Ltd.

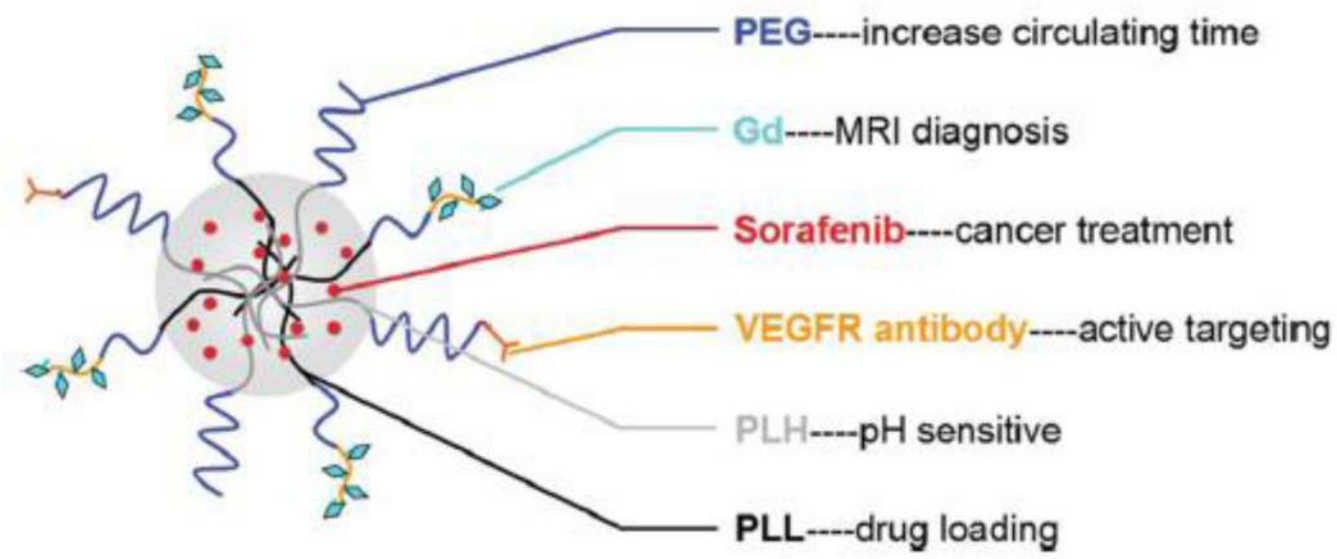

Figure 27.
Design of the multifunctional pH-sensitive polymeric nanoparticle system. Reprinted with permission from Reference 182. Copyright 2014 Royal Society of Chemistry.

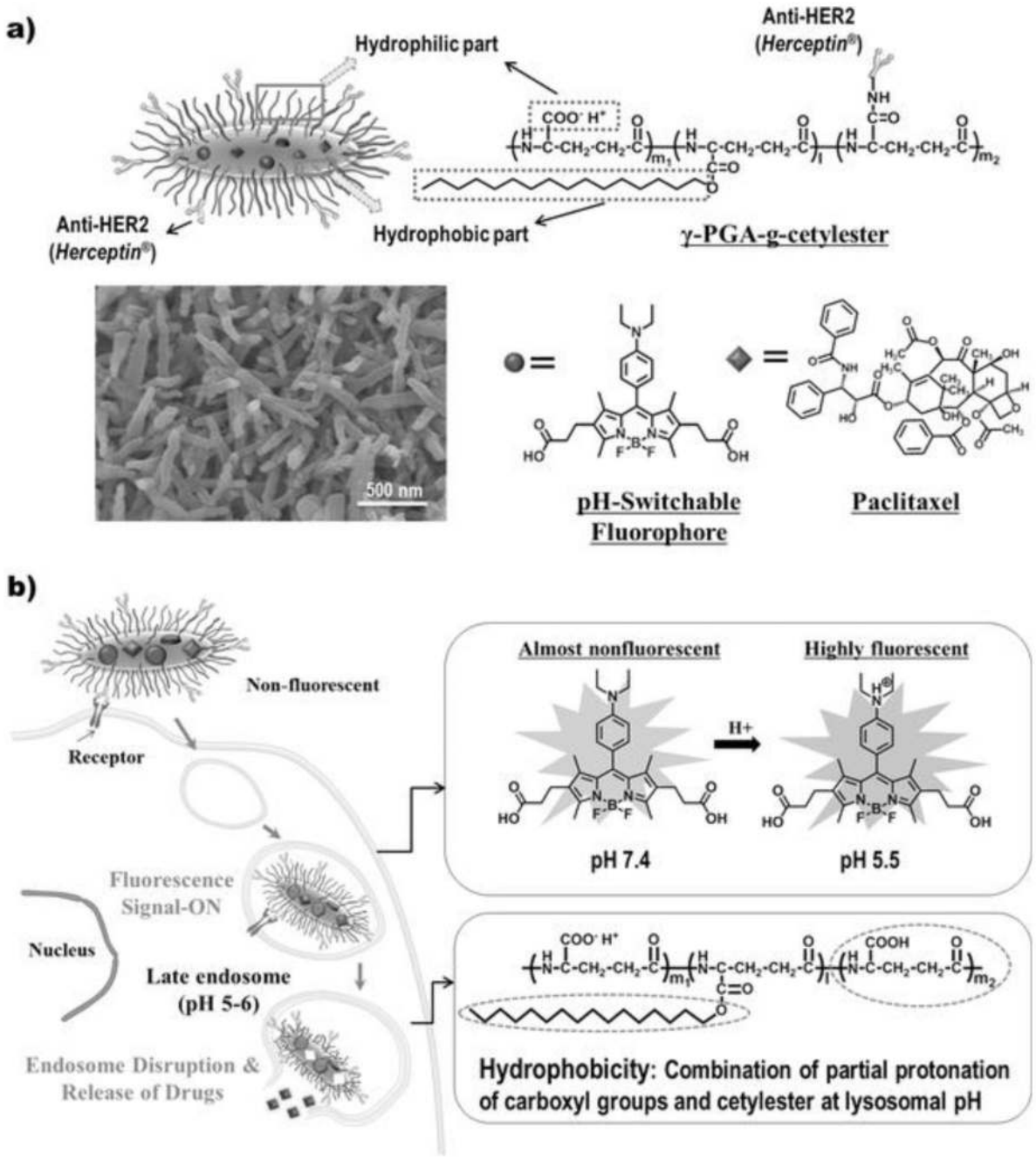

Figure 28.

Design and synthesis of target-selective theranostic nanoparticles mimicking virus entry into cells. a) Schematic illustration and SEM image of the filamentous virus-like theranostic nanoparticles composed of poly(γ-glutamic acid)-*graft*-cetylester (γ-PGA-*g*-cetylester), pH-switchable fluorophores (pSF), therapeutic drugs (paclitaxel), and targeting antibody (Herceptin). b) Target-selective theranosis: receptor-mediated entry of γ-PGA-*g*-cetylester [pSF/paclitaxel] nanoparticles followed by pH-dependent signal-on, hydrophobicity-induced

membrane-disruption and cytosolic delivery of therapeutic drugs. Reprinted with permission from Reference 317. Copyright 2014 John Wiley & Sons, Inc.

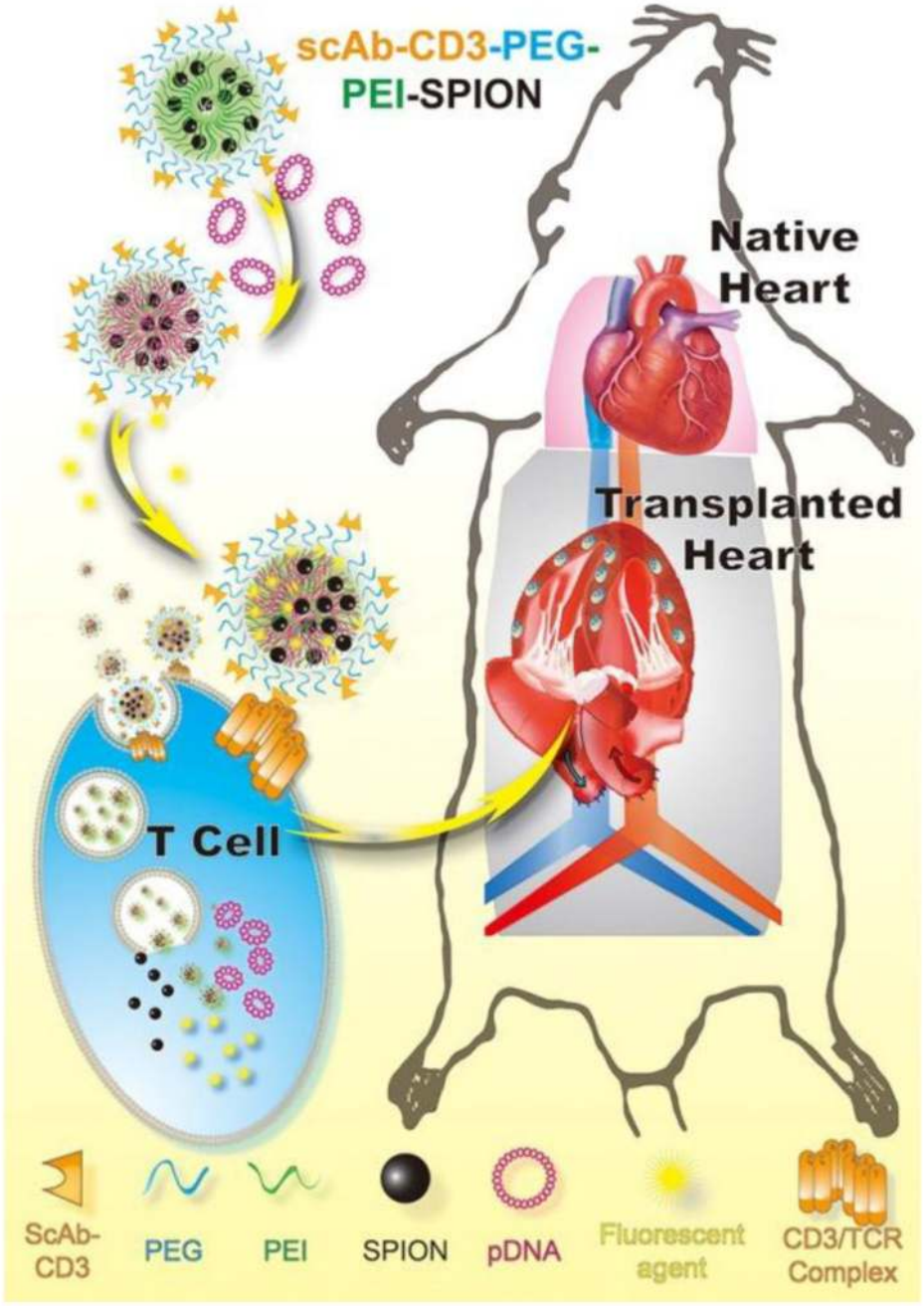

Figure 29.

Schematic diagram of therapeutic process of magnetic targeting polyplex scAbCD3-PEG-*g*-PEI-SPION *in vitro* and *in vivo*. Reprinted with permission from Reference 318. Copyright 2012 American Chemical Society.

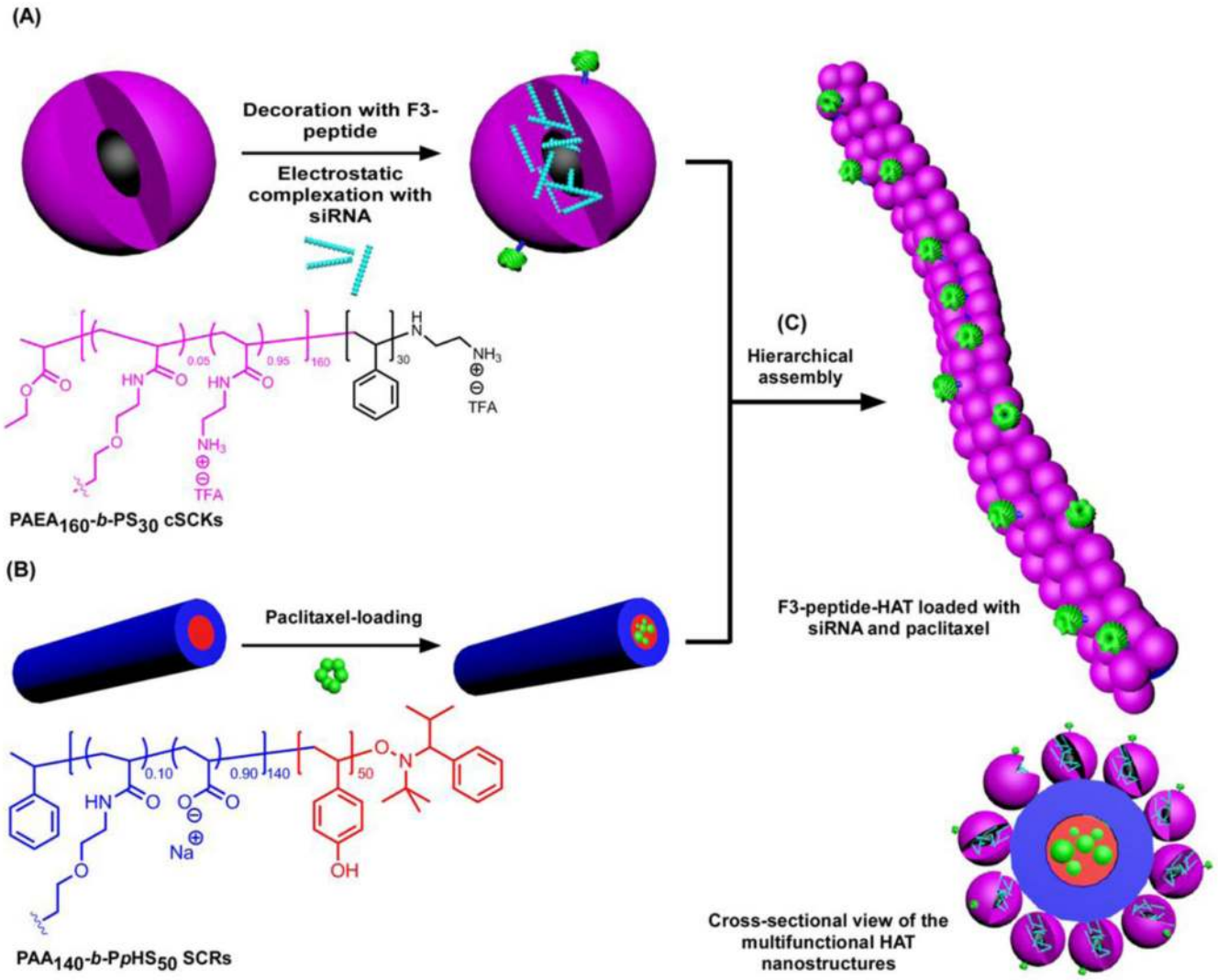

Figure 30.

Construction of HAT nanostructures as a template for the co-delivery of siRNA and paclitaxel: (A) Electrostatic complexation of $PAEA_{160}$-*b*-PS_{30} cSCKs and nucleic acids (*e.g.* siRNA) and decoration of the surface of nanoparticles with targeting ligands (*e.g.* F3 peptides); (B) Loading of hydrophobic drugs (*e.g.* paclitaxel) into SCRs composed of PAA_{140}-*b*-P*p*HS_{50}. (C) Hierarchical-assembly of cSCKs and SCRs to form the HAT nanoassemblies and the cross-sectional view of the multifunctional HAT nanostructures. Reprinted with permission from Reference 320. Copyright 2013 American Chemical Society.

Table 1

Comparison of some key imaging modalities. Adapted with permission from References 33-34. Copyright 2014 and 2010, Springer and Elsevier Ltd., respectively.

Modality	Spatial resolution	Depth limit	Time	Target*	Imaging agents	Probe sensitivity (M)	Advantages	Disadvantages
CT	50–200 μm	None	Seconds -minutes	A, P	Heavy elements *e.g.*, iodine, barium	Not well-characterized	High resolution Relatively lower cost No depth limit	Poor sensitivity Not functional (contrast agents are required for tissue differentiation) Radiation
MRI	25–100 μm	None	Minutes -hours	A, P, M	Superparamagnetic: Fe_3O_4, Fe_2O_3; Paramagnetic: Gd, Mn	10^{-3} to 10^{-5}	High resolution No radiation Functional imaging with modification (fMRI) No depth limit	High cost Low sensitivity Not functional Limited availability for patients with metallic implants
PET and SPECT	1–2 mm	None	Minutes	P, M	Radionuclides PET: ^{18}F, ^{13}N, ^{11}C, ^{15}O, ^{64}Cu, ^{68}Gd, ^{89}Zr, ^{124}I SPECT: ^{99m}Tc, ^{111}In	PET: 10^{-11} to 10^{-12} SPECT: 10^{-10} to 10^{-11}	High sensitivity Functional imaging No depth limit	Low resolution High cost Radiation
Ultrasound	50-500 μm	None	Seconds -minutes	A, P	Microbubbles	Not well-characterized	Low cost Ease of operation No radiation	Low resolution Limited imaging depth
Optical imaging	1–5 mm	mm	Seconds -minutes	P, M	Fluorescent dyes or quantum dots	Bioluminescence: 10^{-15} to 10^{-17} Fluorescence 10^{-9} to 10^{-12}	High sensitivity No radiation Multi-channel imaging	Not for clinical imaging Low resolution Limited imaging depth

*: A, anatomical; P, physiological; M, molecular

Table 2

Main types of nanoparticles that have been utilized for therapy and/or imaging. Adapted with permission from Reference 81. Copyright 2013 Royal Society of Chemistry.

A. Organic nanoparticles:

1. **Macromolecular conjugates (*e.g.* Xyotax®, Oncaspar®):** Conjugating drug to a polymeric or lipidic segment to impart specific properties to the drug to facilitate or direct its delivery.[107-108]
2. **Nanoemulsions (*e.g.* Diprivan®):** Heterogeneous mixture of two immiscible liquids with emulsifier that stabilizes the dispersed droplets. They can be utilized as carriers for hydrophilic or hydrophobic drugs for various therapeutic applications.[109-110]
3. **Polymeric micelles (*e.g.* NK012, NK105, SP1049C, NC-6004, Genexol):** Self-assembly of amphiphilic copolymer chains in aqueous milieu presenting a core/shell architecture with a hydrophobic core and hydrophilic corona. Depending on the structure of the core forming polymer and the forces driving the assembly, they may be classified also as polyion complex micelles or polymer-metal complex micelles.[111-113]
4. **Shell crosslinked knedel-like nanoparticles:** Shell crosslinked polymeric nanoparticles to enhance the kinetic stability and prevent the dissociation upon *in vivo* administration. Degradation of the core is also possible to form nanocages.[90-91,97]
5. **Protein-based and polymeric nanoparticles (*e.g.* Abraxane®, BIND-014):** Colloidal particles with a rigid core that are either made from a polymeric or lipidic matrix in which a drug is dissolved or dispersed or from drug nanocrystals stabilized by a polymer.[97,114-115] Polymer brushes, unimolecular (*e.g.* dendrimers) and hyperbranched structures utilized for drug delivery may also fall into this category.[116-117]
6. **Liposomes (*e.g.* Doxil®, DaunoXome, Ambisome):** spherical vesicles composed of lipid bilayers and a hydrophilic core with capability of solubilizing both hydrophilic and lipophilic drugs into the core and lipid bilayers, respectively.[118-120]
7. **Lipoplexes and polyplexes (*e.g.* ALN-VSP):** Complexes between nucleic acids (DNA/RNA) and cationic lipids or polymers, and when PEGylated are categorized as PEGylated lipoplexes and polyion complex micelles, respectively.[121-124] Stable nucleic acid lipid particles (SNALP) may also fall into this category.[125-126]

B. Inorganic nanoparticles:

1. **Metal and metal-oxide nanoparticles:**
   a. **Gold nanoparticles (*e.g.* Aurimune®):** Nanoparticles that display interesting optical and electrical properties.[127]
   b. **Magnetic nanoparticles (Ferridex, Ferumoxytol, Resovist):** Nanoparticles with magnetic properties (*e.g.* paramagnetic iron oxide nanoparticles).[128-129]
   c. **Other nanoparticles:** Other kinds of nanoparticles do also exist, such as, titanium oxide, platinum- and diamond-based nanoparticles, etc.
2. **Carbon nanotubes:** single wall or multi-wall cylindrical graphene sheets.[129-131]
3. **Quantum dots:** Inorganic semiconductor nanoparticles that are widely used as fluorophores for biological imaging.[129]

Table 3

Multimodal medical imaging using polymeric nanoparticles.

Imaging methods	Polymer modification	Contrast agents (Tracers)	Advantages	Applications
MRI/CT	Poly(acrylic acid) Poly(amidoamine)	Gd^{3+} Gold nanoparticle	Anatomical information High resolution Enhanced images with smaller dosage	Cancer[196-198]
PET/optical	Poly(dextran) nanoparticles; Poly(oligoethylene glycol methyl ether methacrylate)-based hyperbranched polymer	^{89}Zr VivoTag 680 ^{64}Cu NIR-750 Alexa Fluor-647	Anatomical information Quantitative Functional High-contrast High-resolution Time-resolved Therapeutic possibility	Cardiovascular[199] Cancer[200]
MRI/optical	Poly (glycidyl methacrylate)-polyethylenimine Poly(oligoethylene glycol methyl ether methacrylate)-based hyperbranched polymer Poly (lactic acid)-D-α-tocopheryl polyethylene glycol 1000 succinate nanoparticles	SPIO Rhodamine ^{19}F Rhodamine B NIR797 Quantum dot	Anatomical information High resolution High sensitivity Therapeutic possibility	Neuroscience[201] Cancer[202-203]
Ultrasound/optical	Hyaluronic acid	ICG	Anatomical information Functional High resolution Therapeutic possibility	Cancer[204-205]
Trimodal	MRI-PET-optical Poly(dextran) nanoparticles PEG Pyropheophorbide-a-cholic acids-PEG	SPIO ^{64}Cu VT680 Gd^{3+} Yb^{3+}/Er^{3+} ^{124}I	Anatomical information High resolution Functional High sensitivity Therapeutic possibility	Cardiovascular[206] Cancer[207-208]
	MRI-CT-optical PEG	Gd^{3+} Yb^{3+}/Er^{3+} Gold nanoparticle	Anatomical information High resolution Functionl	Cancer[209]